EGG CELL 1 function and stability during double fertilization in *Arabidopsis thaliana*

DISSERTATION

ZUR ERLANGUNG DES DOKTORGRADES
DER NATURWISSENSCHAFTEN (DR. RER. NAT.)
DER FAKULTÄT FÜR BIOLOGIE UND VORKLINISCHE MEDIZIN

UNIVERSITÄT REGENSBURG

vorgelegt von

Svenja Rademacher
aus Darmstadt

im März 2011

Das Promotionsgesuch wurde eingereicht am: 08.03.2011

Die Arbeit wurde angeleitet von: Dr. S. Sprunck

Prüfungsausschuss:

Prof. Dr. W. Tanner (Vorsitzender)

Prof. Dr. T. Dresselhaus

Prof. Dr. H. Tschochner

Prof. Dr. F. Sprenger

TABLE OF CONTENTS

1 SUMMARY

During double fertilization of angiosperms, the two sperm cells are transported conjointly to the female gametophyte, where one sperm cell fuses with the egg cell and the other sperm cell with the central cell. These fusions have to take place in a controlled manner to avoid undesired gamete fusion events and prevent polyspermy. Only little is known about gamete recognition and coordination of gamete fusion in plants. The aim of this work was to characterize the function of the *Arabidopsis* egg cell-expressed *EGG CELL 1* (*EC1*) gene family during gamete recognition and to identify putative interaction partners. The *EC1* gene family comprises five members that encode cysteine-rich proteins, which are secreted from the egg cell during fertilization. Triple knockout mutants were additionally transformed with an RNAi construct targeting the remaining two genes. In these plants ($ec1^{+/-}$) the fusion of the sperm cells with the female gametes was impaired resulting in a reduced seed set.

Detailed analyses of $ec1^{+/-}$ plants showed that in 45% of the ovules of $ec1^{+/-}$ plants sperm cells did not fuse with the female gametes and that non-fused sperm cells were always observed as pairs, which indicated that EC1 might function in sperm cell separation. This hypothesis was supported by the observation that single sperm cells of mutant pollen seemed to be able to fuse in *ec1* ovules. With the aim to identify interaction partners of EC1, a pollen cDNA library was screened using a yeast-two-hybrid approach. Two putative interactors were found: (i) a protein containing two ubiqutin-like (UBL) domains (UbDKγ3), which is probably involved in substrate delivery to the 26S proteasome and (ii) a regulatory subunit of the Phosphatase 2A (PP2A B'θ). The putative interaction with a PP2A subunit and predicted phosphorylation sites at the C-terminus of EC1 indicated that phosphorylation might play a role in EC1. The transient expression of a phospho-mimicking variant of *EC1* fused to *eGFP* in *N. benthamiana* leaves was more stable, i.e. showed fluorescence, compared to the wild type form of EC1. Moreover, a proteasome inhibitor experiment with plants expressing *EC1.1* fused to *eGFP* under control of the *35S* promoter suggested that misexpressed *EC1* is rapidly degraded via the ubiquitin-proteasome pathway. Based on these findings, it was hypothesized that the pollen tube delivers the regulatory subunit of PP2A, which triggers dephosphorylation of the secreted EC1 and

thereby marks it for degradation. This was supported by the observation that misexpressed *PP2A B'θ* in the synergid cell partially phenocopied the *ec1* phenotype.

This work shows that EC1 is essential during double fertilization probably for gamete recognition or sperm cell separation. After fertilization and in all other cells, EC1 is unstable, its degradation is highly regulated and any protein accumulation is avoided.

2 ZUSAMMENFASSUNG

Während der Doppelten Befruchtung bei Angiospermen werden die zwei Spermazellen als Einheit zum weiblichen Gametophyten transportiert, wo eine der Spermazellen mit der Eizelle und die andere mit der Zentralzelle fusioniert. Diese Zellfusionen müssen kontrolliert ablaufen, um ungewollte Fusionen zu verhindern und um Polyspermie zu vermeiden. In Pflanzen ist nur wenig über Gametenerkennung und die Koordinierung der Gametenfusion bekannt. Ziel dieser Arbeit war die funktionelle Charakterisierung der eizell-spezifisch exprimierten Genfamilie *EGG CELL 1* (*EC1*) aus *Arabidopsis* während der Gameteninteraktion und die Identifizierung putativer Interaktionspartner. Die *EC1* Genfamilie umfasst fünf Mitglieder, die cysteinreiche Proteine kodieren, welche während der Befruchtung von der Eizelle sekretiert werden. Dreifachmutanten wurden zusätzlich mit einem RNAi-Konstrukt transformiert, das gegen die übrigen zwei Gene gerichtet ist. In diesen Pflanzen ($ec1^{+/-}$) war die Fusion der Spermazellen mit den weiblichen Gameten beeinträchtigt was sich in einem verringerten Samenansatz äußerte.

Detailierte Analysen der $ec1^{+/-}$ Pflanzen ergaben, dass in 45% der Samenanlagen die Spermazellen nicht mit den weiblichen Gameten fusionierten, und dass nicht-fusionierte Spermazellen immer als Paare beobachtet wurden. Dies deutete darauf hin, dass EC1 an der Trennung der Spermazellen beteiligt sein könnte. Diese Hypothese wurde durch die Beobachtung gestützt, dass einzelne Spermazellen einer Mutante in der Lage zu sein schienen mit einem der weiblichen Gameten in *ec1* Samenanlagen zu fusionieren. Mit dem Ziel Interaktionspartner zu identifizieren, wurde ein Screen einer Pollenschlauch cDNA-Bank mittels Hefe-2-Hybrid System durchgeführt. Zwei putative Interaktionspartner wurden identifiziert: (i) ein Protein, das zwei Ubiquitin-ähnliche (UBL) Domänen enthält (UbDKγ3), welches vermutlich bei der Substratübergabe an das 26S Proteasom eine Rolle spielt und (ii) eine regulatorische Untereinheit der Phosphatase 2A (PP2A B'θ). Die mögliche Interaktion mit der PP2A Untereinheit und vorhergesagte Phosphorylierungsstellen am C-Terminus von EC1 deuteten darauf hin, dass Phosphorylierung eine Rolle bei EC1 spielen könnte. Die transiente Expression einer phospho-mimicking Variante von *EC1* fusioniert mit *eGFP* war stabiler, d.h. zeigte Fluoreszenz, im Gegensatz zur Wildtypform von EC1. Desweiteren ließen

Proteasom-Inhibitor Experimente mit Pflanzen, die *EC1.1-eGFP* unter Kontrolle des *35S* Promotors exprimieren, darauf schließen, dass missexprimiertes *EC1* rasch über den Ubiquitin-Proteasom-Weg abgebaut wird. Auf diesen Ergebnissen basierend wurde die Hypothese aufgestellt, dass der Pollenschlauch die regultorische Untereinheit B'θ der PP2A anliefert, welche dann die Dephosphorylierung des sekretierten EC1 auslöst und dieses dadurch gleichzeitig für den Abbau markiert. Dies wurde duch die Beobachtung bestätigt, dass Missexpression von *PP2A B'θ* in den Synergiden zu einem *ec1*-ähnlichen Phänotyp führte.

Diese Arbeit zeigt, dass EC1 während der Doppelten Befruchtung essentiell ist, vermutlich für die Gametenerkennung oder für die Trennung der Spermazellen. Nach Befruchtung oder in allen anderen Zellen ist EC1 instabil, der ist Abbau streng reguliert und jegliche Akkumulation von Protein wird verhindert.

3 INTRODUCTION

The lifecycle of higher plants alternates between a multicellular, diploid sporophyte and a multicellular, haploid gametophyte (Figure 1). In flowering plants (angiosperms), the major part of the plant body is represented by the sporophyte whereas the gametophytic generations are highly reduced. The sporophyte produces the flower, in which specialized cells undergo meiosis and develop haploid male and female spores that differentiate into the male and female gametophyte, respectively (Figure 1, red background).

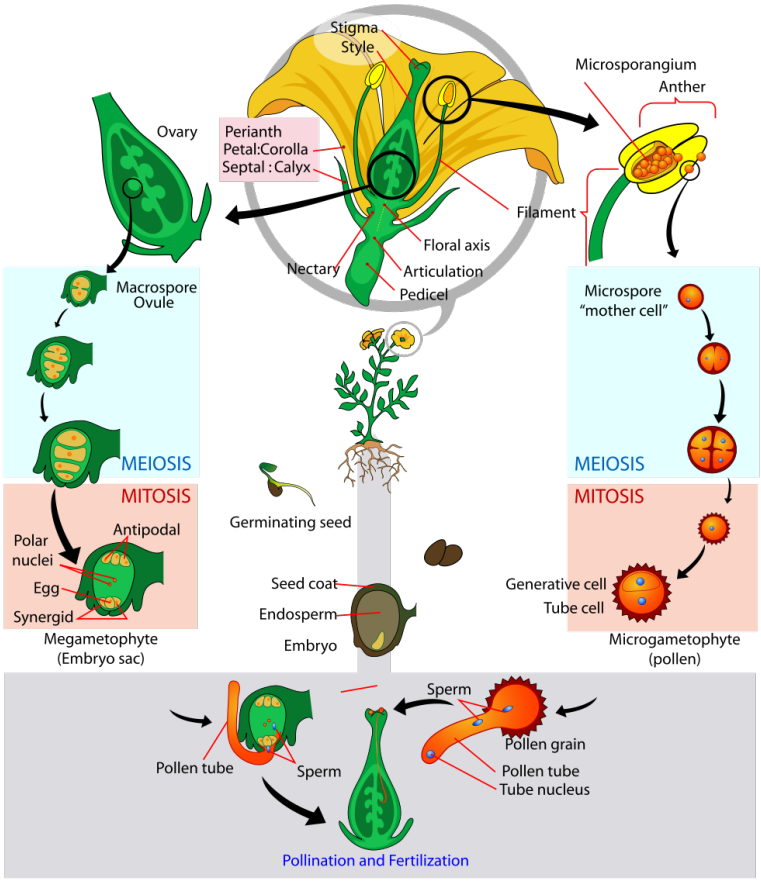

Figure 1: Schematic representation of the life cycle of a flowering plant.
The diploid sporophyte (white background) develops flowers that contain female and male reproductive organs. The female organ (carpel) contains the ovary that encloses one or more ovules in which meiosis takes place. In the anthers of the male organ (stamen) the pollen mother cell differentiates, which undergoes meiosis. The haploid products of meiosis enter several rounds of mitosis resulting in the mature gametophytes, the embryo sac and the pollen grain (red background). The gametes contained in the gametophytes are unified during fertilization (grey background) giving rise to the next diploid generation. Image taken from **www.wikipedia.org**

The major function of the gametophytes is to produce the gametes. In angiosperms, two male gametes, the sperm cells, and two female gametes, the egg and the central cell are produced, both of each participating in the angiosperm characteristic double fertilization. The fusion of sperm and egg cell giving rise to the diploid zygote completes the lifecycle (Figure 1, grey background). From the zygote the embryo develops within the seed and is nurtured by the endosperm, which represents the second fertilization product.

3.1 Development of the male gametophyte

The development of the male gametophyte (pollen grain) takes place in the anther, which is part of the stamen, the male reproductive organ. Male gametophyte development is divided into microsporogenesis and microgametogenesis. During microsporogenesis the diploid pollen mother cell, also called microspore mother cell, undergoes meiosis producing a tetrad of haploid microspores. These haploid microspores are released from the tetrad and develop further into the mature male gametophyte, a developmental process that is called microgametogenesis. The microspores enlarge and polarize before they undergo the first mitosis, which is an asymmetric cell division and is called Pollen Mitosis I (PMI). The daughter cells consist of one large, vegetative cell and the smaller germ cell, representing the male germline. After PMI, the germ cell is engulfed within the cytoplasm of the larger vegetative cell. Some plant species including *Arabidopsis* shed tricelluar pollen. In these species the germ cell undergoes another division, Pollen Mitosis II (PMII), generating the two sperm cells. In most angiosperms however, the pollen is bicellular at anthesis. In these plants, PMII takes place in the growing pollen tube, which is formed by the vegetative cell (reviewed by Borg *et al*., 2009; Borg and Twell, 2010).

3.2 Development of and cell specification in the female gametophyte

The female gametophyte (embryo sac) develops within the ovule, which is located in the ovary and comprises the two phases of megasporogenesis and megagametogenesis, comparably to the development of the male gametophyte. Different types of patterning in the female gametophyte have been observed. The Polygonum-type, first observed in *Polygonum divaricatum*, occurs in most species (Strasburger, 1879; Maheshwari, 1950).

The Polygonum-type female gametophyte results after three rounds of nuclear divisions in a seven-celled structure with four distinct cell types. During megasporogenesis a cell from the nucellus (archesporial cell) differentiates into the megaspore mother cell (MMC, Figure 2A), which undergoes meiosis giving rise to four haploid megaspores (tetrad, Figure 2B). One of these megaspores develops into the functional megaspore, the remaining three megaspores undergo programmed cell death (Figure 2C). In the Polygonum-type of female gametophytes, the functional megaspore undergoes three rounds of nuclear divisions (mitosis without cytokinesis) resulting in a coenocyte with eight nuclei at distinct positions of the female gametophyte (Figure 2E, FG5, FG6).

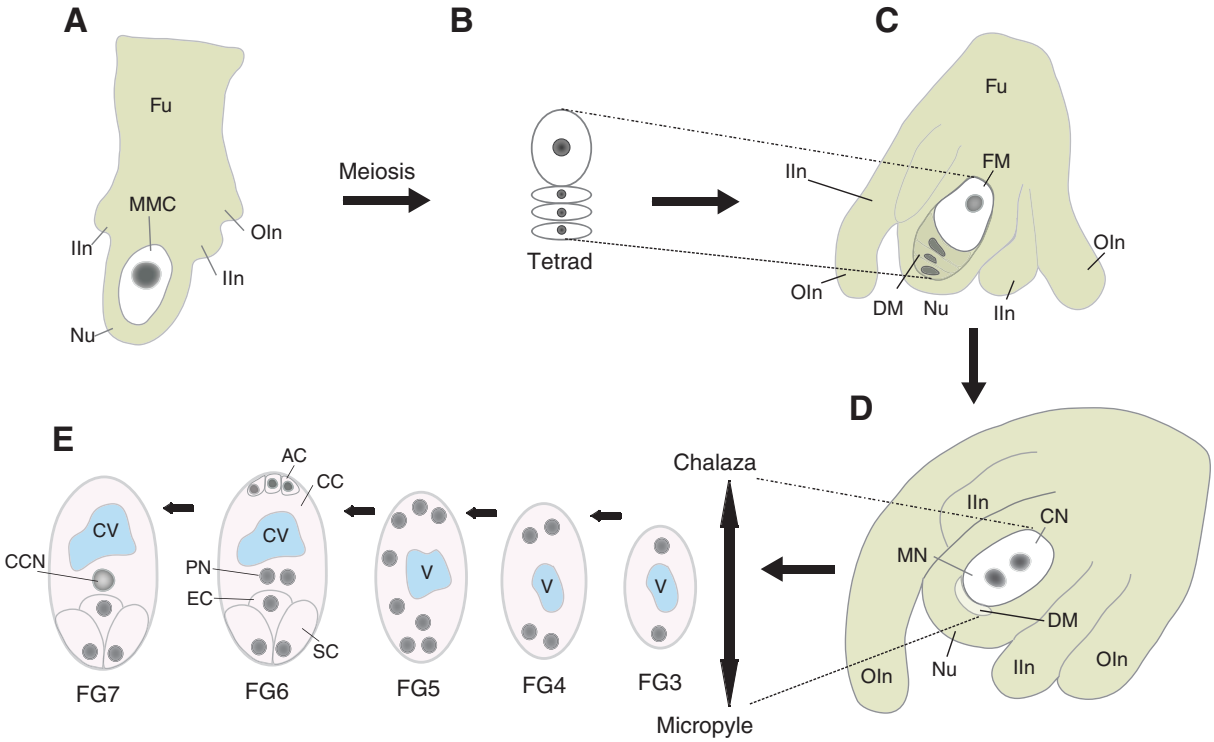

Figure 2: Development of the *Arabidopsis* female gametophyte, schematic representation.
A Ovule primordium: initiation of the formation of outer (OIn) and inner integuments (IIn); archesporial cell within the nucellus (Nu) differentiates into megaspore mother cell (MMC); Fu = funiculus: connection to the septum. **B** Megaspore mother cell undergoes meiosis generating a tetrad of four haploid megaspores. **C** FG1 stage: Three of the megaspores undergo programmed cell death (DM = degenerated megaspores); the integuments continue to grow around the female gametophyte. **D** FG2 stage: after the first mitotic division of the FM the female gametophyte comprises two nuclei, the chalazal nucleus (CN) and the micropylar nucleus (MN). **E** After migration of the CN and MN to the chalazal and the micropylar pole, respectively, a large vacuole is formed in the center (v) (FG3). After two more rounds of nuclear divisions the female gametophyte contains eight nuclei (FG5). After cellularization (FG6) the female gametophyte consists of seven cells: One egg cell (EC) and two synergid cells (SC) at the micropylar pole, one central cell carrying two polar nuclei (PN) and a large central vacuole (CV) and three antipodal cells (AC) at the chalazal pole. In the mature female gametophyte, prior to fertilization (FG7), the polar nuclei have fused to form the central cell nucleus (CCN) and the antipodal cells degenerate. Image taken form Sundaresan and Alandaete-Saez, 2010.

After nuclei migration and cellularization, the female gametophyte contains seven cells: one egg cell and two synergid cells at the micropylar end, two polar nuclei forming the diploid central cell and three antipodal cells at the chalazal pole (Figure 2E). In *Arabidopsis*, the antipodal cells degenerate prior to fertilization. At this developmental stage, the integuments have enlarged and completely surround the female gametophyte except for a small part. Through this opening, called the micropyle, the pollen tube will grow to deliver the two sperm cells during fertilization (reviewed by Yang *et al*., 2010; Sprunck and Gross-Hardt, 2011).

3.3 Early and late events during double fertilization

The major function of the male and the female gametophytes is to produce the gametes and enable their unification during double fertilization. The first step during fertilization is pollination. After a compatible pollen grain has landed on a stigma, adhesion of the pollen grain to a receptive stigma cell and hydration is required for the initiation of pollen tube growth (Figure 3A, 1). Some species are self incompatible, like the *Brassica* species. In these species, self-pollen is rejected and prevented from hydration and germination. Proteins on the pollen coat (S locus cysteine-rich protein, SCR) and on the stigma surface (S locus receptor kinase, SRK) are the main determinants that mediate the incompatibility response. The *Brassica* sporophytic self incompatibility (SSI) system has been studied for years and is currently the probably best understood SI system (reviewed by Fobis-Loisy *et al*., 2004).

After successful hydration, pollen tube growth is initiated. The tip growing pollen tube navigates through the stigma and the style until it reaches the transmitting tract of the ovary (Figure 3A, 2). At some point during the journey the pollen tube changes its direction and grows along the funiculus towards the ovule (Figure 3A, 3+4). Thus, the growth of the pollen tube occurs in a directed manner. A couple of molecules have been identified that mediate the so-called pollen tube guidance. Some molecules important during the sporophytic phase of pollen tube guidance (Figure 3A, 2) have been identified, like for example the arabinogalactan protein TTS from tobacco (Cheung *et al.*, 1995) or chemocyanin, a small basic protein from lily (Kim *et al.*, 2003). In *Arabidopsis*, γ-amino butyric acid (GABA) (Palanivelu *et al.*, 2003) and nitric oxide (NO) signaling have been shown to play a role (Prado *et al.*, 2004; Prado *et al.*, 2008).

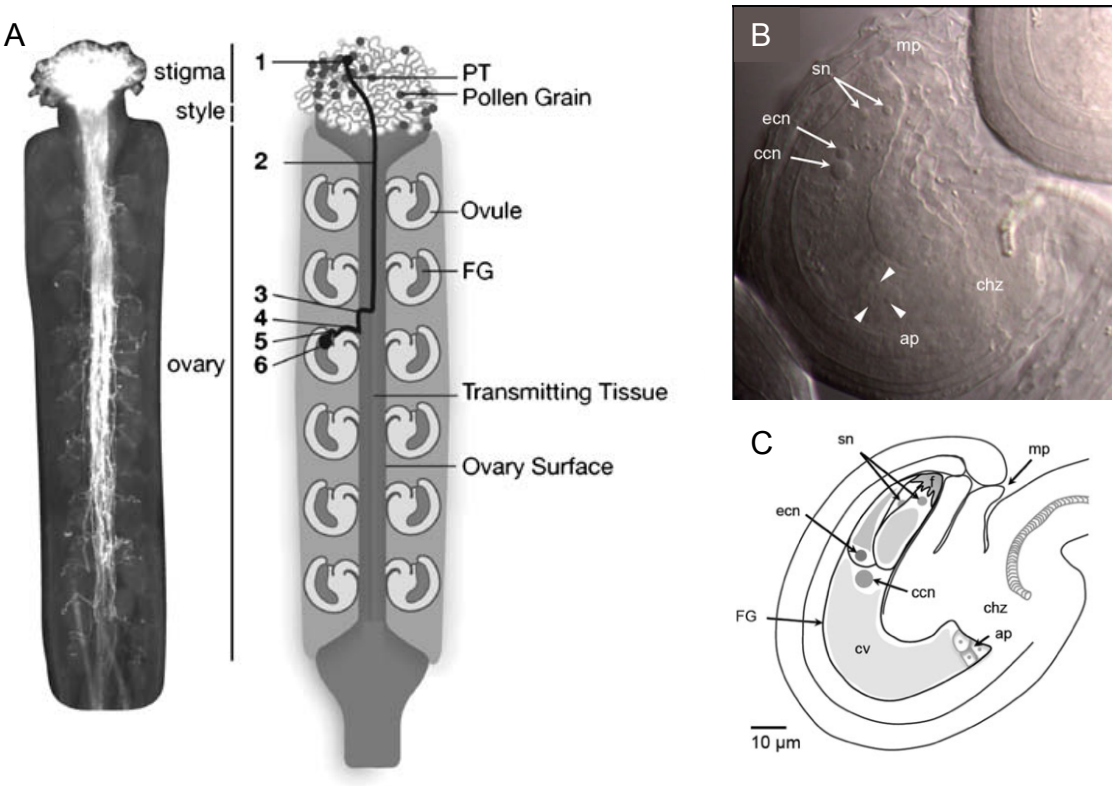

Figure 3: Schematic representation of steps during double fertilization in *Arabidopsis* and structure of the mature ovule.
A Phases of pollen tube guidance. Left: *Arabidopsis* pistil showing the pollen tube path by aniline blue staining; Right: Schematic drawing**. 1** Pollen lands on stigma, pollen tube grows and penetrates the stigmatic tissue. **2** Growth through the transmitting tract. **3** Exit from transmitting tissue. **4** Funicular guidance. **5** Micropylar guidance. **6** Pollen tube reception (A: taken from Johnson and Lord, 2006). **B** DIC microscopy image of a mature *Arabidopsis* ovule. **C** Schematic representation of the mature female gametophyte (FG) of *Arabidopsis* showing the four cell types: egg cell, synergid cell, central cell and antipodal cells. Abbreviations: ap = antipodal cells; ccn = central cell nucleus; chz = chalaza; cv = central vacuole; ecn = egg cell nucleus; f = filiform apparatus; mp = micropyle; sn = synergid nucleus. (B + C: taken from Sprunck and Gross-Hardt, 2011).

In contrast to the early phase of pollen tube guidance, in which the signals are derived from the sporophyte, the signals for funicular (Figure 3A, 4) and micropylar guidance (Figure 3A, 5) are produced by the female gametophyte. Over the past years, considerable progress has been made in identifying genes and proteins involved in the last steps of pollen tube guidance. Recently, the two K^+ transporters CHX21 and CHX23 have been identified as candidates for perception of female gametophytic signals during these phases of pollen tube guidance. *chx21 chx23* pollen tubes grow down the transmitting tract but fail to change their growth direction towards the ovule and to grow along the funiculus. CHX23 co-localizes with ER markers in the pollen tube and may play a role in K^+ and/or H^+ homeostasis. The authors hypothesized that CHX21 and CHX23 play a role in perception of funicular and micropylar guidance signals by affecting membrane trafficking to the tube apex (Lu *et al.*, 2011). Moreover,

two *Arabidopsis* mutants with defective micropylar pollen tube guidance have been described. The *magatama* (*maa*) mutants *maa1* and *maa3*, of which the latter encodes a helicase, show a pollen tube guidance effect. The pollen tubes are normally attracted towards the ovule but fail to enter the micropyle (Shimizu and Okada, 2000; Shimizu *et al.*, 2008). A similar phenotype was observed in *hapless 2* (*hap2*) mutants. In addition to defects in gamete fusion, the loss of *GCS1*/*HAP2* leads to defective micropylar pollen tube guidance. Interestingly, *GCS1*/*HAP2* is specifically expressed in sperm cells indicating an active role of the male gametes in their delivery to the female gametes (von Besser *et al.*, 2006). Higashiyama *et al*. (2001) found already ten years ago, that the synergid cell has the key role in final pollen tube attraction to the female gametophyte (Figure 3A, 5). Single cells of the naked female gametophyte of *Torenia fournieri* were ablated by a laser. These experiments showed that at least one intact synergid cell is needed to attract the pollen tube and that the egg cell and the central cell are not necessary for pollen tube attraction in *Torenia* (Higashiyama *et al.*, 2001). In the last years molecules from different species have been identified that are secreted by the female gametophyte to attract pollen tubes. The maize *EGG APPARATUS 1* (*EA1*) is expressed in the egg cell and the synergid cell and encodes a 94 amino acid protein, which is secreted into the cell walls of the nucellus cells at the micropylar region. Down-regulation of *EA1* results in loss of micropylar pollen tube guidance, i.e. pollen tubes fail to enter the embryo sac (Márton *et al.*, 2005). Moreover, it was shown that the predicted mature EA1 protein directly attracts maize pollen tubes *in vitro* (Márton and Dresselhaus, 2010). Similarly, the defensin-like LURE proteins have been identified as chemoattractants in *Torenia fournieri* (Okuda *et al.*, 2009).

After successful targeting to the micropylar opening, the pollen tube enters the female gametophyte, stops its growth and bursts to release the two sperm cells (Figure 3A, 6). The receptor-like kinase FERONIA (FER) from *Arabidopsis* has been identified in a genetic screen for mutants where the reception of the pollen tube was affected (Huck *et al.*, 2003). After entering a *fer* female gametophyte, pollen tubes fail to arrest and thus continue to grow. Consequently, double fertilization cannot take place. Besides vegetative tissues, *FER* is expressed in the synergid cells and the encoded plant-specific *Catharanthus roseus* Receptor-Like Kinase 1-Like (CrRLK1L) is polarly localized in the synergid plasma membrane at the filiform apparatus. Crossing experiments with *Arabidopsis thaliana* and different *Brassicaceae* species indicated that FER-mediated pollen tube reception acts as a reproductive isolation barrier (Escobar-Restrepo *et al.*,

2007). Similar to *fer*, pollen tubes fail to arrest in *abstinence by mutual consent* (*amc*) and *lorelei* (*lre*) mutants (Boisson-Dernier *et al.*, 2008; Capron *et al.*, 2008). *LRE* is predominantly expressed in the synergid cell and encodes a small, putatively glucosylphosphatidylinositol (GPI)-anchored protein. In contrast to *feronia*, the majority of synergid cells in *lorelei* mutants do not degenerate after pollen tube entry (Capron *et al.*, 2008; Tsukamoto *et al.*, 2010). Similarly, synergid cells do also not degenerate in the *amc* mutant. However, in *amc,* the phenotype of overgrowing pollen tubes only occurs when an *amc* pollen tube grows into an *amc* female gametophyte (Boisson-Dernier *et al.*, 2008). In *Arabidopsis* it was observed that only after direct interaction with the pollen tube, the synergid degenerates (Sandaklie-Nikolova *et al.*, 2007). In other species however, synergid cell death is triggered by pollination (Van Went and Willemse, 1984; Willemse and Van Went, 1984; Russell, 1992).

Over the past years, two proteins have been identified, one of which appears to inhibit premature pollen tube burst before arrival at the synergid cell and the other one induces pollen tube burst allowing discharge of the sperm cells. The *FERONIA* homologs *ANXUR 1* (*ANX1*) and *ANX2* are preferentially expressed in pollen. The respective proteins function redundantly and are localized at the plasma membrane at the tip of the pollen tube. *In vivo*, the majority of *anx1 anx2* pollen tubes stops growth in stigma and style tissues and fail to grow to the female gametophyte (Miyazaki *et al.*, 2009). *In vitro* experiments showed that the disruption of *ANX1* and *ANX2* results in pollen tube burst indicating a role of ANX1 and ANX2 in the timing of pollen tube growth, i.e. inhibition of burst until the pollen tube has reached the female gametophyte (Boisson-Dernier *et al.*, 2009; Miyazaki *et al.*, 2009). Recently it was proposed that ANX1 and ANX2 act as male counterparts of synergid cell-expressed *FER* and that these CrRLKL proteins may play a role in controlling cell wall integrity of the pollen tube tip (Boisson-Dernier *et al.*, 2011). In maize, the synergid cell-expressed *EMBRYO SAC 4* (*ES4*) is essential for gamete delivery. Experiments using a chemically synthesized peptide showed that ES4 induces pollen tube burst *in vitro* in a species dependent manner. This mechanism is induced by the ES4-mediated opening of the potassium channel KZM1 (Amien *et al.*, 2010).

In addition to pollen tube guidance, reception and burst, the synergid cells may also play a role in transporting the two non-motile sperm cells to the site of fusion with the egg and central cell. After pollination, the actin network of the receptive synergid cell reorganizes at the chalazal end and contributes to the formation of an intercellular actin

corona, which is suggested to mediate sperm cell transport to the future fusion site (Huang *et al.*, 1999). Interestingly, on the surface of lily sperm cells, myosin I as been found as a counterpart of actin (Miller *et al.*, 1995) and would thus provide the necessary motive force.

3.4 Gamete interaction

Gamete interaction is a fundamental process in all eukaryotes, nevertheless only little is known about molecular players participating in this process. Some important proteins for gamete recognition and fusion have been identified in mammals (Nixon *et al.*, 2007; Primakoff and Myles, 2007). Here, the egg cell expresses *CD9*, which encodes a member of the tetraspanin superfamily. These proteins are characterized by four transmembrane domains and short, intracellular N- and C- termini. The molecular mechanism of CD9 function is still unclear, but it is discussed to be involved in a binding step or membrane mixing of gametes. Moreover, GPI-anchored proteins appear to be important for gamete fusion. *Pig-a* encodes the first enzyme in the biosynthetic pathway of the GPI-anchor. Female mice with an egg cell-specific knockout of *Pig-a* are infertile. A putative role for GPI-anchored proteins is in establishment or maintenance in specific lipid microdomains of the plasma membrane. However, until now there is no experimental evidence. *IZUMO* is testis-specifically expressed and encodes an immunoglobulin superfamily (IgSF) type I transmembrane protein with one extracellular domain that is essential for gamete fusion in mammals. A member of the epididymal produced cysteine-rich secretory proteins (CRISPs), called DE or CRISP-1, is tightly associated with the sperm plasma membrane but also binds to the fusogenic region of the egg cell and may be essential for fertilization. Other possible players in mammalian gamete recognition and fusion of the sperm cell may be the ADAM (A Disintegrin And Metalloprotease) family of integral membrane proteins (Rubinstein *et al.*, 2006). Most of the putative players have been identified by means of monoclonal antibodies that inhibit egg-sperm fusion. However, for some of the candidates the exact function remains to be determined.

In plants the situation is even more elusive (Sprunck, 2010); only one protein has been described that seems to be essential for gamete fusion. The *GENERATIVE CELL SPECIFIC 1/HAPLESS 2 (GCS1/HAP2)* gene form *Arabidopsis* is specifically expressed in sperm cells and encodes a protein with an extracellular N-terminus, which

is indispensible for gamete interaction, one transmembrane domain and a histidine-rich C-terminus. Mutant *gcs1* sperm cells are delivered to the female gametophyte but fail to fuse with the egg and the central cell (Mori *et al.*, 2006; von Besser *et al.*, 2006; Mori *et al.*, 2010). However, direct participation of GCS1 in the membrane fusion step has not been shown in *Arabidopsis* gametes.

Orthologs of *GCS1* have also been identified in red and green algae and in the malaria parasite *Plasmodium* (Mori *et al.*, 2006). In *Plasmodium* and *Chlamydomonas*, it could be shown that GCS1 is directly involved in membrane fusion after the membrane merger during gamete interaction (Hirai *et al.*, 2008; Liu *et al.*, 2008). In addition to GCS1, the surface protein P48/45 of the 6-cys family from *Plasmodium* has a central role in fertilization. The 6-cys family seems to be *Apicomplexan* specific and encodes proteins with a double six-cysteine domain. The P48/45 protein is present on the surface of male and female gametes, however only the male P48/45 knockout gametes are affected during fertilization, being unable to attach to or penetrate female gametes (van Dijk *et al.*, 2001). Recently, other members of the 6-cys family in addition to P48/45 have been identified, termed P230 and P47. Similar to P48/45, P230 is essential for male fertility, whereas P47 plays a role in female gamete fertility. In knockout mutants of P230 and P47 the attachment of *Plasmodium* gametes is disturbed. The failure of gamete attachment in 6-cys family mutants indicates that these proteins function upstream of GCS1, which is essential for gamete fusion (van Dijk *et al.*, 2010).

3.5 The versatile roles of small cysteine-rich proteins

Small, cysteine-rich proteins (CRPs) play key roles in diverse mechanisms of cell-cell communication during development and plant reproduction (Higashiyama, 2010; Marshall *et al.*, 2011). Common features of these proteins are a small size of less than 160 amino acids, an N-terminal region with a signal peptide for secretion and a C-terminal part containing 4 to 16 cysteine residues (Marshall *et al.*, 2011). However, not many pairs of receptors and cysteine-rich proteins as ligands have been identified so far.

Root growth and development involve CRP-mediated signaling. The class of cysteine-rich Rapid Alkalinization Factor (RALF) proteins has been shown to negatively influence root growth (Pearce *et al.*, 2001) and probably also plays a role in other plant developmental aspects. RALF proteins are named after their ability to induce alkalinization of the medium in cell suspension cultures by binding to a cell surface

receptor and inhibiting a membrane bound H^+-ATPase. Besides, the process of stoma patterning and differentiation also seems to involve CRPs as signaling molecules. *EPIDERMAL PATTERNING FACTOR 1* (*EPF1*) and *EPF2* are expressed in stomatal precursor cells and negatively regulate stomata development (Hara *et al.*, 2007; Hara *et al.*, 2009). It is suggested that EPF signals are perceived by receptor-like kinase TOO MANY MOUTHS (TMM) and receptor kinases of the ERECTA (ER) family, that are critical for proper patterning and differentiation of stomata (Shpak *et al.*, 2005). Recently, the cysteine-rich protein STOMAGEN has been identified as positive regulator of stomata development (Sugano *et al.*, 2010).

In plant defense mechanisms, cysteine-rich proteins of the defensin and defensin-like class play important roles. First hints that defensins induce a pathogen response by affecting ion fluxes at the fungal membrane were obtained by works with *Neurospora crassa* and an anti-fungal peptide from radish (Terras *et al.*, 1992a; Terras *et al.*, 1992b). CRPs are not only involved in plant defense but also in symbiosis between plant and bacteria. Scheres *et al*. (1990) found that in pea the two genes encoding the cysteine-rich peptides ENOD3 and ENOD14 are expressed exclusively during nodulation and are important for the interaction of nitrogen fixing bacteria and the host plant. Also in the leguminous plant *Medicago truncatula* a number of nodule-specific CRPs have been identified (Mergaert *et al.*, 2003).

In addition to roles in developmental processes and plant-microbe interaction, CRPs are also involved in various steps of plant reproduction (Figure 4) (Higashiyama, 2010; Marshall *et al.*, 2011). As described in section 3.3, among the S-locus proteins there is one CRP, called SCR (Schopfer *et al.*, 1999) or SP11 (Suzuki *et al.*, 1999) playing an important role as the male determinant in the self-incompatibility response. Contrarily, in poppy, the female determinant of SI encodes a CRP named *Papaver rhoeas* stigma S-determinant (PrsS) (Foote *et al.*, 1994; Wheeler *et al.*, 2009). In tomato, receptor-ligand pairs with LRRs as receptors and CRPs as ligands have been identified that are essential for pollen germination and fertilization. *Lycopersicon esculentum* Pollen-specific Receptor Kinase 1 (LePRK1), LePRK2 and LePRK3 bind, among other CPRs, the pollen-specific, LAT52, which is a small CRP of the Kunitz trypsin inhibitor class, and the stigma-expressed *LeSTIG1* (Muschietti *et al.*, 1994; Tang *et al.*, 2004). From lily, a CRP of the lipid-transfer protein class called Stigma/style Cysteine-rich Adhesion (SCA) has been isolated that mediates the adhesion of the pollen tube wall to the epidermis cells of the transmitting tract (Mollet *et al.*, 2000; Park *et al.*, 2000). The

defensin-like LURE proteins secreted from synergid cells in *Torenia fourinieri* have been shown to be essential for the final step of micropylar pollen tube guidance (Okuda *et al.*, 2009). Moreover, defensin-like proteins are also involved in pollen tube burst. Similar to mechanisms in pathogen defense, the ES4 protein of maize leads to changes in ion fluxes by mediating the opening of the potassium channel KZM1, which causes pollen tube burst (Amien *et al.*, 2010). Additionally, CRPs play a role after fertilization in seed development. In maize, CRPs have been identified that are specifically expressed in distinct domains of the endosperm like *AE1*, *BAP* and *ZmESR-6* that may regulate the transfer of nutrients to the developing embryo (Magnard *et al.*, 2000; Serna *et al.*, 2001; Balandin *et al.*, 2005). Moreover, the paternally imprinted *MATERNALLY EXPRESSED 1* (*MEG1*) from maize, which is endosperm transfer cell-specifically expressed and important for the correct development of these cells might function in nutrient trafficking from the maternal tissue into the developing seed (Gutierrez-Marcos *et al.*, 2004; Marshall *et al.*, 2011).

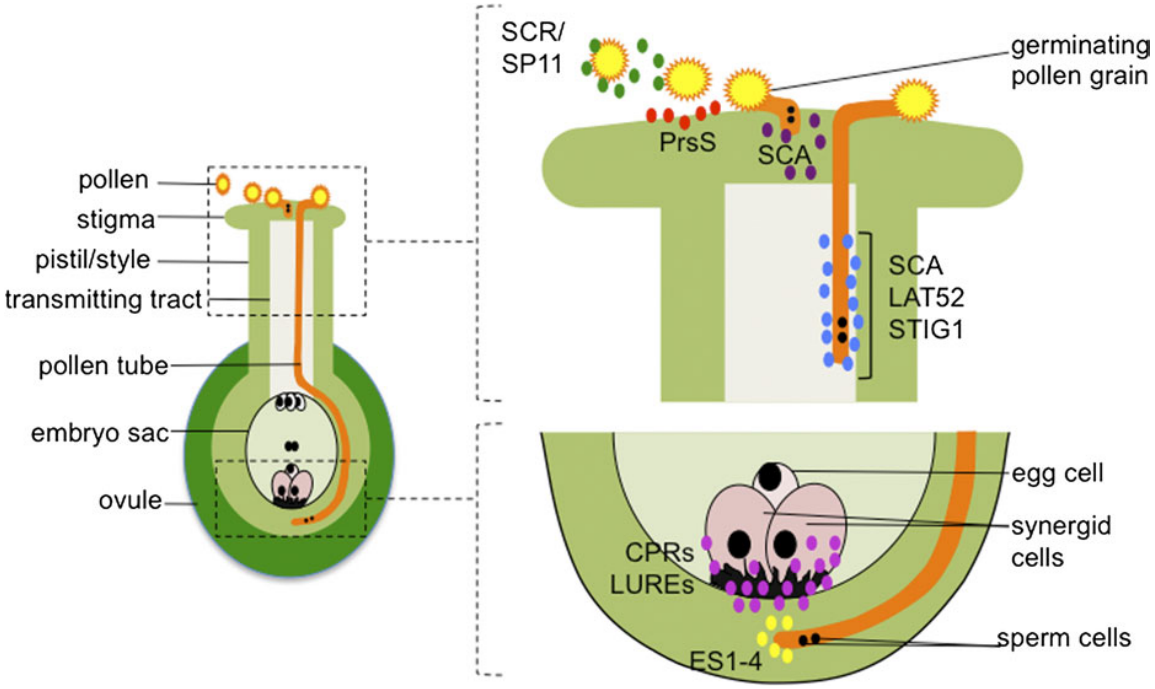

Figure 4: Schematic drawing showing cysteine-rich proteins (CRPs) involved in cell-cell communication during reproduction.
Left side: Pollination of an ovary (schematic drawing). Right side, top image: CRPs involved in pollen-stigma interaction, pollen germination and pollen tube growth are illustrated. Right side, bottom image: CRPs that play a role in male and female gametophyte interactions are shown. Image taken from Marshall *et al.*, 2011.

3.6 Identification of the *EGG CELL 1* gene family

The egg cell-specific gene family encoding *Triticum aestivum* EGG CELL 1 (TaEC1) was found as the largest cluster of expressed sequence tags (ESTs) in a cDNA library of isolated egg cells from wheat (Sprunck *et al.*, 2005). In BLAST searches a gene family comprising five members was identified that encode EC1 homologous proteins in *Arabidopsis thaliana*. One gene is located on chromosome 1 and was therefore named *AtEC1.1*, two genes in tandem on chromosome 2 (*AtEC1.2a* and *AtEC1.2b*), one on chromosome 4 (*AtEC1.4*) and one on chromosome 5 (*AtEC1.5*). The proteins encoded by the *EC1* genes have a predicted N-terminal signal peptide for secretion and a conserved pattern of six cysteine residues in the middle part. The C-terminus is more variable and contains numerous predicted phosphorylation sites.

Several approaches were taken to analyze, whether this gene family also shows egg cell specific expression in *Arabidopsis*: (i) *EC1* promoter activities were analyzed in transgenic plants driving the expression of the reporter gene *β-glucuronidase* (*GUS*) or of a nuclear localized *eGFP*, (ii) mRNA of *EC1.1*, *EC1.2a* and *EC1.5* was detected using *in situ* hybridization and (iii) *Arabidopsis* plants expressing a fusion of *eGFP* and the *EC1.1* coding sequence under control of the *EC1.1* promoter were analyzed regarding protein localization. The results showed an egg cell-specific expression for the *Arabidopsis EC1* gene family and a rapid loss of transcriptional activity after fertilization.

Detailed analyses of ovules expressing *EC1.1* fused to *eGFP* under control of the endogenous promoter showed that the fusion protein is located in vesicle-like structures in mature egg cells before fertilization. However, this pattern changes during fertilization. The fusion protein appears to be secreted at the site where fusion of egg cell and sperm cell will take place. The secretion of EC1 is probably triggered by pollen tube reception or burst (S. Sprunck, unpublished observation).

To study the function of the *EC1* gene family, T-DNA insertion lines were analyzed. Single knockout lines of *EC1.1*, *EC1.4* and *EC1.5* as well as double and triple mutants did not display any phenotype regarding seed set. To achieve a knockdown of the entire gene family an RNAi construct was generated targeting *EC1.2a* and *EC1.2b* simultaneously. In these plants, homozygous for the T-DNA insertion in *EC1.1*, *EC1.4* and *EC1.5* and heterozygous for the RNAi construct, a reduced seed set of about 50% was observed. Pollination experiments with a sperm cell marker line (Ingouff *et al.*,

2007) and the analysis of Feulgen stained mutant ovules revealed that sperm cells are delivered into the female gametophyte but were still detectable 24 to 40 hours after pollination indicating a defect in gamete interaction.
(Sprunck, S., Rademacher, S., *et al*., in preparation)

3.7 Aims of this work

The *EC1* genes encode small cysteine-rich proteins. One goal of this thesis was to determine and evaluate the phylogenetic relation of the EC1 proteins to other members of the recently annotated and classified superfamily of CRPs in *Arabidopsis* (Silverstein *et al.*, 2007). Moreover, homologous proteins to EC1 in other species should be identified and subjected to bioinformatic analyses. Another objective of this thesis was to continue the characterization of the phenotype of *EC1* knockdown plants in detail. This included transmission analysis of the RNAi construct, dissection of the fertilization process, quantification of phenotypes and functional analyses by ectopic overexpression of *EC1* in vegetative tissues. With the aim to perform biochemical approaches, the *EC1* genes should be heterologously expressed and applied in bioassays to address the mechanistic role of EC1. To understand the molecular mechanism of EC1 function, another goal was to identify EC1-interacting proteins using the yeast-two-hybrid system. After verification of interaction, identified candidates should then be functionally characterized by analyzing knockdown mutants and overexpressing plants.

4 MATERIAL & METHODS

4.1 Standard molecular biology work

Standard methods of molecular biology were performed according to Sambrook *et al*. (1989) using molecular grade reagents.

4.2 Bioinformatic analyses

To gather general information about genes, nucleotide and protein sequences, The Arabidopsis Information Resource (TAIR, http://arabidopsis.org/) and the National Center for Biotechnology Information (NCBI, http://www.ncbi.nlm.nih.gov/) were consulted. For analysis of protein sequences, structures and proteomic tools, programs on the ExPASy page (Expert Protein Analysis System, http://expasy.org/) were used. For mass spectrometry (MS)-digest searches ProteinProspector was used (http://prospector.ucsf.edu/prospector/mshome.htm). To predict the subcellular localization of proteins TargetP (http://www.cbs.dtu.dk/ services/TargetP/) was used, for the prediction of signal peptide cleavage sites SignalP was used (http://www.cbs.dtu.dk/services/SignalP/) and putative serine, threonine and tyrosine phosphorylation sites in eukaryotic proteins were identified by NetPhos (http://www.cbs.dtu.dk/services/NetPhos/). For prediction of disulfide bond formation, DISULfind was used (http://disulfind.dsi.unifi.it/, Ceroni *et al*., 2006). For all prediction programs, standard settings were applied and, if possible, eukaryote or plant was chosen as organism group. *In silico* expression analysis were performed using Genevestigator (https://www.genevestigator.com/gv/index.jsp, Hruz *et al.,* 2008) or the Arabidopsis eFP Browser (http://bar.utoronto.ca/efp/cgi-bin/efpWeb.cgi, Winter *et al*., 2007). Vector NTI® 9.0.0 (Invitrogen) was used for *in vitro* cloning procedures.

For the construction of phylogenetic trees of CRP classes (Silverstein *et al.*, 2007), namely ECA1 gametogenesis related proteins and defensin-like proteins (DEFLs), the protein sequences were aligned using the multiple sequence alignment program ClustalW2 at the European Bioinformatic Institute (EBI) (http://www.ebi.ac.uk/ Tools/msa/clustalw2/). The output .dnd-file was saved and the deduced phylogenetic

tree was illustrated with PhyloDraw 0.8 software (Graphics Application Lab, Pusan National University).

The EC1.1 protein sequence was used as a query for the Basic Local Alignment Search Tool ("BLAST searches") to identify *EC1*-related genes in *Arabidopsis* (http://blast.ncbi.nlm.nih.gov/). The BLASTP algorithm was run on the non-redundant protein sequence (nr) collection of *Arabidopsis thaliana*. Similarly, for the identification of EC1 homologs in different plant species, BLASTP and TBLASTN searches were performed at different genome databases, namely the plant genome database (http://www.plantgdb.org/), the *Brachypodium distachyon* database, (http://www.brachypodium.org/) and the *Medicago truncatula* database, version MT3.0 (http://www.medicago.org/). All BLAST searches were performed with default settings. The corresponding nucleotide sequences of the identified proteins were downloaded and the alignment on the amino acid level was performed in SeaView 4.2.4 (Gouy *et al.*, 2010) using the muscle algorithm. For the construction of phylogenetic trees, the aligned sequences were imported to MEGA 4.1 and converted into the respective format (.meg). The phylogenetic trees based on nucleotide sequences were calculated using the Neighbor Joining (NJ) method treating gaps with Pairwise Deletion. To test the support of the relationship, the Bootstrap method with 10,000 replicates was applied. For illustration of the alignment GeneDoc 2.7.000 was used.

The BLAST searches to identify EC1 orthologs were performed from April to August 2010 and searches for EC1 related proteins were performed in the end of 2010.

4.3 Work with plants

4.3.1 Plant material and growth conditions

The *Arabidopsis thaliana* Columbia accession (Col-0) was used as wild type and for transformation. Seeds were put on soil (mixture of 65% substrate, 25% sand and 10% expanded clay), stratified at 4°C in the dark for two days and subsequently transferred into plant growth chambers under short day conditions with 8 hours light and 16 hours dark at 22°C and about 70% humidity. After four weeks, plants were transferred to long day chambers (16 hours light/8 hours dark) to induce flowering. Transformation of *Arabidopsis thaliana* plants was carried out using the floral dip method as previously described by Clough and Bent (1998). Plants transformed with the *bar* or *pat* gene

(Phosphinotricin-Acetyltransferase) as a selection marker conferring BASTA® resistance, were sprayed with BASTA® (Bayer Crop Science) with a concentration of 200 mg/l glufosinate ammonium supplemented with 0.1% Tween-20 three days after germination. Spraying was repeated three more times with an interval of two days. For growing plants under sterile conditions, seeds had to be surface sterilized. The desired amount of seeds was filled into a 1.5 ml reaction cup, incubated with 700 µl 70% ethanol for 3 min and repeatedly vortexed. After 15 sec of centrifugation ethanol was replaced by an aqueous solution containing 1% NaOCl and 0.1% Mucasol® (Merz Consumer Care GmbH). After 2 min incubation the seeds were centrifuged again for 15 sec. The seeds were washed by adding 1 ml of sterile H_2O, vortexed and subsequently centrifuged for 15 sec. This step was repeated four more times. The sterile seeds were dispersed in a sterile 0.1% agarose solution and sowed out on solid ½ x MS medium containing vitamins and MES buffer (Murashige & Skoog, Duchefa) prepared with 0.8% Phytagar (Duchefa). For selection of plants carrying the *hph* gene (Hygromycin B Phosphotransferase) as a selection marker, the medium was supplemented with 30 µg/ml Hygromycin. Seeds were stratified for two days at 4°C in the dark and then transferred to a short day plant growth chamber.

4.3.2 mRNA isolation and reverse transcriptase (RT)-PCR

For general expression analysis of genes in various tissues, mRNA was extracted directly and reversely transcribed into cDNA. For mRNA isolation, the Dynabeads® mRNA DIRECT™ Micro Kit (Invitrogen) was used and the extraction was carried out following the manufacturer's instructions. Directly after isolation, mRNA was treated with DNase I, Amplification Grade (Invitrogen). Briefly, 8 µl DEPC-treated H_2O, 1 µl 10 x DNase I Reaction Buffer, 1 µl DNase I together with the mRNA attached to Oligo$(dT)_{25}$ Dynabeads® were incubated for 15 min at RT. For inactivation of DNase I, 1 µl of 25 mM EDTA was added and the sample was incubated at 65°C for 10 min. First-strand synthesis of cDNA was carried out using oligo$(dT)_{18}$ primers and RevertAid™ M-MuLV Reverse Transcriptase according to the manufacturer's instructions (MBI Fermentas). For following PCR reactions, 1 µl of cDNA was used as template.

4.3.3 Dissection of ovules and clearing

For microscopy analysis, ovules and developing seeds had to be dissected using a stereomicroscope. First, the pistil or silique was freed by removing all other floral organs. Afterwards, the pistil or silique was cut along the septum at both sides using a hypodermic needle (0.4 x 20 mm, Braun) so that the carpels could be detached. For fluorescence microscopy, the pistil was then transferred into 50 mM sodium phosphate buffer pH 7.5, the placenta was separated lengthwise into two halves using two hypodermic needles and directly analyzed at a fluorescence microscope with the respective filter set. For differential interference contrast (DIC) microscopy, the preparations were cleared using chloral hydrate clearing solution (80 g chloral hydrate; 10 ml glycerol; ad 50 ml H_2O). In this case, the ovules or developing seeds were dissected in clearing solution instead of phosphate buffer. After 30 min to 2 hours, depending on the developmental stage of the ovule or developing seed, the preparations were analyzed at the Axioskop FL (Zeiss) with DIC optics.

4.3.4 GUS staining of ovules

For analysis of pollen tube guidance and reception, flowers were pollinated with the marker line *ARO1:GUS* (Gebert *et al.*, 2008) and subsequently histochemically stained. The *ARO1* promoter is active in pollen and pollen tubes and was thus used for the above-mentioned analyses. Therefore, stage 12 flowers were emasculated and two days later pollinated with flower stage 13 (stages according to Smyth *et al.*, 1990) *ARO1:GUS* pollen. One day after pollination, the pistils were detached from the inflorescence, carefully cut with a hypodermic needle along the septum, transferred to GUS-staining solution (10 mM EDTA, 2 mM $K_4Fe(CN)_6$, 2 mM $K_3Fe(CN)_6$, 0.1% Triton X-100, 1 mg/ml X-Gluc (Applichem) in 50 mM sodium phosphate buffer pH 7.0) and incubated at 37°C overnight (modified from Vielle-Calzada *et al.*, 2000). The preparations were washed three times in sodium phosphate buffer before they were dissected in clearing solution as described in section 4.3.3 (page 21).

4.3.5 *In vitro* pollen germination

Pollen germination medium consisted of 18% sucrose, 0.01% boric acid, 1 mM $MgSO_4$, 1 mM $CaCl_2$, 1 mM $Ca(NO_3)_2$ and 0.5% agar (ultrapure, granulated;

Merck) as previously described by Li *et al*. (1999). At first, a two fold concentrated solution containing sucrose, boric acid, $MgSO_4$, $CaCl_2$ and $Ca(NO_3)_2$ was prepared in sterile H_2O by dissolving in a 50°C water bath. Agar (1%) was dissolved in H_2O using a microwave and afterwards cooled to 50°C in a water bath. Equal amounts of the salt/sucrose solution and the agar were combined and the pollen germination medium was poured into small petri dishes (30 mm in diameter) under the clean bench. The plates were kept open under the clean bench and dried for exactly one hour. Fresh pollen from stage 13 flowers (Smyth *et al.*, 1990) was dipped onto the plate. The plates with closed lid were put into a plant growth chamber (22°C, approximately 70% humidity, 16 hours light/8 hours dark) and incubated 5 to 20 hours.

4.3.6 Bioassay with purified GST-EC1.1 and sperm cells released from *in vitro* germinated pollen

Pollen of the sperm cell marker line *HTR10-mRFP1* was germinated *in vitro* for six hours as described in section 4.3.5, page 21. To induce pollen tube burst and release of the sperm cells from the tube, the petri dish was place under an inverted microscope, a drop (app. 5 µl) of mannitol solution (285 mosmol/kg H_2O) was pipetted onto the sample and pollen tube burst induced by the osmotic shock was observed under the microscope. Subsequently, 10 µl of the 1 ml fraction of refolded and purified GST-EC1.1 fusion protein was applied in the same way.

For DAPI staining of burst pollen tubes, the staining solution (aqueous solution containing 2.5 µg/ml 4',6-diamidino-2-phenylindole (DAPI), 0.01% Tween-20, 5% DMSO, 50 mM phosphate buffered saline (PBS) (pH7.2)) was carefully pipetted onto the samples on the petri dish. Samples were analyzed for DAPI fluorescence after 30 min using the Nikon ECLIPSE TE2000-S inverted microscope with an UV-MBE41300 filter set (340-380 nm excitation, 435-485 nm emission).

4.3.7 Generation of *P_{35S}:EC1.1-eGFP* plants and proteasome inhibitor assay

The EC1.1-eGFP fusion construct was amplified from p7U-EC1-GFP (Sprunck *et al*., unpublished) using the primer pair *AtEC1.1 SalI+1f/GFP SalI rev* and ligated into the binary vector pCHF5 behind the *CaMV35S* promoter via *Sal*I restriction sites. The construct was named pRAS7 and used for transformation of *Arabidopsis thaliana* wild type plants with the floral dip method (Clough and Bent, 1998). For proteasome

inhibitor studies, T2 generation seeds were germinated on solid ½ x MS medium enriched with 2% sucrose. Two weeks after sowing, the seedlings were transferred to solid ½ x MS medium with 2% sucrose and containing 100 µM MG132 (Sigma-Aldrich, 100 mM stock solution in DMSO) or just DMSO as a control. The seedlings were kept on these plates for 16 hours or 24 hours, respectively and then harvested for microscopy analysis or protein extraction. For microscopy analysis, agar blocks containing roots were cut out of the plate, placed on a microscope slide and covered with a cover slip. eGFP fluorescence was observed by using a Nikon ECLIPSE TE2000-S inverted microscope with an F36-525 filter set (472/30 nm excitation, BP 520/35 nm). For Western Blot analysis, 15 seedlings were frozen in liquid nitrogen together with two steel balls in 2 ml Eppendorf cups and homogenized using a CryoMill (Retsch). Afterwards, proteins were extracted by adding 300 µl extraction buffer (20 mM Tris-HCl, pH7.5; 150 mM NaCl; 1 mM EDTA; 10 mM DTT, one "Complete" protease inhibitor pellet (Roche)). The lysate was furthermore vortexed until it was homogenous. After 30 min centrifugation at 20,000 x g at 4°C, the supernatant was transferred into a clean cup and the protein concentration was determined by a Bradford Assay (Bradford, 1976). Pistil proteins were extracted in a stepwise procedure by consecutive centrifugation steps to separate microsomal and cytoplasmic fractions. For this purpose, 50 pistils of stage 12 flowers (Smyth *et al.*, 1990), that had been emasculated two days before, were collected in 2 ml Eppendorf cups and immediately frozen in liquid nitrogen. The tissue was homogenized in the cup by grinding with a plastic pestle. After adding 300 µl of homogenization buffer (330 mM sucrose; 100 mM KCl; 1 mM EDTA; 50 mM Tris/0.05% MES pH7.5; 5 mM DTT; one "Complete" protease inhibitor pellet (Roche)) the sample was centrifuged for 15 min at 1,000 x g. The supernatant was transferred into a fresh cup and centrifuged again for 15 min at 10,000 x g. Again, the supernatant was transferred into a fresh cup and centrifuged one more time for 75 min at 48,000 x g. The resulting pellet represents the microsomal fraction and the supernatant contains the cytoplasmic fraction of proteins. The supernatant was precipitated by adding first 1/100 vol. of 2% DOC (sodium deoxycholate). After vortexing and incubation at 4°C for 30 min, 1/10 vol. of 100% TCA (trichloroacetic acid, 100% = 454 ml H_2O/kg TCA) was added. Precipitation was carried out overnight at 4°C. The sample was centrifuged for 15 min at 15,000 x g at 4°C. The supernatant was discharged and the pellet was dried. For SDS-PAGE (SDS polyacrylamide gel electrophoresis), the pellet was resuspended in 20 µl of 1 x SDS

sample buffer. For titration against some residual TCA, NH_3 gas was passed through the sample using a Pasteur pipette. After separating the proteins by SDS-PAGE, they were transferred to a PVDF membrane (Bio-Rad) by the tank-blot procedure. The membrane was blocked for 1 h with blocking solution (1% skimmed milk powder, 0.1% Triton X-100 in 1 x TBS). The GFP was visualized with indirect two-step immunodetection. using a 1:5,000 dilution of monoclonal anti-GFP antibody (Roche) in blocking solution and a secondary goat anti-mouse antibody conjugated with HRP (Horseradish Peroxidase, Sigma-Aldrich) were used, 1:5,000 diluted in blocking solution. The Immobilon Western Detection Reagent (Millipore) served as a substrate for the HRP enzyme.

4.3.8 Cloning of the *EC1.1* phospho-mimicking variant and transient expression in *N. benthamiana* leaves

In order to phospho-mimick the three putatively phosphorylated serine residues at the C-terminus of EC1 (S151, S152, S154) a primer was designed through which the serines were replaced with aspartate residues (*AtEC1.1 3xSD*). For the amplification of the construct, *AtEC1.1 3xSD* was used as reverse primer, *P-mim EC1.1 fw* as forward primer and pRAS7 served as a template. Finally, the construct was recombined into pB7FWG2 (Karimi *et al.*, 2007) via an LR-Clonase reaction (Invitrogen) to create a translational fusion of the *EC1.1* phospho-mimicking variant with *eGFP* under control of the viral *CaMV35S* promoter (pRAS28). For transient expression in *N. benthamiana* leaves, *Agrobacterium tumefaciens* (C58C1) was transformed with pRAS28. For infiltration into *N. benthamiana* leaves, Agrobacterium cells were grown overnight in 5 ml selective medium. After 15 min centrifugation at 3,500 x g, cells were resuspended in infiltration buffer (10 mM $MgCl_2$; 10 mM MES-KOH, pH5.7; 100 µM aceto—syringone) and adjusted to OD_{600} = 1. The cell suspension was infiltrated at the abaxial side of the leaf using a 5 ml syringe and applying slight pressure on the opposite side with a finger. eGFP fluorescence in leaf epidermis cells was analyzed one to three days after infiltration by confocal laser scanning microscopy (Zeiss Axiovert 200 M microscope equipped with a confocal laser scanning unit LSM 510 META) using the 488 nm-line of the argon laser for excitation and a BP 505-550 filter for selective GFP detection.

4.3.9 Expression of *PP2A B'θ* in synergid cells and pollination experiments

For the misexpression of *PP2A B'θ* in synergid cells, the respective ORF (open reading frame) was amplified from a clone (U85787) ordered at the ABRC (Arabidopsis Biological Resource Center, http://abrc.osu.edu/). The synergid cell-specific *DD31* promoter (Steffen *et al.*, 2007) was amplified from genomic DNA using *DD31 prom fw (SacI)*/*DD31 prom rev (SpeI)* and cloned into the Gateway® Destination vector pB7FWG2 (Karimi *et al.*, 2007) via *Sac*I and *Spe*I restriction sites. Finally, the translational fusion of *PP2A B'θ* and *eGFP* under control of the *DD31* promoter was created by LR Clonase® reaction (pRAS56). Col-0 *Arabidopsis* plants were transformed, seeds of the T0 generation were germinated and transgenic plants were selected (see section 4.3.1, page 19). For analysis of the fertilization process, stage 12 flowers (Smyth *et al.*, 1990) were emasculated. Two days after emasculation, pistils were pollinated with flower stage 13 (Smyth *et al.*, 1990) pollen of the sperm cell marker line *HTR10-mRFP1* (Ingouff *et al.*, 2007). For microscopy analysis, ovules were prepared as described above (see section 4.3.3, page 21). The preparation was then analyzed for eGFP and mRFP1 fluorescence at the Nikon ECLIPSE TE2000-S inverted microscope with the F36-525 filter set (472/30 nm excitation, BP 520/35 nm) for eGFP visualization and with the filter set F36-506 (575/15 nm excitation; BP 624/40) for mRFP1 detection.

4.4 Work with yeast

4.4.1 Yeast-two-hybrid screening

The yeast-two-hybrid (Y2H) screen was carried out using the Matchmaker™ Library Construction & Screening Kits (Clontech-Takara Bio Europe). For generation of the bait construct, a truncated version of *EC1.1* without the predicted leader peptide was amplified from genomic DNA (*EC1* genes do not contain introns) using the primer pair *AtEC1.1 EcoRI+82f*/*AtEC1.1 EcoRI+477r* and cloned via *Eco*RI restriction sites into pGBKT7 vector (Clontech-Takara Bio Europe) to create a translational fusion of the GAL4 DNA binding domain and the open reading frame of *EC1.1*. The resulting construct was named pRAS4. The yeast strain Y187 (Harper *et al.*, 1993) was transformed with pRAS4 according to "Yeast Protocols Handbooks" (Clontech-Takara

Bio Europe). For the construction of the ovule cDNA library material from 132 flowers was used in total. Two days after emasculation of stage 12 flowers carpels were removed from the pistils (see section 4.3.3, page 21) and ovules attached to the placenta were frozen in liquid nitrogen and stored at -80°C. mRNA was extracted using Dynabeads® mRNA DIRECT™ Micro Kit according to the manual (Invitrogen). To determine the concentration of the mRNA, Dynabeads® were removed from the mRNA directly after boiling at 90°C for 2 min while the tube was still standing in the thermocycler. Afterwards, the mRNA was immediately cooled on ice. The concentration of mRNA was determined using a NanoDrop ND-1000 spectrophotometer (Thermo Scientific) and was 30 ng/µl. First strand synthesis using random hexamer primer (CDSIII/6 Primer) and Long-Distance (LD) PCR were carried out according to the manual (Matchmaker™ Library Construction & Screening Kits, Clontech-Takara Bio Europe). After purification of the cDNA, the yeast strain AH109 (James *et al.*, 1996) was transformed with pGADT7 rec and the ovule cDNA to generate the yeast-two-hybrid library following the instructions of the manual. The transformation efficiency was 2.1 x 10^6 transformants and agreed approximately with the expected number according to the manual (1 x 10^6 transformants). After pooling of transformants, the library titer was calculated to be 1.8 x 10^9 cfu/ml, which above the minimum according to the manual (2 x 10^7 cfu/ml). Mating of bait and prey yeast strains and selection of interacting clones on triple dropout medium (SD/-His/-Leu/-Trp) was carried out according to the manual. The mating efficiency was 1.6%. As a positive control for mating and for interacting proteins the strains AH109 and Y187 were transformed with the vectors pGADT7-T and pGBKT7-53, respectively, which were included in the kit. The construction of the pollen tube cDNA library in the yeast strain AH109 is described elsewhere (Gebert, 2008) and served as prey. The titer of the pollen tube cDNA library was calculated to be 1.6 x 10^7 cfu/ml, which was slightly below the expected minimum of 2 x 10^7 cfu/ml according to the manual. Mating of bait and prey yeast strains and selection of interacting clones on triple dropout medium was carried out according to the manual. The mating efficiency of the bait strain with the pollen tube cDNA library was approximately 1%.

In total, 564 and 480 diploid yeast colonies were picked after mating of the *EC1.1* bait strain with the ovule and pollen tube cDNA library, respectively and resuspended in 100 µl sterile water in 96 well plates and replica plated onto triple (SD/-His/-Leu/-Trp) and quadruple dropout medium (SD/-Ade/-His/-Leu/-Trp) to select for more strongly

interacting partners. After 6 days of growth at 30°C, an X-Gal-Assay was performed to analyze the activation of the *lacZ* (β-Galactosidase) reporter gene. For covering one plate of 150 mm in diameter, 20 ml of 1 M sodium phosphate buffer pH 7.0, 2.4 ml of DMFA (N, N-dimethylformamide), 400 µl of 10% SDS (sodium dodecyl sulfate) and 400 µl X-β-Gal (5-bromo-4-chloro-3-indolyl-β-D-galactopyranoside, 20 mg/ml in DMFA) were combined. 20 ml 1% BactoAgar in H_2O was boiled, afterwards cooled down in a water bath to 60°C and finally added to 20 ml of the above described staining solution. The agar plate was carefully laminated with the X-Gal staining solution, solidified for 30 min under the clean bench and then incubated at 30°C overnight. From diploid colonies that activated the *lacZ* reporter gene, i.e. colonies showing blue staining, the prey-plasmids were isolated like previously described (Robzyk and Kassir, 1992) and used for transformation of *E. coli* for propagation and subsequent sequence analysis. To confirm the putative interactions, AH109 was transformed with the rescued plasmids and mated with the bait strain (see "Yeast Protocols Handbook", Clontech-Takara Bio Europe). Mating with Y187 carrying the empty bait vector pGBKT7 was used as a control to evaluate auto-activation of the identified positive clones.

4.4.2 Yeast-two-hybrid direct interaction tests

For the interaction analysis of full length clones of PP2A B'θ and UbDK3γ, the coding sequence was amplified from a clone (U85787) ordered at the ABRC (Arabidopsis Biological Resource Center) and from pollen cDNA using the primer pair *PP2AB'theta SmaI+1f/ PP2AB'theta XhoI+1479r* and *UbDk3gamma SmaI fw/ UbDK3gammaXhoI rev*, respectively. Afterwards, the cDNA was cloned into pGADT7 via *Sma*I and *Xho*I restriction sites. The resulting vectors were named pRAS9 and pRAS64. For GCS1-EC1 interaction analysis, only the N-terminal, extracellular part of GCS1/HAP2 (amino acid position 25 to 550) without the predicted signal peptide (amino acid position 1 to 24) was amplified using *GCS1c+73f EcoRI/ GCS1c+1650r EcoRI* and cloned into pGADT7 via *Eco*RI restriction sites (pRAS13). The resulting vectors were transformed into AH109 and mated with Y187 carrying pRAS4 or the empty bait vector pGBKT7 (see "Yeast Protocols Handbook", Clontech-Takara Bio Europe) and grown on selective medium to evaluate interaction of target proteins.

4.4.3 Expression of *EC1.1* in *Pichia pastoris*

For heterologous expression of *EC1.1* in *Pichia pastoris*, the EasySelect™ *Pichia* Expression Kit (Invitrogen) was used. The *EC1* coding sequence without the predicted signal peptide was amplified from genomic DNA using the primer pair *AtEC1.1 Pichia fw*/ *AtEC1.1 Pichia rev* and cloned into pPICZα via *Eco*RI and *Xba*I restriction sites (pRAS10). In pPICZα, the α-factor secretion signal from *Saccharomyces cerevisiae* upstream of the multiple cloning site leads to secretion of the target protein into the growth medium. For protein purification, the target protein is C-terminally tagged with c-myc and 6xHis. Moreover, the expression in *P. pastoris* is under control of the methanol inducible *AOX1* promoter. pRAS10 was integrated into *P. pastoris* (X-33) genome by electroporation according to the manual (BioRad electroporator; voltage: 1.25 V; resistance: 200 Ω; capacity: 25 μF). Induction of target protein expression was carried out according the manual. To avoid clogging of the column during purification, the cells were removed from the medium by two times centrifugation at 15,000 x rpm for 15 min. Purification of recombinant EC1.1 was carried out using Ni-NTA agarose (Qiagen) via column with gravity flow or the batch method according to the guidelines of "The QIA*expressionist*™" (Qiagen). Additionally, a HisTrap™ column (5 ml) connected to an Äkta™ System (both GE Healthcare) was used for EC1.1 purification (flow rate: 4 ml/min). For the latter method, loading of the column and washing (5 column volumes) was performed at 4°C. Protein elution was achieved with 50 mM NaH_2PO_4, 300 mM NaCl, 500 mM imidazole, pH 8.0 and was carried out gradually at room temperature.

4.5 Expression of *EC1* in *E. coli* and protein purification

For heterologous expression of *EC1.1* and *EC1.2a* in *E. coli*, the coding sequences lacking the predicted N-terminal signal peptide were amplified from genomic DNA using the primer pair *AtEC1.1+82f GW*/*AtEC1.1 rev GW* and *AtEC1.2a+67f GW*/*AtEC1.2a rev GW*, respectively, and recombined into two different Gateway® vectors with different tags for purification. To generate a translational fusion of EC1.1 with N-terminal GST (Glutathion-S-Transferase) the pGEX-2-GW vector (pGEX-2T [GE Healthcare] derived, gateway cassette was introduced) was used and the resulting construct was named pRAS37. In this construct, the target gene is under

control of the synthetic *tac* promoter, enabling inducible target protein expression by adding IPTG (isopropyl-β-D-thiogalactopyranosid). Additionally, an inducible *T7* promoter based expression system was used. Here, the EC1.2a was fused to a N-terminal His•Tag® and a C-terminal Strep•Tag®II by using the pET-53-DEST™ vector (Novagen). The resulting construct was named pRAS42. The expression vectors were used for transformation of various *E. coli* expression strains with different properties regarding target protein expression: Rosetta™(DE3) (Novagen), ArcticExpress™(DE3) (Stratagene), Origami™(DE3) (Novagen), Lemo21(DE3) (NEB), LemoGami (combination of Origami™(DE3) and pLemo plasmid). For protein extraction from Rosetta™(DE3), ArcticExpress™(DE3), Origami™(DE3) or LemoGami transformed with the expression vector, a preculture of 5 ml LB medium with respective antibiotics was grown overnight. 50 ml of LB medium including antibiotics was inoculated with 1 ml of the preculture and grown to OD_{600} = 1. Target protein expression was induced by adding 1 mM IPTG. After 4 h of growth, the cells were harvested by 20 min centrifugation at 4,000 x g. Either, the cells were resuspended in 0.1 culture volume phosphate buffered saline (PBS) pH 7.4 including protease inhibitors ("Complete" protease inhibitor pellet (Roche), without EDTA for purification of His-tagged proteins) and lysed by adding 1 mg/ml lysozyme and subsequent sonication (20 s at 60%, 20 s on ice; 7 cycles) or by using the BugBuster® Protein Extraction Reagent according to the manufacturer's instructions (Novagen). Inclusion body solubilization and protein refolding was carried out as described in the manual of the Protein Refolding Kit (Novagen). GST-EC1.1 fusion protein expressed in the Rosetta™(DE3) strain was solubilized in 50 mM CAPS, pH 11.0, 0.3% N-lauroylsarcosine (sodium salt) and 1 mM DTT. After dialysis and refolding, the GST-EC1.1 fusion protein was purified via GSTrap™ 4B column (GE Healthcare), connected to a peristaltic pump. The purification was carried out at 4°C with a flow rate of 0.5 ml/min according to the manufacturer's guidelines. Growth conditions and induction of target protein expression in Lemo21(DE3) was carried out according to the manufacturer's instructions with 400 µM IPTG at 28°C for 4 h. Eventually, the protein extracts and fractions of purification were analyzed by SDS-PAGE and stained with PageBlue™ (MBI Fermentas) according to the manufacturer's instructions.

5 RESULTS

5.1 Small cysteine-rich proteins in the *Arabidopsis* female gametophyte

The subject of research of this thesis, the *EC1* gene family, encodes cysteine-rich proteins. To identify the proteins most closely related to the EC1 family, BLASTP searches were performed. These revealed a group of nine proteins (Table 1) with highest similarity to EC1 that were named EC1-related (ECR). Interestingly, one of the *ECR* genes, namely At2g27315 has been shown to be expressed synergid cell-specifically (Punwani *et al.*, 2008) and two others, At5g54062 and At5g52975, are predominantly expressed in the synergid cells (Jones-Rhoades *et al*., 2007; Steffen *et al*., 2007).

Table 1: Identification of EC1-related (ECR) proteins. BLASTP results with EC1.1 as a query. Accession, AGI, E value and term are indicated. Expression data of previously published work is also quoted. SY = synergid cell, EC = egg cell, CC = central cell. N. d. = not determined/no expression data available.

Accession	AGI	E value	Term	Expression
AAU44598.1	At5g54062	4e-05	ECR6	SY (EC) (Steffen *et al*., 2007; Jones-Rhoades *et al*., 2007)
NP_680764.1	At4g35165	5e-05	ECR2	n. d.
NP_00107789.1	At2g14378	2e-04	-	n. d.
NP_68118.1	At3g48675	4e-04	-	n. d.
NP_568782.1	At5g52975	0.006	DD8/ECR4	SY (EC, CC) (Steffen *et al*., 2007)
AAM60965	At2g27315	0.011	ECR1	SY (Punwani *et al*., 2008)
NP_680427.1	At5g52965	0.014	ECR3	n. d.
NP_680430.1	At5g53905	0.1	-	n. d.
NP_001078753.1	At5g53742	0.26	ECR5	n. d.

The multiple sequence alignment of EC1 and ECR proteins is shown in Figure 5A. The two groups share the same conserved cysteine pattern but differ in other parts, which are only conserved within the EC1 and the ECR proteins, respectively (Figure 5A, blue line and yellow line, respectively). Moreover it is evident that At5g54062 has a

duplicated cysteine pattern. In this case, the second cysteine pattern is aligned to the sequence of the remaining ECR proteins. The phylogenetic tree shows that EC1 and ECR proteins are clustering in two clearly distinct groups (Figure 5B).

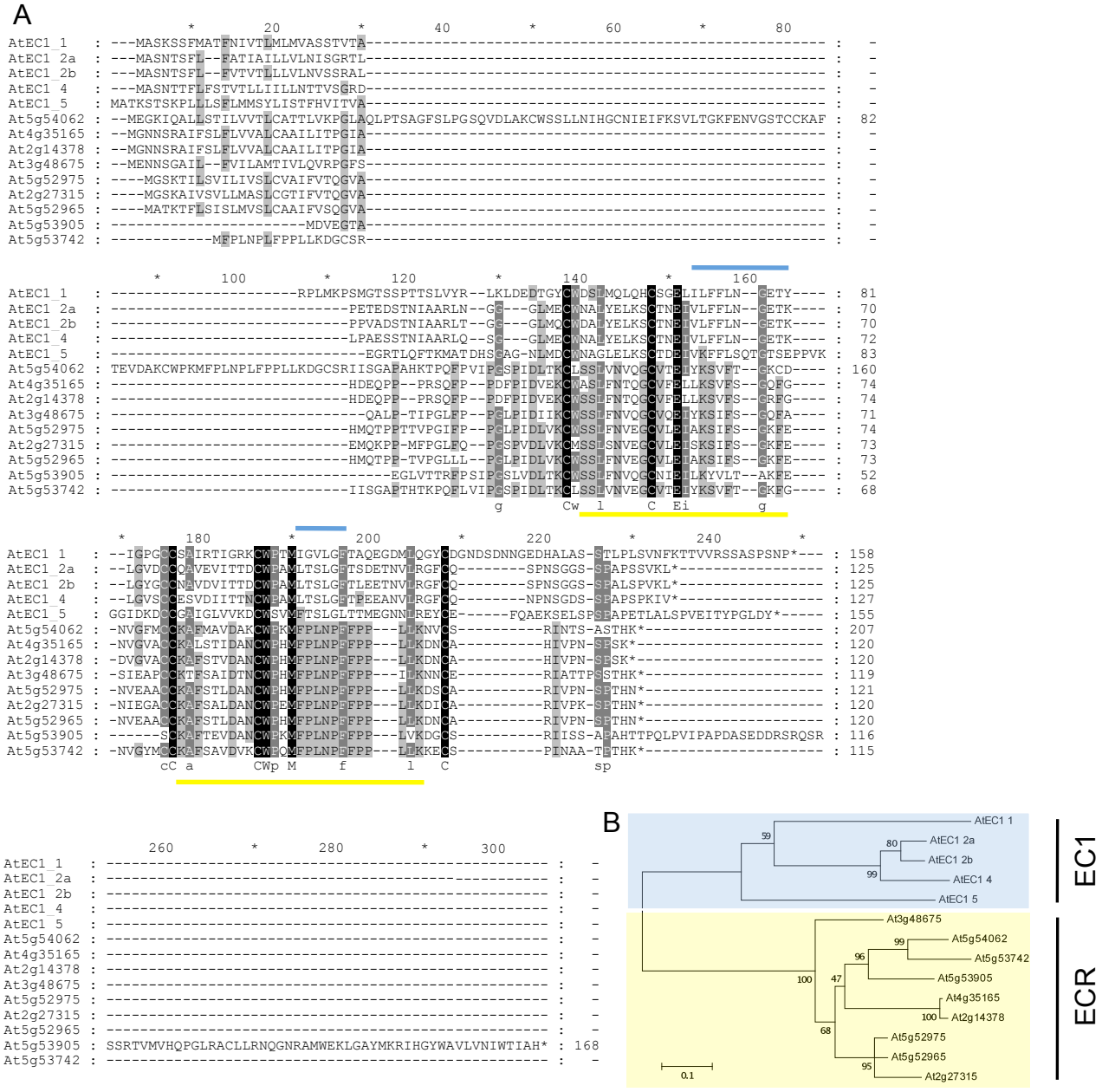

Figure 5: Similarity between EC1 and ECR proteins.
A Multiple sequence alignment of EC1 and ECR proteins. Conserved amino acids between both groups are shown with a black background, consensus sequence is shown below the alignment. EC1-group conserved residues are indicated by the blue line and ECR-conserved residues by the yellow line. **B** Phylogenetic relation of the EC1- (blue) and the ECR-group (yellow). The number on each node represents the probability that supports the relationship (determined with Bootstrap Method). The branch length is the measurement of divergence between two nodes. Bar = 0.1 nucleotide substitutions per site.

The interest in the different roles of small cysteine-rich proteins (CRPs) has strongly increased within the last few years. Silverstein *et al*. (2007) identified 825 genes in the *Arabidopsis* genome encoding CRPs. These predicted proteins were classified into

different groups and classes according to the number of cysteine residues and their pattern. Both EC1 and ECR proteins fall into the class called 'ECA1 gametogenesis related family protein'. Moreover, Jones-Rhoades *et al*. (2007) showed that the expression of genes encoding CRPs drastically decreased in ovules lacking a female gametophyte.

To gain an overview about the relation of EC1 proteins, ECR proteins and other members of this class of CRPs, an unrooted phylogenetic tree was constructed (Figure 6A). Interestingly, the five EC1 proteins (blue) as well as the ECR proteins cluster in an isolated clade. The complete ECR-group comprises nine members, which are highlighted in yellow (Figure 6A). The relationship of both groups is well supported by a bootstrap value of 98 and 91, respectively. The *EC1* gene family is exclusively expressed in the egg cell and the genes cluster in one phylogenetic clade. Also the ECR-group might be expressed predominantly in one cell type within the female gametophyte, the synergid cell in this case (Steffen *et al*., 2007, Jones-Rhoades *et al*., 2007, Punwani *et al*., 2008). Possibly, all genes that cluster in one phylogenetic group show the same expression pattern. Based on this hypothesis the phylogenetic trees of the ECA1 and the DEFL class were used to search for more groups of genes that may be specifically expressed in one cell type of the female gametophyte.

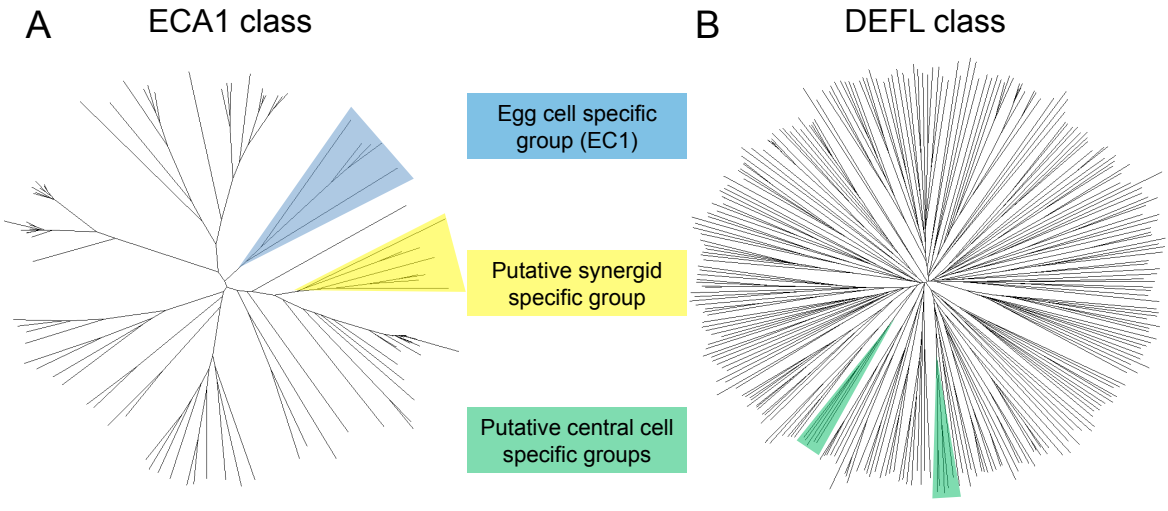

Figure 6: Unrooted phylogenetic trees of ECA1 gametogenesis related proteins (encoded by 118 genes) and DEFL class proteins (encoded by 291 genes). Classification according to Silverstein *et al.* (2007).
A Unrooted tree of the ECA1 class of CRPs. The distinct clade of the five EC1 proteins is highlighted in blue. The ECR-group, putatively synergid cell-specific, is highlighted in yellow. **B** Unrooted tree of the DEFL class of CRPs. The two candidate groups for central cell-specific expression are highlighted in green.

Based on publicly available expression data and microarray data of isolated egg, central and synergid cells (Šoljić *et al*., in preparation) two more, putative central cell groups among the DEFL class of CRPs were identified (Figure 6B). Steffen *et al*. (2007) showed that DD22/LCR80, a member of the first group comprising six proteins is specifically expressed in the central cell. The members of this family have been annotated as 'low-molecular-weight-cysteine-rich' (LCR) before and will be termed the LCR-group here (Table 2). The second group comprising five genes was chosen because At5g54220 is specifically expressed in the central cell, according to microarray data (Šoljić *et al*., in preparation). Moreover, this gene and At2g25305 are similar to central cell-specific genes that were identified in EST analyses of maize female gametophytes and egg cells (Yang *et al.*, 2006). The members of this group comprise eight cysteine residues in total, including a characteristic triple-cysteine motif at the C-terminus. For that reason this group was termed CCC-group here.

Table 2: LCR- and CCC-candidate gene families for central cell-specific gene expression. The LCR-group comprises six members and the CCC-group comprises five members. AGI, term and expression data of previously published work are indicated. N. d. = not determined/no expression data available.

AGI	Term	Expression
At4g30074	LCR19	n. d.
At5g42242	LCR57	n. d.
At5g38317	LCR58	n. d.
At4g30070	LCR59	n. d.
At4g30067	LCR63	n. d.
At5g38830	DD22/LCR80	CC (Steffen *et al*., 2007)
At1g24062	CCC1	n. d.
At5g54220	CCC2	mentioned in Yang *et al*., 2006
At2g25305	CCC3	mentioned in Yang *et al*., 2006
At5g54215	CCC4	n. d.
At5g54225	CCC5/LCR83	n. d.

Taken together, three new candidate groups for female gametophyte cell-specific expression were found including one putative synergid-group of the ECA1 class, the ECRs, and two putative central cell-groups of the DEFL class, the LCR-group and the CCC-group. A precondition for a real candidate for cell specific expression within the female gametophyte is the absence of transcript in all kinds of other tissue. To test this,

the candidate genes were subjected to reverse transcriptase (RT) - PCR with various tissues (Figure 7).

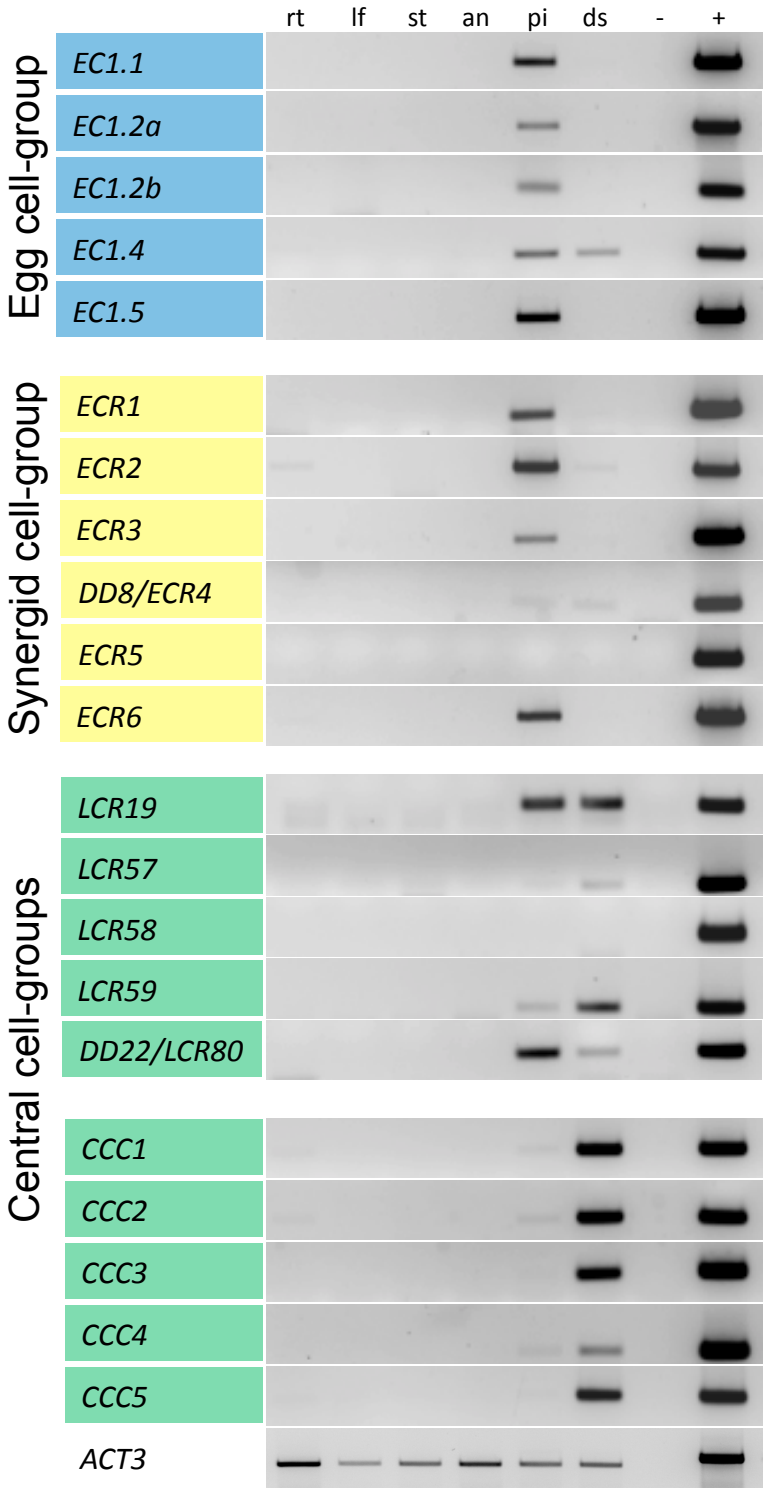

Figure 7: Expression analysis of candidate groups for cell-specific expression within the female gametophyte by reverse transcriptase (RT) - PCR.
Gel electrophoretic separation of PCR products after amplification from cDNA of different tissues. rt = root; lf = leaf; st = stem; an = anther, ps = pistil; ds = developing seed; - = non template control; + = genomic DNA control. Internal standard: *ACTIN3* (*ACT3*). Fragment sizes and oligo nucleotide sequences are given in the appendix.

The female gametophyte-specific expression of *EC1* could be confirmed. The *EC1* transcript was not detected in any of the tested vegetative tissues (root, leaf, stem). All of the five genes are expressed in pistils; only *EC1.4* is also detectable in developing seeds. *ECR1, ECR2* and *ECR3* show the strongest expression in pistils, whereas the *ECR2* transcript is also weakly detectable in roots and developing seeds. *ECR4/DD8* is very weakly expressed in pistils and developing seeds. For *ECR5*, a transcript was not detected in the tested tissues and *ECR6* is only expressed in pistils. *LCR19* shows signals in pistils and developing seeds. *LCR57* and *LCR59* show both a weak signal in pistils and a stronger signal in developing seeds, whereas *LCR80*/*DD22* shows a stronger signal in pistils than in developing seeds. For *LCR58*, a transcript was not detected in any of the tested tissues. All five members of the CCC group show a strong signal in developing seeds and a much weaker signal in pistils.

In summary, all of the analyzed genes are preferentially expressed in tissues containing the female gametophyte or the embryo and the endosperm. The central cell candidate group is even more strongly expressed in the developing seed than before fertilization in the pistil. Taken together, these gene families are interesting for further, more detailed expression analysis and functional analysis to elucidate their roles during female gametophyte development, fertilization and early seed development.

5.2 EC1 homologs in different species

BLASTP searches were performed to identify EC1 homologous proteins in other species. Interestingly, homologs were only found angiosperms. Homologs of *Arabidopsis* EC1 were neither identified in gymnosperms nor in bryophytes (*Physcomitrella patens*), nor in ferns (*Adiantum sp*.) nor in algae. The *Arabidopsis lyrata* genome encodes five EC1 proteins like *Arabidopsis thaliana*. In *Populus trichocarpa*, two homologs were identified, in *Ricinus communis* four and in *Vitis vinifera* two. From the monocots, three EC1 homologs were identified in *Brachypodium distachyon*, the ECA1 protein from *Hordeum vulgare* was found as a homolog, three EC1 homologs in *Oryza sativa*, two in *Sorghum bicolor* and two in *Zea mays* (Table 3; see Appendix for detailed BLAST search results, page 102).

Table 3: Number of identified EC1 homologs in different species.
Division, name of the species and number of identified homologs are indicated. EC1 homologs are only found in angiosperms (dicots and monocots). Homologous proteins were not found in gymnosperms, ferns (pteridophyta), moss (bryophyta) or algae (chlorophyta).

Division	Species	Number of EC1 homologous proteins
Angiosperms	*Arabidopsis thaliana*	5
	Arabidopsis lyrata	5
	Medicago truncatula	2
	Populus trichocarpa	2
	Ricinus communis	4
	Vitis vinifera	2
	Brachypodium distachyon	3
	Hordeum vulgare	1
	Oryza sativa	3
	Sorghum bicolor	2
	Triticum aestivum	1
	Zea mays	2
Gymnosperms	*Abies sp.*	0
	Larix sp.	0
	Picea sp.	0
	Pinus sp.	0
Pteridophyta	*Adiantum sp.*	0
Bryophyta	*Physcomitrella patens*	0
Chlorophyta	*Volvox sp.*	0
	Chlamydomonas sp.	0

Figure 8 shows a multiple sequence alignment of all identified EC1 homologs. In the middle part of the sequence a region with high similarity was identified: **C W** x_8 **C** x_7 **F** x_{2-4} **G** x_{7-13} **C C** x_9 **C W** x_{7-9} **G** x **T** x_2 **E** x_3 **L** x_3 **C**. This sequence does not only contain the characteristic cysteine pattern but additional conserved amino acids like tryptophan, phenylalanine, glycine, threonine, glutamate and leucine.

AtEC1.5 and AlEC1.5 have an insertion of eight amino acids within the second and the third cysteine residue. This insertion does not appear in any of the other homologs (Figure 8) and is also noticeable in the phylogeny where AtEC1.5 and AlEC1.5 form a small outgroup (Figure 9).

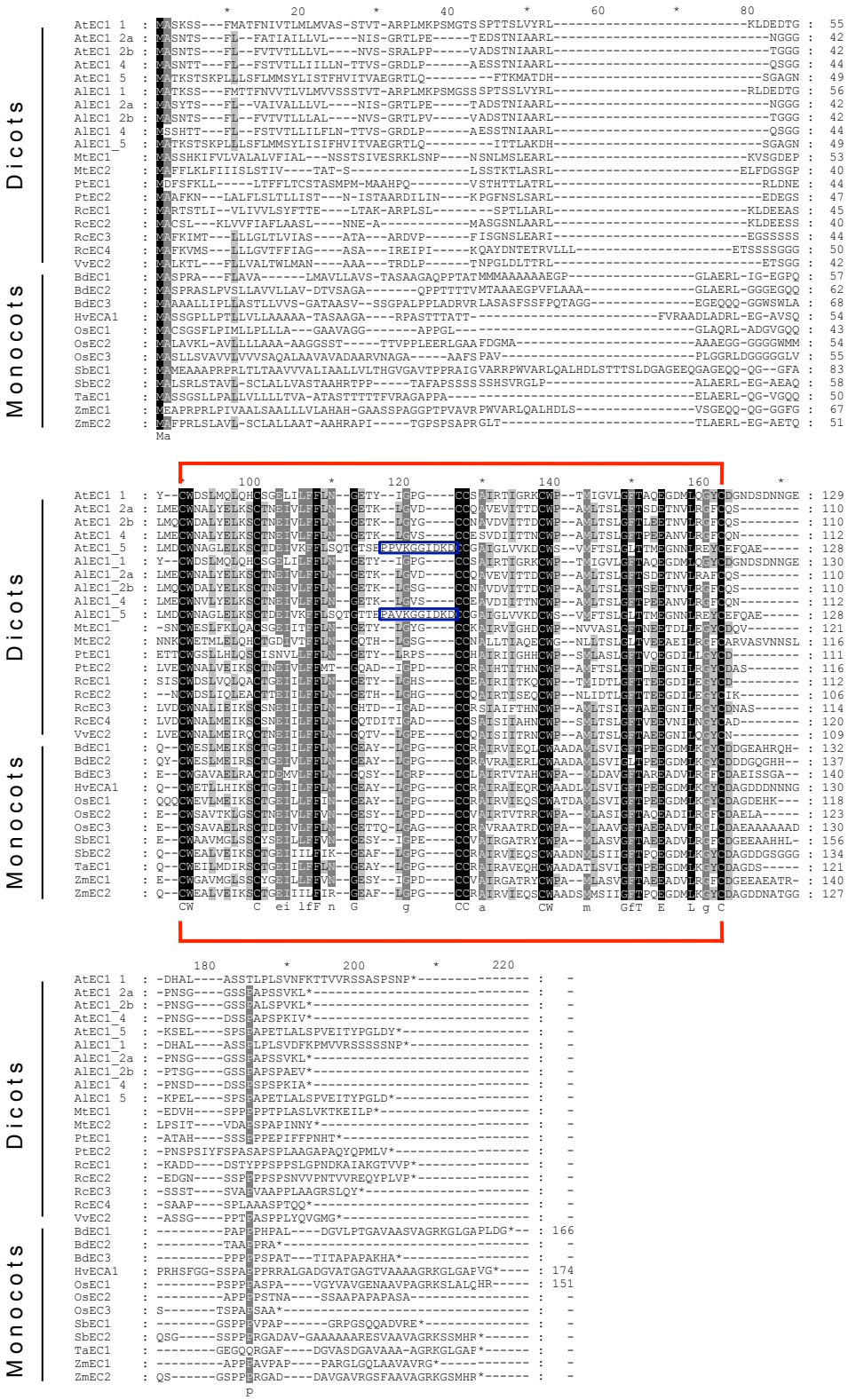

Figure 8: Multiple sequence alignment of the identified EC1 homologs from different species.
Upper part of the alignment: sequences of dicots, lower part: monocot sequences of EC1 homologs. Highly conserved residues are shown with a black background. Consensus sequence is shown below the alignment. The protein domain containing the conserved cysteine pattern is indicated by the red box. Insertion of amino acids in AtEC1.5 and AlEC1.5 is highlighted by the blue boxes. At = *Arabidopsis thaliana*; Al = *Arabidopsis lyrata*; Mt = *Medicago truncatula*; Pt = *Populus trichocarpa*; Rc = *Ricinus communis*; Vv = *Vitis vinifera*; Bd = *Brachypodium distachyon*; Hv = *Hordeum vulgare*; Os = *Oryza sativa*; Sb = *Sorghum bicolor*; Ta = *Triticum aestivum*; Zm = *Zea mays*.

The construction of a phylogeny based on the alignment shown above (Figure 8) indicates that EC1 proteins in dicots and monocots evolved independently (Figure 9).

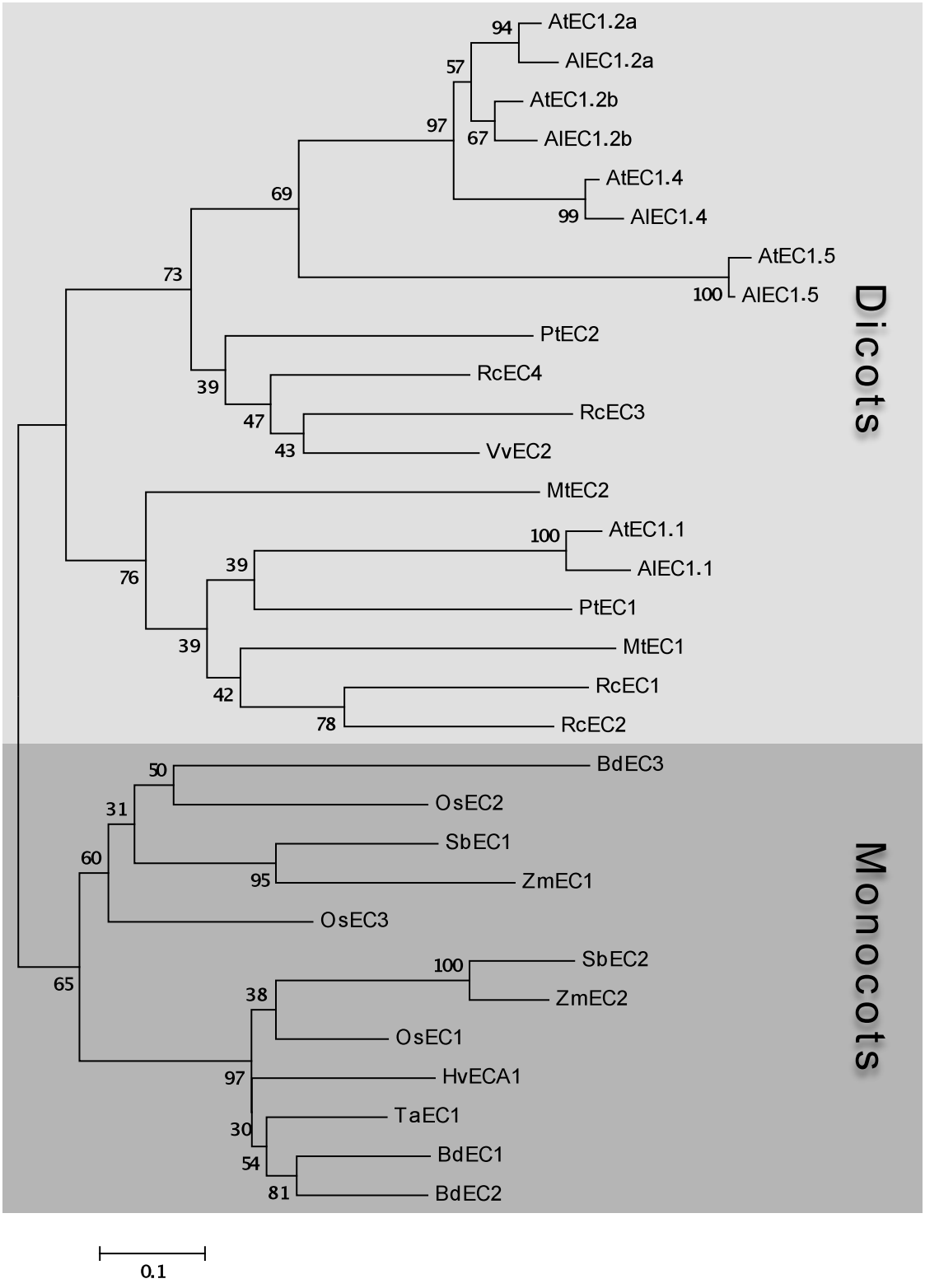

Figure 9: Phylogenetic tree of EC1 homologs.
The upper part of the phylogenetic tree represents members of dicots (light grey) and the lower part members of monocots (dark grey). The number on each node represents the probability that supports the relationship (determined with Bootstrap Method). The branch length is the measurement of divergence between two nodes. Bar = 0.1 nucleotide substitutions per site.

The ancestors of *Arabidopsis thaliana* and *Arabidopsis lyrata* diverged from one another approximately 5 million years ago (Koch *et al.*, 2000). Because of this, the EC1 proteins show a high degree of similarity (Table 4).

Table 4: Similarity table of EC1 proteins between *Arabidopsis thaliana* and *Arabidopsis lyrata*. The percentage of similarity is indicated. Percentages of the respective five pairs are underlined and written in bold letters.

	AtEC1.1	AtEC1.2a	AtEC1.2b	AtEC1.4	AtEC1.5	AlEC1.1	AlEC1.2a	AlEC1.2b	AlEC1.4	AlEC1.5
AtEC1.1	100	29	32	30	20	**91**	29	32	32	21
AtEC1.2a		100	87	80	35	29	**96**	87	77	35
AtEC1.2b			100	81	34	32	87	**93**	78	35
AtEC1.4				100	33	32	78	82	**95**	34
AtEC1.5					100	21	35	34	35	**95**
AlEC1.1						100	29	32	33	22
AlEC1.2a							100	86	76	35
AlEC1.2b								100	78	34
AlEC1.4									100	35
AlEC1.5										100

The 158 amino acids (aa) comprising EC1.1 protein shows 91% similarity between both species with only 13 exchanges, one insertion and one deletion. The smaller proteins EC1.2a (125 aa), EC1.2b (125 aa) and EC1.4 (127 aa) show only seven, eleven and nine exchanges and have a similarity degree of 96%, 93% and 95%, respectively. The EC1.5 proteins of *A. thaliana* and *A. lyrata* with its characteristic insertion show a similarity of 95%.

5.3 Functional analysis of the *EC1* gene family

To study the function of *EC1*, T-DNA insertion lines were identified in a previous project (S. Sprunck, personal communication). The analyzed T-DNA insertion lines of *EC1.1*, *EC1.4* and *EC1.5* were complete knockout lines, i.e. no transcript was detectable anymore. However, single, double and triple knockout lines of these three genes did not display any phenotype. Since T-DNA insertion lines were not available for *EC1.2a* and *EC1.2b*, the triple mutant was transformed with an RNAi construct targeting these two genes and will be termed *ec1*$^{+/-}$ hereafter. After knockdown of the complete *EC1* family, a reduced seed set was observed (Figure 10A). These plants were homozygous for the T-DNA insertions in *EC1.1*, *EC1.4* and *EC1.5* and heterozygous for the RNAi construct. At the beginning of this project preliminary data about the phenotype of *ec1*$^{+/-}$ were available (see section 3.6, page 16). The goal of my PhD thesis was to examine the fertilization process in *ec1*$^{+/-}$ plants step by step and to quantify the observed phenotypes in order to achieve a detailed and precise functional characterization of the *EC1* gene family.

5.3.1 Quantification of seed set in *ec1*$^{+/-}$ mutants

Three independent lines were analyzed in detail regarding seed set of selfed flowers (Figure 10B). Line *ec1*$^{+/-}$*-9* showed a seed set of approximately 67% compared to 99.5% in wild type. The remaining 33% of the seeds in *ec1*$^{+/-}$*-9* were aborted, probably resulting from undeveloped ovules. The lines *ec1*$^{+/-}$*-16* and *ec1*$^{+/-}$*-18* exhibited 54% and 64% normally developed seeds, respectively. Seeds that had a normal size but had a white color instead of green probably resulted from defects during seed maturation. This phenotype only occurred at a frequency of 0.2% in line *ec1*$^{+/-}$*-18* and was thus not further analyzed. Two further categories, shriveled seeds of brown or white color occurred rarely and were detected at a maximum of 1% of all ovules. Taken together, in average 38% of seeds were aborted from three independent *ec1*$^{+/-}$ lines. Within the siliques, aborted and developed seeds were randomly distributed (Figure 10A). This suggests that the reduced seed set is caused by the loss of *EC1* function rather than by abiotic or plant growth effects.

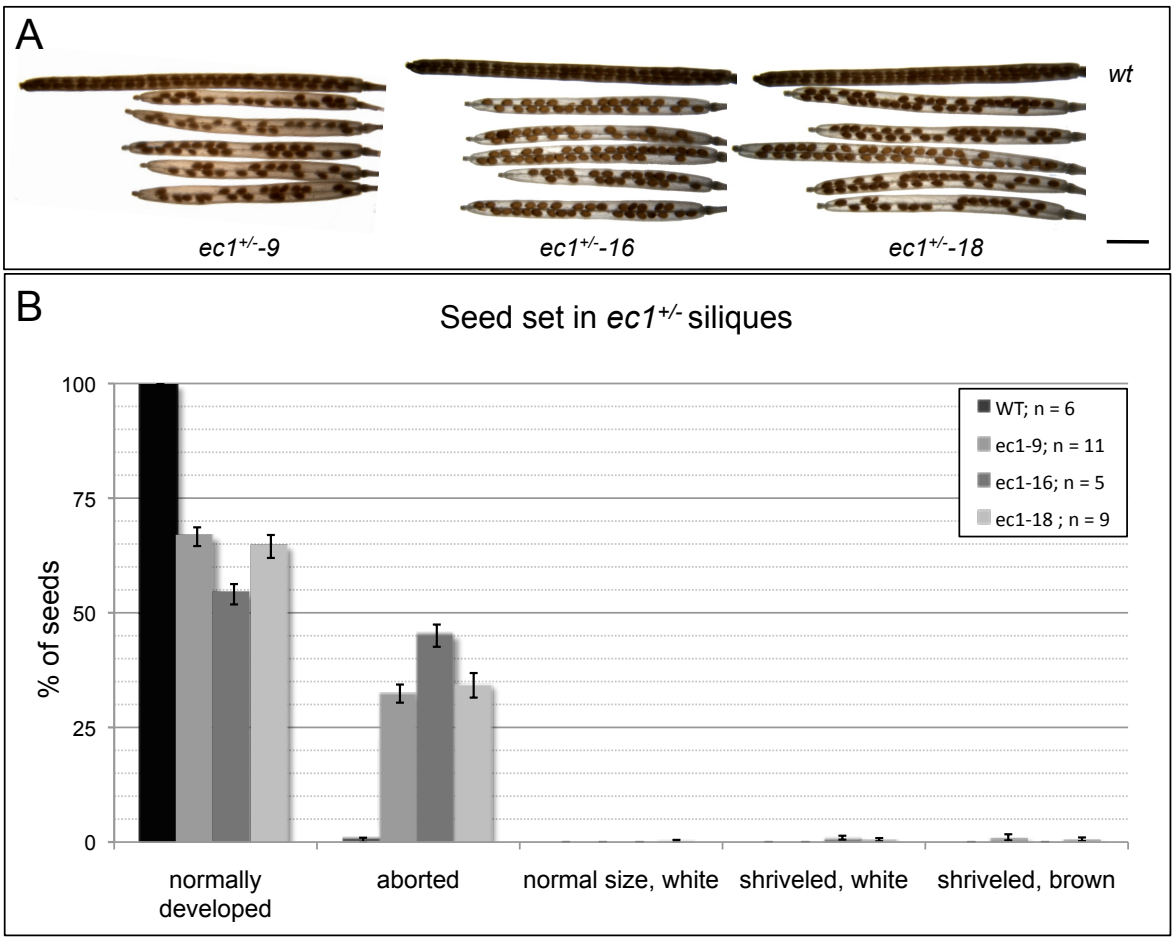

Figure 10: Siliques of *ec1*$^{+/-}$ plants show a reduced seed set (selfed plants).
A Images of siliques of three independent *ec1*$^{+/-}$ lines (-9, -16, -18). Wild type silique is shown in the uppermost row of each column. Aborted seeds are recognizable as gaps. Pictures were taken by B. Bellmann. Bar = 2 mm. **B** Wild type siliques have 99.5% normally developed seeds, three independent *ec1*$^{+/-}$ lines (-9, -16, -18) have a seed set of 67%, 54% and 64%, respectively; the remaining ovules were mainly aborted. n = number of siliques counted ± standard error (bars).

5.3.2 Heredity and transmission analysis of RNAi lines

In order to determine whether a sporophytic or gametophytic effect caused the fertility defect, the offspring of selfed *ec1*$^{+/-}$ plants was analyzed regarding its sensitivity to Hygromycin B. The resistance against the antibiotic is linked to the transmission of the RNAi construct and was thus used as a scorable marker.

The progeny of *ec1*$^{+/-}$*-9* (n = 232) was resistant to Hygromycin at 52.2%. Of the seedlings of the *ec1*$^{+/-}$*-16* progeny (n = 258) and the *ec1*$^{+/-}$*-18* progeny (n = 296) 53.1% and 51.4% of the seedlings were resistant to Hygromycin, respectively. The dead to alive ratio of seedlings was 1:1.09 for *ec1*$^{+/-}$*-9,* 1:1.1 for *ec1*$^{+/-}$*-16* and 1:1.06 for *ec1*$^{+/-}$*-18.* Taken together, in each of the three independent lines, the segregation of

Hygromycin-sensitive to Hygromycin-resistant plants was approximately 1:1. As expected, this ratio strongly suggests a gametophytically caused defect.

To analyze the transmission efficiency via the female and the male gametophyte, respectively, reciprocal backcrosses with wild type plants were performed. First, the percentage of developed seeds after hand-pollination of wild type was determined (Table 5, first row). Approximately 84% of the seeds developed normally. This value served as a control and also showed the efficiency of hand-pollination. Moreover, it was also above the accepted limit of 80% successfully fertilized ovules.

Table 5: Transmission efficiency of the *ec1* allele (RNAi construct). Reciprocal crossings of *ec1*$^{+/-}$ (*ec1/EC1*) with wild type (*EC1/EC1*): parental genotypes, percentage of normally developed and aborted seeds are indicated. n = number of counted seeds.

Parental genotype (female x male)	Normal %	Aborted %	n
EC1/EC1 x EC1/EC1	83.8	17.2	187
ec1-9/EC1 x EC1/EC1	50.2	49.8	181
EC1/EC1 x ec1-9/EC1	82.6	17.4	278
ec1-16/EC1 x EC1/EC1	50.1	49.9	252
EC1/EC1 x ec1-16/EC1	87.3	12.7	139
ec1-18/EC1 x EC1/EC1	58.9	41.1	366
EC1/EC1 x ec1-18/EC1	83.7	17.3	186

These crossing experiments showed that transmission through the female, but not the male gametophyte was severely affected (Table 5). The seed set of *ec1*$^{+/-}$*-9* plants pollinated with wild type pollen was reduced to 50%, whereas pollination of wild type plants with *ec1*$^{+/-}$*-9* resulted in approximately 83% normally developed seeds. Siliques with *ec1*$^{+/-}$*-16* as mother and wild type as father had only about 50% developed seeds whereas the reciprocal crossing resulted in 87% normally developed seeds. Similar results were obtained for *ec1*$^{+/-}$*-18*. In this case the transmission via the female

gametophyte was not as strongly affected, which was reflected by almost 59% normally developed seeds. Nevertheless, there was still a clear difference to the reciprocal crossing of wild type plants pollinated with *ec1*$^{+/-}$*-18* resulting in 84% developed seeds.

5.3.3 Morphology analysis of *ec1*$^{+/-}$ female gametophytes

The transmission analysis described in the previous section indicated that the reduced seed set in *ec1*$^{+/-}$ plants was caused by a defect of the female gametophyte. To examine the morphology and maturity of *ec1* female gametophytes, ovules were dissected from *ec1*$^{+/-}$ pistils and analyzed by differential interference contrast (DIC) microscopy.

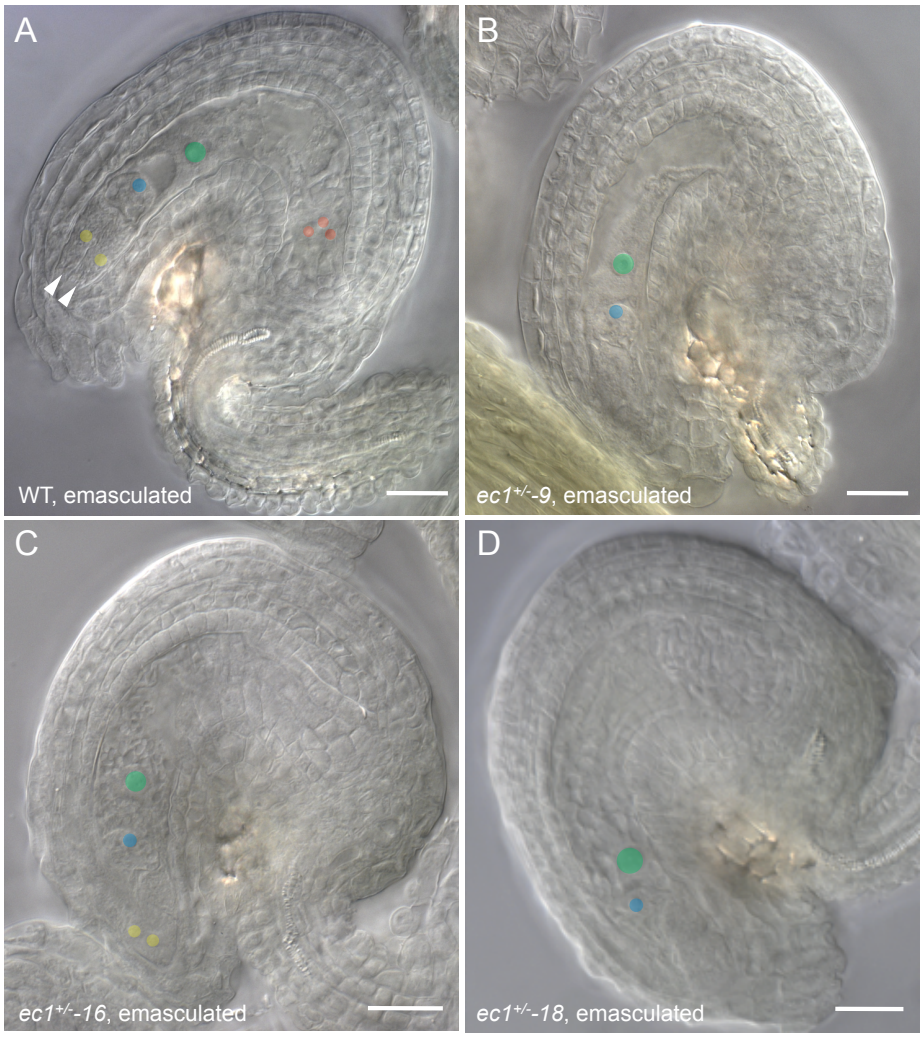

Figure 11: DIC microscopy analysis of dissected and cleared mature ovules of *ec1*$^{+/-}$ lines two days after emasculation.
Nuclei of the different cell types of the female gametophyte were artificially colored: egg cell: blue; central cell: green; synergid cells: yellow; antipodal cells: red. **A** Wild type ovule, dissected from the pistil. Arrowheads point to the filiform apparatus. **B** *ec1*$^{+/-}$*-9* ovule. Egg and central cell are in focus plane. **C** *ec1*$^{+/-}$*-16* ovule. Egg and central cell nuclei and the two synergid nuclei are visible. **D** *ec1*$^{+/-}$*-18* ovule. Egg and central cell nuclei are in focus. Bars = 20 μm.

Figure 11 shows representative images of wild type and *ec1*$^{+/-}$ ovules dissected from pistils two days after emasculation. In the wild type ovule the four cell types of the female gametophyte can be clearly seen (Figure 11A): both female gametes, haploid egg cell and diploid central cell as well as two synergid cells at the micropylar pole and three antipodal cells at the chalazal pole. Due to the focus plane, not all cell types are visible in the preparations shown in Figure 11B, C and D like in the image of the wild type preparation (Figure 11A). Nevertheless, morphological analyses of *ec1* female gametophytes did not reveal any aberrations compared to wild type.

5.3.4 Pollen tube guidance ability of *ec1*$^{+/-}$ ovules

At this point the results suggested that *ec1*$^{+/-}$ ovules contain fully mature female gametophytes but exhibited a defect during fertilization. To explore at which step during the fertilization process the aberrations occur, the pollen tube guidance ability of *ec1*$^{+/-}$ ovules was analyzed. Therefore, *ec1*$^{+/-}$ flowers were pollinated with a pollen tube marker line, in which *GUS* expression was driven by the *ARO1* promoter that has been shown to be strongly active in pollen and pollen tubes (Gebert *et al*., 2008).

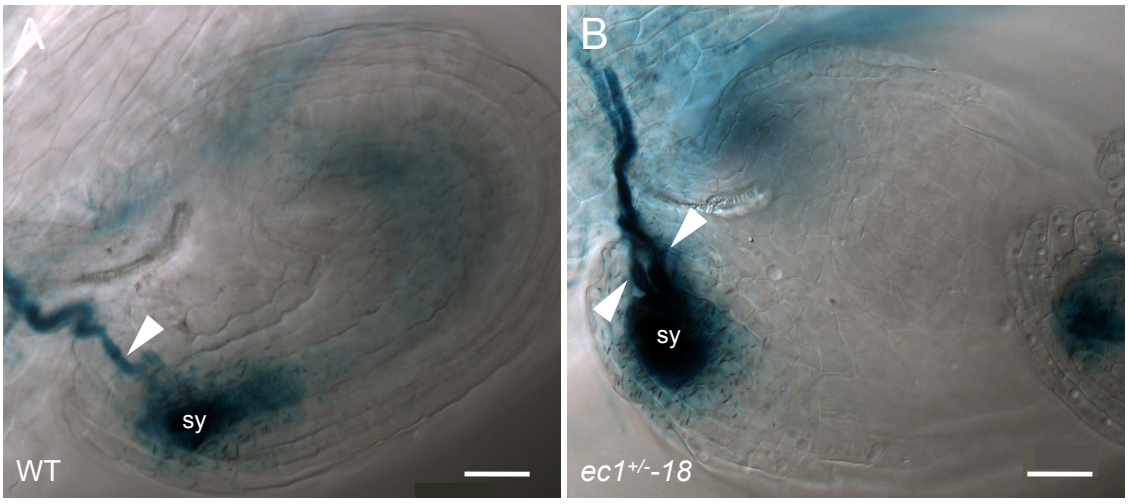

Figure 12: DIC microscopy analysis of pollen tube guidance of *ec1*$^{+/-}$ ovules. GUS histochemical staining after pollination with the pollen tube marker line P_{ARO1}*:GUS*.
A Wild type ovule targeted by one pollen tube (blue GUS staining, arrowhead). Receptive synergid cell (sy) is stained blue. **B** *ec1*$^{+/-}$*-18* ovule targeted by two pollen tubes (blue GUS staining, arrowheads indicating the entry of multiple pollen tubes). Receptive synergid cell shows strong GUS staining (sy). Bars = 20 μm.

Figure 12A shows a wild type ovule targeted by one pollen tube visualized through histochemical GUS staining. In addition to the pollen tube also the synergid cell was

strongly stained. This effect can be explained by pollen tube rupture and subsequent release of its content into the receptive, degenerating synergid cell. Ovules of *ec1*$^{+/-}$ plants also attracted pollen tubes. This experiment showed that pollen tube attraction was not altered in *ec1*$^{+/-}$ ovules, moreover, that pollen tubes stop growth as in wild type ovules and that pollen tube reception occurs as indicated by the pollen tube rupture and release of its content. This conclusion was evidenced by the blue staining of the synergid. This fact in turn means that the receptive synergid cell must have degenerated before pollen tube reception, as reported by Sandaklie-Nikolova *et al*. (2007). In some cases also multiple pollen tubes entered *ec1*$^{+/-}$ embryo sacs (Figure 12B, arrowheads, see section 5.3.5, page 47). Apart from this, pollen tube growth and targeting towards mutant ovules seemed to be comparable to the wild type situation.

5.3.5 Quantification of non-fused sperm cells within *ec1*$^{+/-}$ ovules

Ovules in wild type pistils are reached by pollen tubes approximately five to eight hours after pollination. Karyogamy between female and male gametes takes place after three to four additional hours (Ingouff *et al.*, 2007). Wild type and *ec1*$^{+/-}$ lines were hand pollinated with pollen of the sperm cell marker line *HTR10-mRFP1* (Ingouff *et al.*, 2007) and the developing seeds were analyzed by fluorescence microscopy 30 to 40 hours later. As mentioned before (see section 3.6, page 16), the phenotype of non-separating and non-fusing sperm cells had already been observed in *ec1*$^{+/-}$ mutant ovules (Figure 13A, B). In order to get more information about this phenotype, quantifications of pollination experiments with the sperm cell marker line were performed (Figure 13C).

Four independent lines were analyzed in more detail (*ec1*$^{+/-}$*-4*, *-9*, *-16* and *-18*). In wild type siliques, sperm cells were only detectable in 3% of the ovules. In these few cases probably multiple pollen tube attraction accidently occurred. In 97% of the ovules seeds were developing normally, i.e. sperm cells had been delivered, separated and fused with the female gametes and were thus no longer detectable. Fluorescence of mRFP1 is becoming weaker due to chromatin decondensation, which starts about two hours after sperm cell discharge. Later after fertilization HTR10-mRFP1 is no longer detectable, because paternally contributed HISTONE 3 (H3) variants including HTR10 are actively removed from the zygote within a few hours and the *HTR10* promoter is switched off (Ingouff *et al.*, 2007; Ingouff *et al.*, 2010).

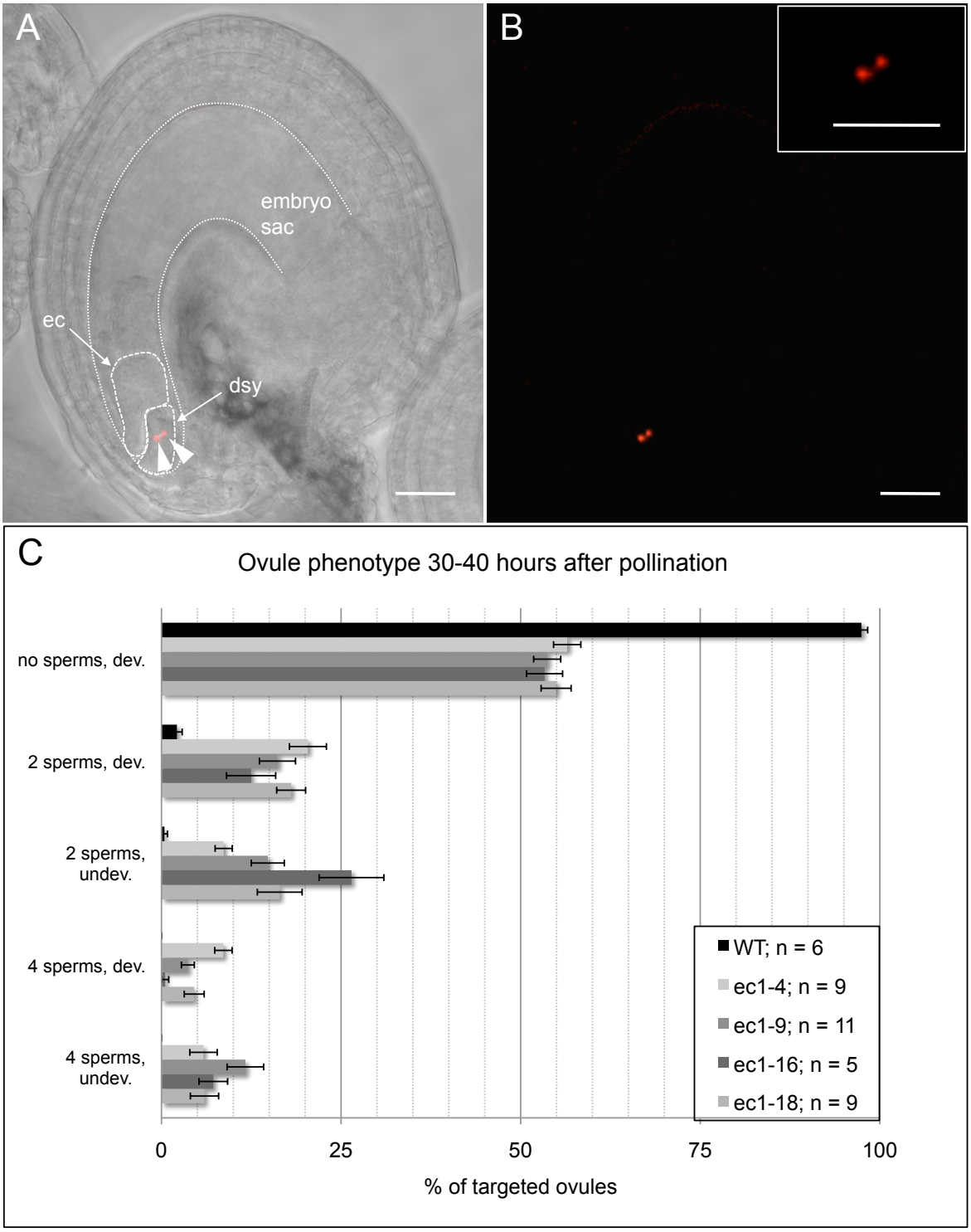

Figure 13: Fluorescence microscopy analysis and quantification of the *ec1*$^{+/-}$ ovule phenotype during double fertilization.
A Overlay of DIC and mRFP1 fluorescence channel. Fluorescence of HTR10-mRFP1 in sperm cell nuclei is shown in red (arrowheads). Sperm cells are located within the degenerated synergid cells (dsy). The margins of the egg cell (ec) and the embryo sac, respectively, are indicated by a dotted line. **B** mRFP1 fluorescence channel only of the same preparation. The sperm cell nuclei are shown in red. Inset: close up of the sperm cell pair. Bars = 20 µm. **C** Quantification of phenotypes in % of targeted ovules, divided into five different categories: Dev. = developed; enlarged embryo sac; undev. = undeveloped; small embryo sac. n = number of siliques counted ± standard error (bars).

Sperm cells that had been delivered to *ec1*$^{+/-}$ ovules fused only in 53.3% to 56.7% of all ovules and were thus not detectable any more (Figure 13C). Instead, four additional phenotypes were observed at significantly high percentages in *ec1*$^{+/-}$ ovules. A pair of two sperm cells within a rather small, likely unfertilized embryo sac was observed in 8.7% to 26.5% of ovules. A sperm cell pair within an enlarged embryo sac was observed in 16.1% to 20.4% of the ovules. At frequencies of less than 10% and 12%, respectively, four sperm cells were observed in enlarged embryo sacs and small embryo sacs, respectively (Figure 13C). Deduced from these data, multiple pollen tube attraction occurred in at least 13% of *ec1*$^{+/-}$ ovules (mean value of four independent lines). In summary, in approximately 45% of the ovules of *ec1*$^{+/-}$ plants non-fused sperm cells were observed within the female gametophyte.

5.3.6 Microscopy analysis of developing seeds from *ec1*$^{+/-}$ siliques

The pollination experiment described in the previous section revealed a phenotype-frequency of about 45%, which was not consistent with the percentage of seed abortion in *ec1*$^{+/-}$ plants with only 38% of aborted seeds. This suggests that some of the ovules accumulated EC1 protein over time thus enabling the sperm cells to eventually fuse with the egg cell and the central cell. To investigate this hypothesis, the morphologies of developing seeds from 5 mm siliques of selfed *ec1*$^{+/-}$ plants were analyzed in detail by DIC microscopy.

Of wild type seeds from 5 mm siliques 99% contained embryos at the four-celled or the octant-stage (Figure 14A, G). These stages were only observed in about 43% of ovules of *ec1*$^{+/-}$ plants (Figure 14B, G). The remaining phenotypes mainly comprised either ovules that were not fertilized but containing intactly appearing central and egg cells (Figure 14C, G) or ovules that seemed to be degenerating without any clearly detectable cell structure within the female gametophyte (Figure 14D, G). Delayed developmental stages like zygote or two-celled proembryo with only two or four endosperm nuclei were also observed, but only at frequencies below 5% (Figure 14E, F, G). This indicates that the phenotype of the unfertilized ovules with intact egg and central cells could be regarded as intermediates that have not been fertilized yet but are still capable of being fertilized.

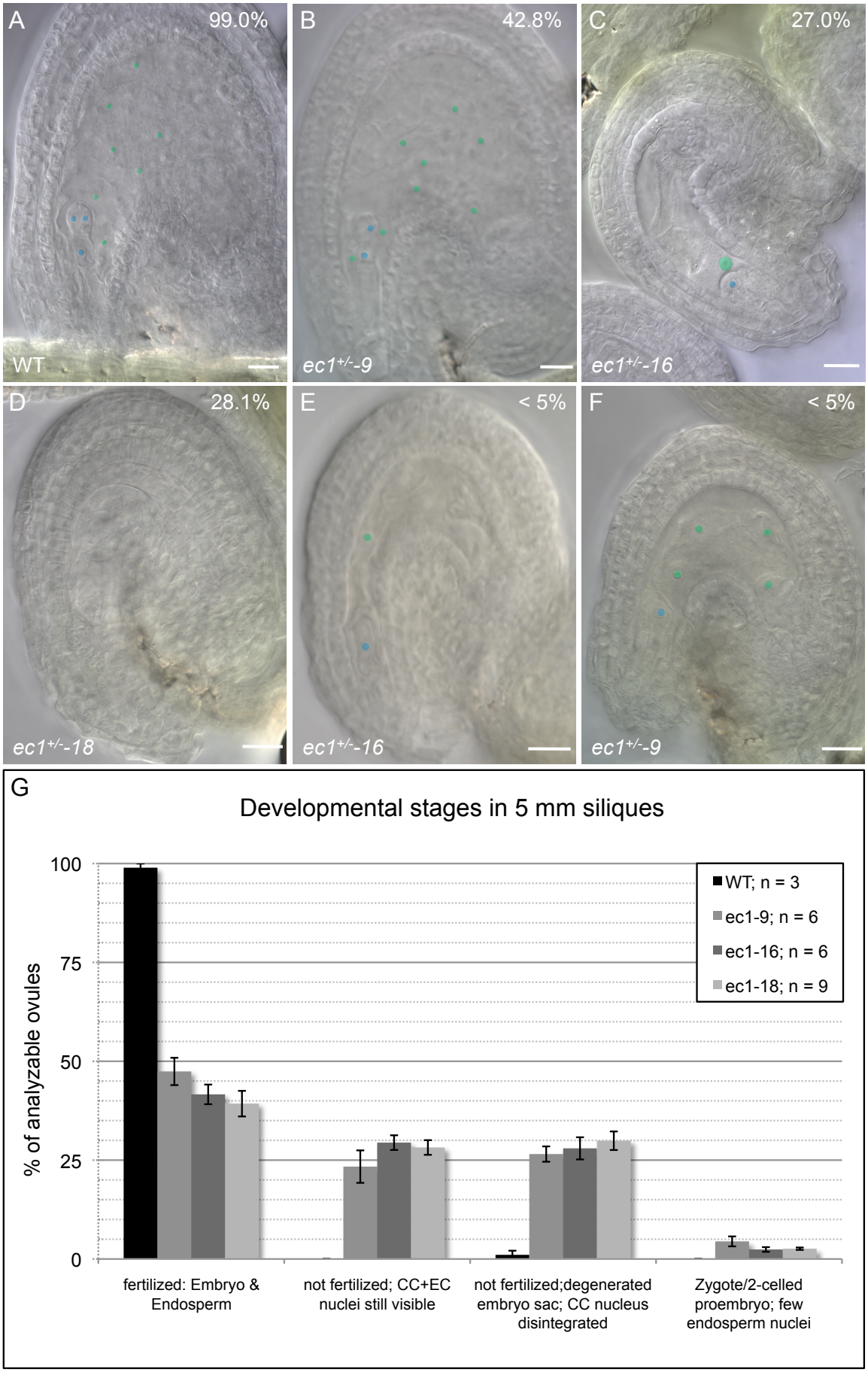

Figure 14: legend on next page

Legend for Figure 14: Developmental stages of developing seeds in 5 mm siliques of *ec1*$^{+/-}$ plants.
A – **F** DIC microscopy analysis of developing seeds of 5 mm siliques after clearing. Egg cell, zygote or embryo nuclei are artificially colored in blue; endosperm or central cell nuclei are artificially colored in green. The frequency of the observed phenotype is given in the upper right corner of the image. Bars = 20 μm. **A** Wild type seed at the four-celled embryo stage. **B** Ovule at the four-celled embryo stage of an *ec1*$^{+/-}$*-9* line. **C** Unfertilized ovule of an *ec1*$^{+/-}$*-16* line. Central and egg cell nuclei are clearly detectable. **D** Degenerating ovule of an *ec1*$^{+/-}$*-18* line. Identification of cell structures within the female gametophyte is not possible. **E** *ec1*$^{+/-}$*-16* ovule at the elongated zygote stage with its nucleus in the middle. The endosperm is probably two-celled. **F** Two-celled proembryo in an ovule of an *ec1*$^{+/-}$*-9* line with four endosperm nuclei. **G** Quantification of various phenotypes shown in A-F in wild type and three independent *ec1*$^{+/-}$ lines (-9, -16, -18). n = number of siliques counted ± standard error (bars).

5.3.7 Pollination of *ec1*$^{+/-}$ plants with single sperm pollen

The genetic and cellular data indicate, that EC1 is necessary during gamete fusion. However, because the sperm cells were always observed as a pair we asked whether the EC1 protein is required for gamete fusion or rather for gamete separation. To address this question, a genetic approach was used. Iwakawa *et al*. (2006) and Nowack *et al*. (2006) characterized the *Arabidopsis* mutant *cyclin dependent kinase a;1* (*cdka;1*) that has a defect during the second mitotic division in pollen development. A mature *Arabidopsis* pollen grain is tricellular consisting of one vegetative and two sperm cells. The defect in *CDKA;1* leads to bicellular pollen consisting of one vegetative cell and only one sperm-like cell. Developing seeds resulting from a single fertilization event abort later on, but since the single sperm is able to fertilize the egg cell (Iwakawa *et al.*, 2006; Nowack *et al.*, 2006) this mutant was used to analyze its ability to fuse with *ec1* female gametes. If EC1 was exclusively required for sperm cell separation, then the single sperm cell would be expected to fuse with one of the female gametes and would not be visible 30 hours after pollination. If, however, EC1 was needed for fusion of male and female gametes, the single sperm would not be expected to fuse. The numbers of single sperm pollen within the pool of all pollen grains of a heterozygous *cdka;1*$^{+/-}$ plant differ among the analyzing labs: Iwakawa *et al*. (2006) reported 48.7% bicellular pollen and Nowack *et al*. (2006) 41.9%. Recently, Aw *et al*. (2010) found that the number of bicellular pollen decreases continuously during *in vitro* pollen tube growth assays. After 20 hours only 34% of the pollen tubes contained one sperm cell (Aw *et al.*, 2010). Since these variations might be caused by different growth conditions (A. Schnittger, F. Berger, personal communications), the number of single sperm cells in pollen grains and in pollen tubes after 20 hours of germination was determined for *HTR10-mRFP1/cdka;1*$^{+/-}$ plants grown in our growth chambers by counting red

fluorescing sperm cell nuclei. At anthesis, *HTR10-mRFP1/cdka;1*$^{+/-}$ plants contained 48% bicellular pollen grains (n = 4424). Eight to nine hours after germination 43% of pollen tubes contained single sperm cells (n = 402) and 20 hours after germination 40% of pollen tubes contained single sperms (n = 428). These results further supported the above described findings that the ability of *cdka;1* sperm cells to undergo the second mitotic division during pollen tube growth might dependent on growth conditions and male germline maturation.

Based on these data and on the pollination experiments of *ec1*$^{+/-}$ plants with *HTR10-mRFP1* pollen, the expected numbers for the two possible scenarios after pollination of *ec1*$^{+/-}$ with *HTR10-mRFP1/cdka;1*$^{+/-}$ were calculated as described in Figure 15.

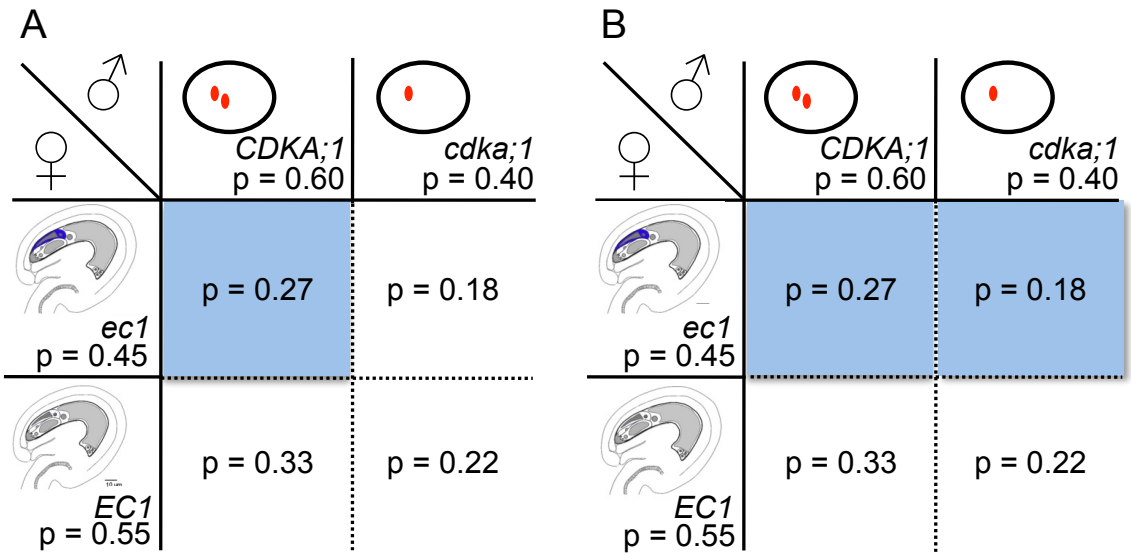

Figure 15: Expected numbers of phenotype combination after pollination of *ec1*$^{+/-}$ plants with *cdka;1*$^{+/-}$ pollen.
Probability of phenotypes of parental plants are indicated (single sperm cell, wild type sperm cells (sperm cell pair)); *ec1* embryo sac with later non-fusing sperms, wild type embryo sac, later fusing sperms). Numbers in big squares represent the probability of phenotype combination during pollination/fertilization. Blue squares represent the proportion of ovules with non-fused sperm cells. **A** Single sperms are able to fuse; i.e. only sperm cell pairs will not fuse in *ec1* ovules (27%). **B** Single sperms are also not able to fuse with *ec1*; i.e. 45% of all ovules show non-fused sperm cells (27% plus 18%).

The probability for a pair of sperm cells (mainly of *CDKA;1* genotype) to be delivered to an *ec1* mutant ovule would be 27% and for a single sperm 18%. If the single sperm cell was able to fuse with one of the female gametes in *ec1* ovules, then this category would add on the wild type ovule category, in which fusion of a sperm pair or a single sperm takes place. This means that non-fused sperm cells would occur in 27% of all ovules (Figure 15A, blue square). However, if the single sperm cell was

also not able to fuse in *ec1* ovules, then the same percentage of fused and non-fused sperm cells would be expected like in pollination experiments with wild type pollen (45% non-fused).

In wild type ovules hardly any non-fused sperm cells were detectable, no matter whether wild type or single sperm pollen was used for pollination (Figure 16, black bars). In contrast, there was a clear difference in *ec1*$^{+/-}$ ovules after wild type and single sperm pollination. As described before, pollination with wild type pollen resulted in non-fused sperms in 45% of the ovules. When pollen of the *cdka;1*$^{+/-}$ mutant was used, the number of ovules with non-fused sperm cells was about 23% (Figure 16, mean value of three independent lines). A t-test was performed and revealed a significant difference between the pollination with wild type and *cdka;1*$^{+/-}$ pollen for all three independent lines ($p \leq 0.01$).

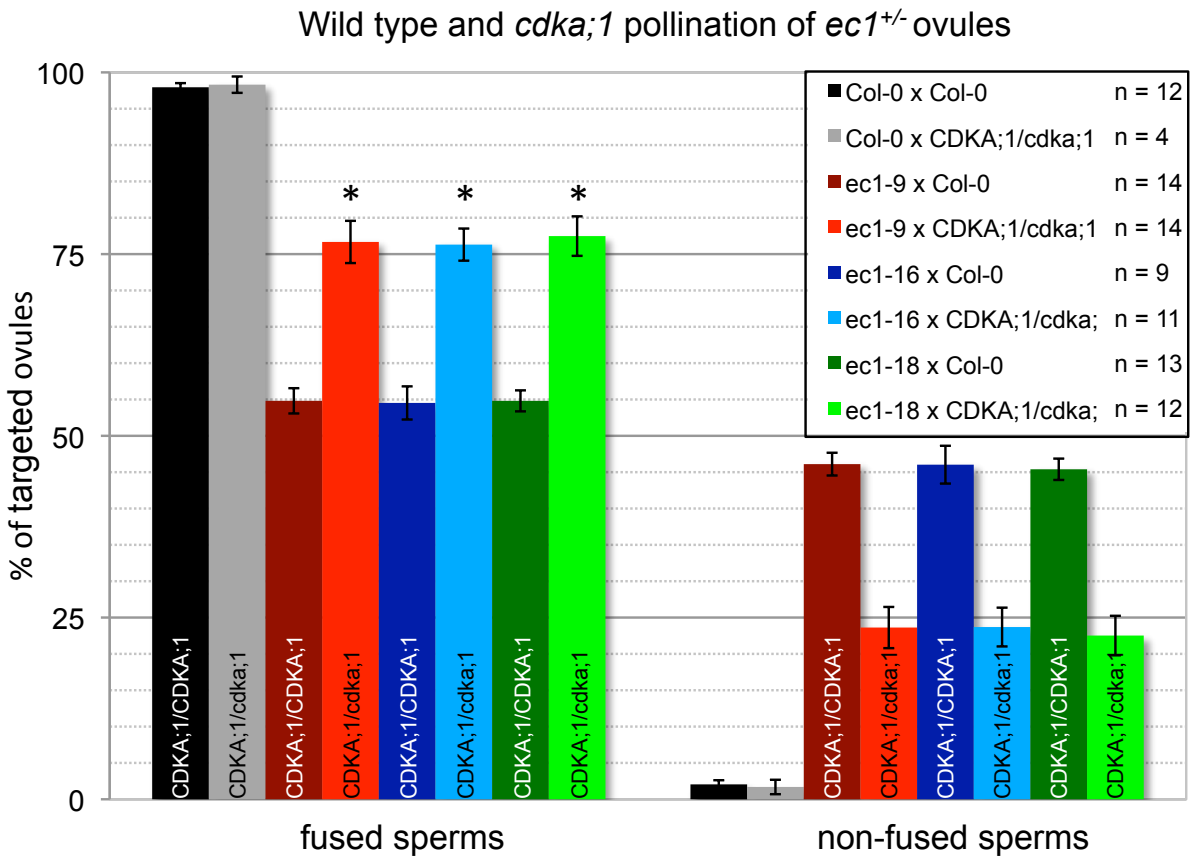

Figure 16: Pollination of *ec1*$^{+/-}$ plants with wild type pollen and pollen from *cdka;1*$^{+/-}$ plants.
Wild type and *ec1*$^{+/-}$ (*-9, -16, -18*) plants were pollinated with HTR10-mRFP1 marked wild type pollen or pollen of *cdka;1/CDKA;1* plants (also marked with HTR10-mRFP1). Fluorescence microscopy analysis was performed 30 to 40 hours after pollination. The number of targeted ovules was determined in two categories fused sperms and non-fused sperms (comprising all categories of non-fused sperms). The number of siliques counted is indicated (n) ± standard error (bars). * significant difference between wild type and *cdka;1/CDKA;1* pollination.

The percentage of ovules with non-fused sperms was even slightly smaller than expected. This finding can be explained by the fact that if single sperms fuse, multiple pollen tube attraction may not occur in these ovules, but happens in a considerable amount of *ec1* ovules when pollinated with wild type pollen. Single non-fused sperm cells were detected in rare cases (below 5%) in *ec1*$^{+/-}$ as well as in wild type ovules. This pollination experiment indicated that EC1 is required rather for a process upstream of gamete fusion, for example sperm cell separation.

5.3.8 Pollination of *ec1*$^{+/-}$ plants with *generative cell specific1* mutant pollen

Mori *et al*. (2006) and von Besser *et al*. (2006) characterized a mutant that shows a phenotype similar to *ec1*$^{+/-}$. *GENERATIVE CELL SPECIFIC 1* (*GCS1*) is specifically expressed in sperm cells and encodes a protein with an N-terminal extracellular domain, one transmembrane domain and a C-terminal histidine-rich part of unknown function. A mutation of *GCS1* leads to defects in pollen tube guidance and gamete fusion defects. Transmission of the mutant allele by the male gamete is severely affected (Mori *et al.*, 2006).

The *ec1*$^{+/-}$ lines were pollinated with *HTR10-mRFP1/gcs1*$^{+/-}$ and the number of ovules with non-fused sperm cells was determined by fluorescence microscopy as in the previously described experiments. Since the *ec1* phenotype is only transmitted through the female side, whereas the *gcs1* phenotype is exclusively caused by a defect on the male side, an additive phenotype related to the frequency was expected. In control experiments, where wild type plants were pollinated with *gcs1*$^{+/-}$pollen, non-fused sperms were observed in 22% of all ovules (n = 97). This value served as a reference and is similar to previously published results (Mori *et al.*, 2006). Importantly, only 71% of the ovules developed into seeds. The remaining 7% ovules seemed to contain a collapsed female gametophyte, which may result from the additional pollen tube guidance defect that has been reported for this mutant (von Besser *et al.*, 2006). The pollination of *ec1*$^{+/-}$ with *gcs1*$^{+/-}$ resulted in 45% of all ovules exhibiting non-fused sperms, whereas fertilization only occurred in 36% of all ovules (n = 252). In this experiment the female gametophyte had collapsed even in 19% of the ovules.

Taken together, after pollination of *ec1*$^{+/-}$ plants with wild type and *gcs1*$^{+/-}$ pollen the ratio of ovules with non-fused sperms to ovules with fused sperm cells changed from 1:1.2 to 1:0.8. As expected the amount of ovules with non-fusing sperms increased compared to the crossing of wild type plants with *ec1*$^{+/-}$ and *gcs1*$^{+/-}$ plants, respectively.

The experiments described above show that the egg cell-specific, small and secreted protein EC1 seems to be necessary for gamete interaction during double fertilization. The loss of *EC1* lead to a reduced seed set due to defects in double fertilization. Pollen tube guidance, reception and burst as well as gamete delivery were not affected. However, the sperm cells did not separate and as a consequence fusion with the female gametes did not take place. Pollination experiments with single sperm pollen supported the hypothesis that sperm cell separation was affected in *ec1*$^{+/-}$ ovules rather than gamete fusion.

5.4 Expression of *EC1* and protein purification

In addition to the genetic data about *EC1* function, biochemical approaches were taken to further understand the function and mechanistic activity of the protein. Therefore, *EC1* was fused to various tags and overexpressed *in planta* or heterologously in yeast or *E. coli* for subsequent affinity purification. The protein should then be used in a bioassay to analyze its ability to separate the two sperm cells *in vitro*. Moreover, the EC1 protein could be used to study the binding capacity to the sperm cell surface.

5.4.1 Expression of *EC1.1 in planta*

First, it was aimed to purify the protein from plants because EC1 proteins are cysteine-rich and the correct formation of disulfide bonds in heterologous systems is critical and might cause problems especially in *E. coli* (see Appendix for predicted disulfide bond formation, page 104). *Arabidopsis* plants expressing *EC1.1* under control of the strong *Cauliflower Mosaic Virus 35S* (*CaMV35S*) promoter had already been generated in a previous project (B. Bellmann). The transgenic plants did not display an altered phenotype in comparison to wild type plants. Although the transcript of *EC1* was detected in leaves by reverse transcriptase-PCR in large amounts in all lines tested (data not shown), the presence of the protein remained questionable since there was no antibody for immunodetection available. To circumvent this problem, plants were generated that expressed a fusion of *EC1.1* and *enhanced Green Fluorescent Protein* (*eGFP*) under control of the *CaMV35S* promoter (RAS7). The fusion protein should then be easily detectable by fluorescence microscopy. However, eGFP fluorescence was not detected in all tissues tested. To exclude that the transgene was not transcribed, the presence of transcript was proven by RT-PCR. A possible reason for the absence of the protein might be down-regulation or translational inhibition in stably transformed plants since the EC1.1 protein might be harmful for cells. Therefore, the *EC1.1-eGFP* construct was expressed transiently in *Nicotiana benthamiana* by agrobacteria infiltration. A fusion of the amino acid transporter CAT6 and eGFP, which localizes to Golgi vesicles and the plasma membrane (U. Hammes, unpublished), was used as a positive control. For the evaluation of autofluorescence a non-infiltrated leaf served as a negative control. Agrobacteria were transformed with the respective constructs (pRAS7, P_{35S}:CAT6-eGFP) and infiltrated into the abaxial side of *N. benthamiana* leaves. Two

and three days after infiltration, eGFP fluorescence was analyzed microscopically. The control experiment showed strong eGFP fluorescence in Golgi vesicles and the plasma membrane as expected (Figure 17B). However, fluorescence was not detected in leaves infiltrated with EC1.1-eGFP (Figure 17A). These leaves were not distinguishable from leaves that had not been infiltrated (Figure 17C).

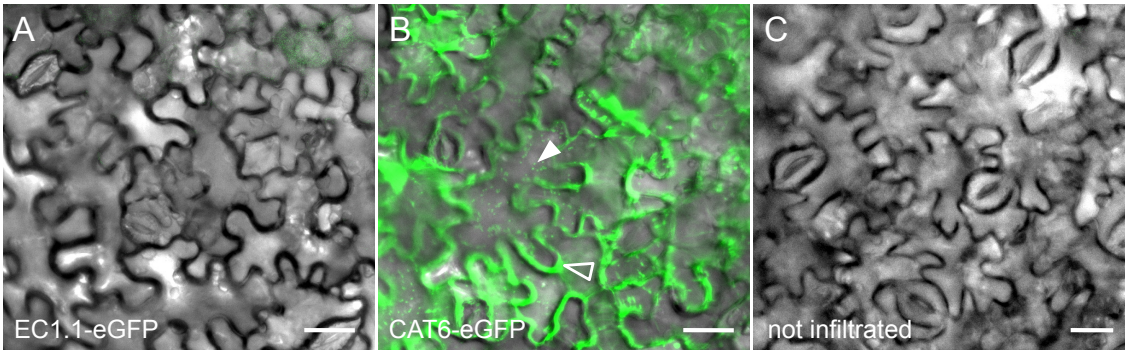

Figure 17: Fluorescence microscopy of transiently expressed *EC1.1-eGFP* in *N. benthamiana* leaf epidermal cells, 48 hours after infiltration.
A Leaf after infiltration with *EC1.1-eGFP*. eGFP fluorescence was not detectable. **B** Control experiment: *CAT6-eGFP* infiltrated leaf showing strong eGFP fluorescence in Golgi vesicles (closed arrowhead) and the plasma membrane (open arrowhead). **C** Negative control: non-infiltrated leaf. All images are overlays of bright field and eGFP fluorescence channels. Bars = 20 μm.

Taken together, the EC1.1-eGFP fusion protein seemed not to be present in stably transformed *Arabidopsis* plants as well as in transiently transformed *N. benthamiana* leaf epidermal cells, at least not above the fluorescence detection limit. These two *in planta* systems were thus not suitable for *EC1.1* expression and purification of the protein.

5.4.2 *EC1.1* expression in *Pichia pastoris*

The protein expression system in *Pichia pastoris* has been reported to be very useful (Macauley-Patrick *et al.*, 2005), especially for expression of genes encoding cysteine-rich proteins (Invitrogen). The EasySelect™ *Pichia* Expression Kit from Invitrogen can be used with a vector comprising an N-terminal α-factor secretion signal from *Saccharomyces cerevisiae* targeting the protein to the medium. Since EC1 is also a secreted protein, this vector was used to ensure similar targeting and similar conditions like pH and redox status. Moreover, this system comprises a methanol inducible promoter (*AOX1*). To the 3' end of the *EC1.1* coding sequence a c-myc-tag and a 6xHis-tag were fused for later protein purification.

The *Pichia pastoris* strain expressing *EC1.1* and the respective wild type strain (X-33) were grown in the respective medium. Samples of the growth medium were taken before induction (t = 0), 24 hours (t = 24 h) and 48 hours after induction (t = 48 h) and analyzed for target protein induction by Western Blot analysis using a c-myc antibody (Figure 18A). Before induction, a signal was not detected in wild type or in the *EC1.1* expressing strains. After 24 hours of induction, a clear signal was detected in the strain expressing *EC1.1*, which became even stronger 48 hours after induction. The signal did not appear in a clear, distinct band but was rather diffuse. The calculated molecular weight of EC1.1-c-Myc-6xHis including the tags was 17.5 kDa, which approximately overlapped with the size of the bands detected on Western Blots (Figure 18A, B, lower image).

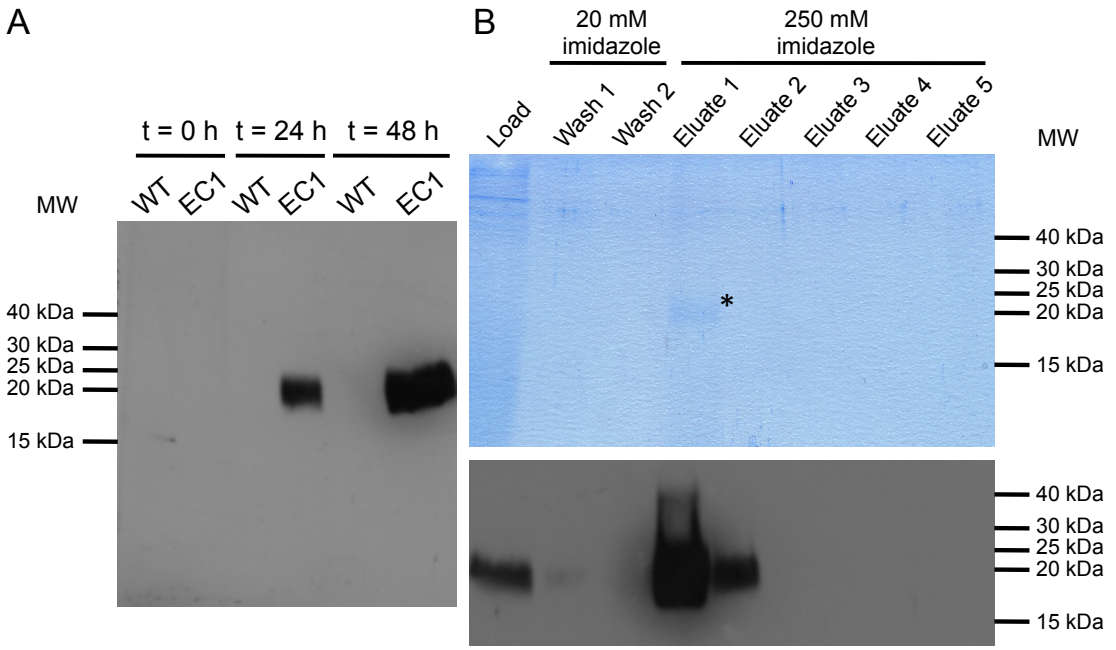

Figure 18: Induction of *EC1* expression in *Pichia pastoris* and purification with Ni-NTA agarose.
A Western Blot: accumulation of EC1 protein in the medium at 24 hours and 48 hours after induction of target protein expression cells with methanol. 5 µg of total protein was loaded (concentration determined by a Bradford assay). EC1-c-Myc-6xHis was detected with a c-myc antibody. **B** Purification of EC1-c-Myc-6xHis with Ni-NTA agarose via gravity flow. Upper image: Coomassie stained SDS-gel after separation of different fractions of purification. A faint, diffuse band of approximately 20 kDa is detectable in the eluate 1 fraction (asterisk). Lower image: Western Blot with the same samples as shown on the Coomassie stained gel above. EC1-c-Myc-6xHis was detected with a c-myc antibody.

For EC1.1 purification, cells were grown for 48 hours in induction medium. After cells had been removed by centrifugation, the supernatant was loaded onto a Ni-NTA column via gravity flow. The column was washed with sodium phosphate buffer containing 20 mM imidazole and the protein was eluted with 250 mM imidazole in five

fractions. The analysis of the different fractions on a Coomassie stained SDS-gel revealed poor purification efficiency. Only a very faint, diffuse band occurred in the first fraction after elution (Figure 18B, asterisk). Another gel, loaded with the same samples was blotted onto a PVDF membrane after gel electrophoresis. After immunodetection with an anti-c-myc antibody, a very strong band was detected in the first fraction of elution. Signals were also detectable in the fraction that was loaded onto the column and in the first washing fraction, whereas the latter one was very weak (Figure 18B, lower image). The faint Coomassie band seemed to correlate in size with the signals on the Western Blot.

To improve the purification efficiency, the experiment was scaled up by increasing the culture volume. In the experiment described above, the supernatant was 100 ml and had been loaded after 4.5 hours. However, after upscaling, the time for loading the column was up to ten hours, which might have been the reason for even worse results after purification. Bands were no longer detectable on Coomassie stained gels and much weaker signals occurred on the Western Blot. To reduce and minimize the time of the whole purification procedure, the batch method by incubating Ni-NTA agarose with the supernatant and subsequent packing of the column was carried out. Since also this method did not lead to satisfying results, purification of EC1.1 produced in *P. pastoris* was carried out using a HisTrap™ column that was connected to an Äkta™ purification system. First, the supernatant was loaded with a peristaltic pump, which strongly reduced the time of loading by at least ten fold so that protein purification of larger culture volumes could be carried out. The Äkta™ purification profile of the supernatant of *EC1.1* expressing *P. pastoris* with a HisTrap™ column is shown in Figure 19A. The photometric measurement at 280 nm (Figure 15A, blue line) during protein purification shows only a small peak in the elution fractions A4 to B8. Nevertheless, these 17 fractions were combined and analyzed by SDS-PAGE. The Coomassie stained SDS gel showed a clear enrichment of one band of about 30 kDa. Since this size did not agree with the calculated molecular weight of 17.5 kDa for EC1.1-c-Myc-6xHis, the same samples were also blotted onto a PVDF membrane after gel electrophoresis to check for specificity. However, the signal on the Blot had a size of about 20 kDa as it had already been observed in the experiments before (Figure 18). The band of the enriched protein on the Coomassie stained gel was not identical to the signal obtained on the Western Blot, which means that another protein but not EC1.1-c-Myc-6xHis had been purified.

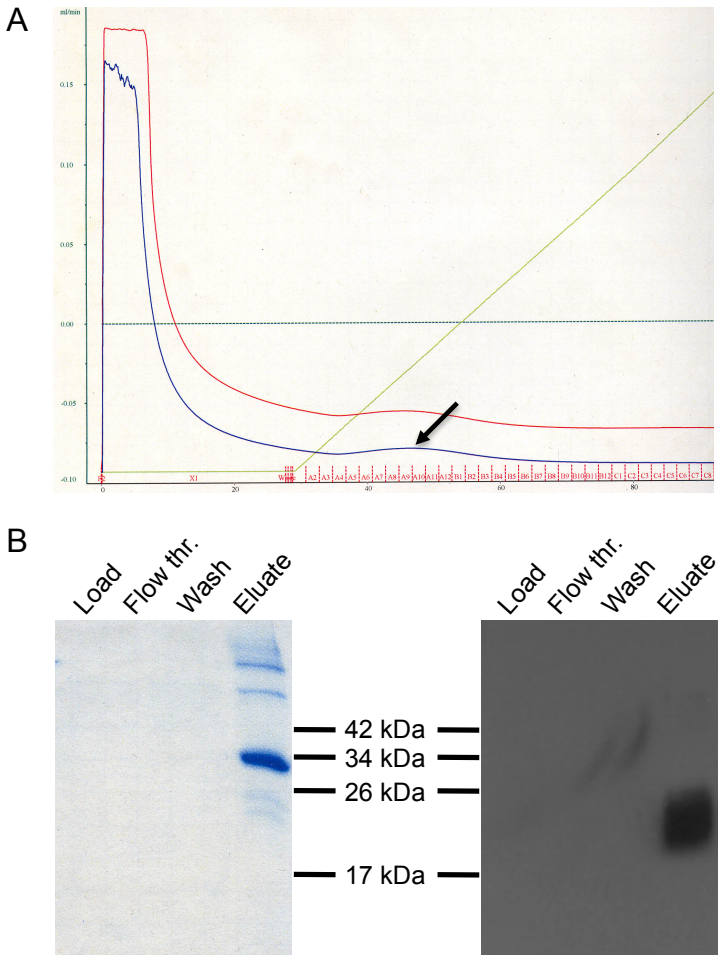

Figure 19: HisTrap™ purification of the supernatant of *EC1.1* expressing *P. pastoris* strain.
A Äkta™ purification profile of the supernatant of *P. pastoris* expressing *EC1.1*. The blue line shows the absorption of protein in each fraction by photometric measurement at 280 nm. A slight peak is visible in fraction A4 to B8 (arrow). These fractions were combined for SDS-PAGE and Western Blot analyses shown in B. The red line shows the absorption at 260 nm. The light green line indicates the applied gradient of increasing imidazole concentration during the elution and the dark green line shows the constant flow rate of 4 ml/min. **B** Coomassie stained SDS gel (left side) and Western Blot after detection of EC1.1-c-Myc-6xHis with an anti-c-myc antibody. Coomassie stained gel shows a strong band in the eluate fraction of approximately 30 kDa. Signal on the Western Blot in the eluate fraction corresponds to a size of about 20 kDa.

Since obviously a non-target protein from the *Pichia* growth medium had a much higher affinity to Ni-NTA agarose, the *Pichia* system was set aside for heterologous expression and purification of EC1.1.

5.4.3 Expression of *EC1* in *E. coli*

The EC1 proteins possess six cysteine residues that may form up to three disulfide bonds. Therefore, *E. coli* was not the expression system of first choice because disulfide bond formation in the reducing *E. coli* cytoplasm occurs only rarely. Nevertheless, *EC1*

genes were expressed in different *E. coli* strains because all other attempts of heterologous expression failed. The coding sequences without the predicted signal peptide of all five *EC1* genes (*EC1.1*, *EC1.2a*, *EC1.2b*, *EC1.4* and *EC1.5*) were recombined into the pGEX-2-GW vector generating translational fusions of an N-terminal glutathione-S-transferase (GST) and EC1. For *EC1.2a*, the coding sequence was additionally recombined into pET-53-DEST™ for N-terminal His•Tag® fusion and C-terminal Strep•Tag®II fusion. First, all expression vectors were used for transformation of the Rosetta™ strain and target protein expression was analyzed by SDS-PAGE four hours after induction with IPTG. For the *E. coli* strain transformed with the GST-EC1.2b fusion, the expression of a protein of 26 kDa was induced, which is the size of the GST alone. In all other strains expressing *EC1.1*, *EC1.2a*, *EC1.4* or *EC1.5* the size of the induced protein overlapped with the calculated molecular weight of the fusion proteins of 40 to 44 kDa (data not shown). However, the fusion proteins were insoluble (see also Figure 21 for GST-EC1.1), probably aggregating in inclusion bodies.

To avoid solubilization of EC1 from inclusion bodies and refolding of the protein before purification, EC1 solubility was analyzed in different *E. coli* strains. First, ArcticExpress™ cells were transformed with the expression vectors. ArcticExpress™ cells carry a plasmid with genes encoding cold-adopted chaperonins. These possibly enhance the solubility of critical target protein expression in cells grown at 4 to 12°C. However, SDS-PAGE analyses of samples before and after induction showed that target protein expression did not occur at all, only one of the chaperonins was detectable in large amounts (not shown). Therefore, the expression of *EC1* in ArcticExpress™ was no longer followed up.

The Origami™ *E. coli* strain carries mutations in the thioredoxin reductase (*trxB*) and the glutathione reductase (*gor*) gene, which strongly enhance disulfide bond formation in the cytoplasm. SDS-PAGE analyses of Origami™ cells expressing *GST-EC1.1* or *6xHis-EC1.2a-Strep* revealed that also in these cells the target protein is insoluble (not shown).

Finally, expression of *EC1.2a* was carried out in the Lemo21 strain that carries the pLEMO plasmid encoding lysozyme. Lysozyme is an inhibitor of the T7 RNA Polymerase and is under control of an L-rhamnose inducible promoter on pLEMO. The target protein expression from *T7* based inducible promoters can thus be tuned depending on the amount of added L-rhamnose. Indeed, a proportion of

6xHis-EC1.2a-Strep was found in the soluble fraction of proteins, using this expression system (not shown).

To combine the property of the Origami™ strain allowing disulfide bond formation in the cytoplasm and of Lemo21 to achieve solubility of the target proteins, Origami cells were simultaneously transformed with pLEMO and the *EC1.2a* expression vector. It seemed that in these newly generated LemoGami cells, some target protein was soluble. Figure 20 shows Coomassie stained gels after SDS-PAGE of LemoGami samples grown with different concentrations of L-rhamnose.

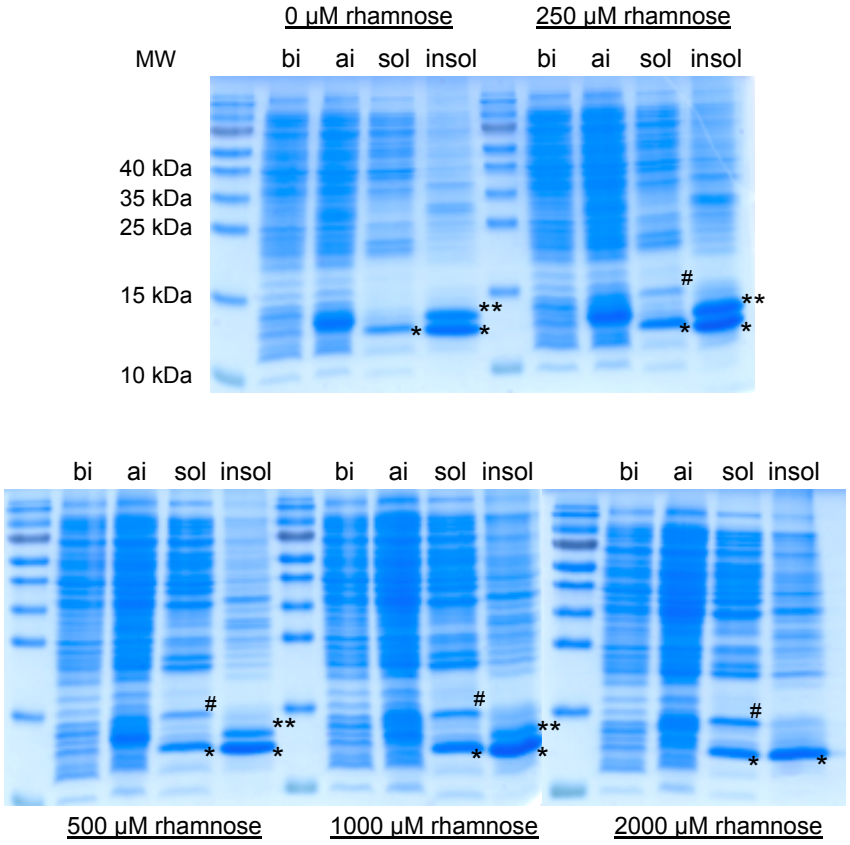

Figure 20: Analysis of *6xHis-EC1.2a-Strep* expression in LemoGami cells by SDS-PAGE (Coomassie staining).
Expression of *6xHis-EC1.2a-Strep* was analyzed without L-rhamnose and with 250 µM, 500 µM, 1000 µM and 2000 µM L-rhamnose during induction of target protein expression with IPTG. Increasing intensity of the lysozyme band (#, 14 kDa) is detectable. Two additional bands of different sizes (*, **) are also visible in the soluble (sol) and the insoluble (insol) fraction of proteins. bi = cells before induction; ai = cells after induction.

The band that only appeared after the addition of L-rhamnose and became stronger with increasing L-rhamnose concentrations represents lysozyme (Figure 20, sharp) with an expected size of approximately 14 kDa. Moreover, two other bands occurred that seemed to be induced. Without addition of L-rhamnose, one band is detectable in the soluble and the insoluble fraction (Figure 20, asterisk) and another more slowly

migrating band only occurs in the insoluble fraction (Figure 20, two asterisks). The more L-rhamnose was added to the medium, the fainter this band became until it eventually disappeared at 2000 µM L-rhamnose. With the larger band becoming fainter, the intensity of the smaller one seemed to increase. The calculated molecular weight of 6xHis-EC1.2a-Strep was 16.3 kDa. Because of that, EC1 would have been expected to migrate more slowly than lysozyme, however, this was not the case. Nevertheless, it was tried to purify the 6xHis-EC1.2a-Strep fusion from LemoGami cells, but without success. After SDS-Page and Coomassie staining only unspecific bands were detected in the elution fractions without any enrichment of the target protein (not shown).

Due to the lack of success with the expression of recombinant EC1 protein in other *E. coli strains*, the inclusion bodies from *GST-EC1.1* expressing Rossetta™ cells were solubilized with the detergent N-lauroylsarcosine. After dialysis and refolding, the fusion protein was purified via GSTrap™ 4B column. Although most of the GST-EC1.1 protein did not bind, which became evident by the strong signal in the flow through, a single, clean band of the expected size occurred in three of the elution fractions (Figure 21, E2- E4).

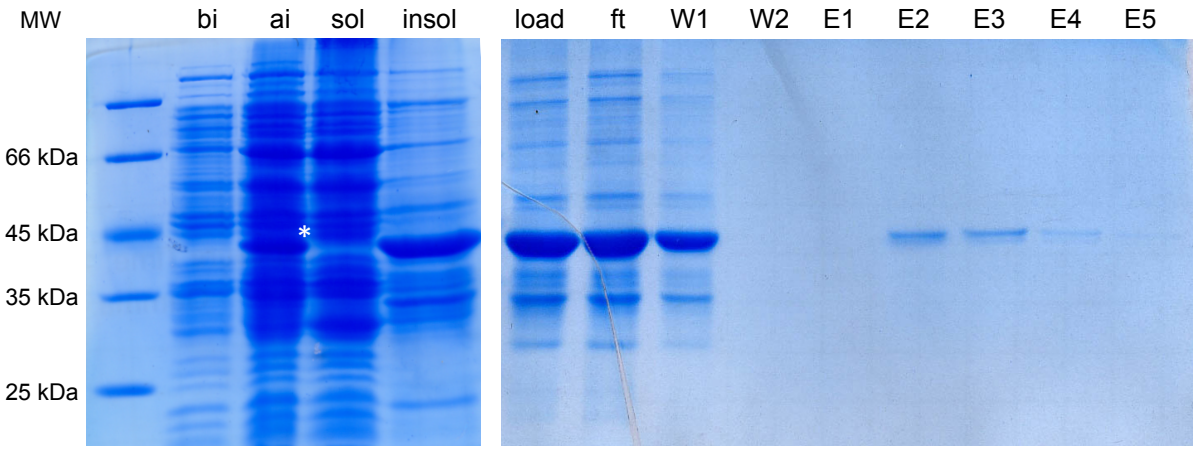

Figure 21: Purification of GST-EC1.1 from Rosetta™ cells after solubilization and refolding.
First two lines represent the cells before induction (bi) and after induction (ai) of target protein expression (asterisk). Target protein cannot be detected in the soluble fraction of proteins (sol), whereas a strong signal appeared in the insoluble fraction (insol). After dialysis and refolding with reduced and oxidized glutathione, the protein was loaded onto the GSTrap column (load). Most of the GST-EC1.1 was detected in the flow through (ft). The first washing fraction (W1) showed as well a strong signal of GST-EC1.1. The elution fractions E2, E3 and E4 only showed clear signals at the size of the GST-EC1.1 fusion (44 kDa).

To confirm, that these signals were indeed the GST-EC1.1 fusion protein, the bands were cut out, digested with trypsin and the fragment sizes were mass spectrometrically analyzed by Matrix-assisted laser desorption/ionization (MALDI). Comparison of the obtained data with the predicted fragment sizes after trypsin digestion revealed that the purified band indeed reflected the GST-EC1.1 fusion protein (see Appendix, page 104).

5.4.4 Application of the GST-EC1.1 fusion protein in a bioassay

In order to analyze whether the GST-EC1.1 fusion protein possesses the ability to separate the two sperm cells *in vitro*, a bioassay was established. Therefore, pollen of the sperm cell marker line was germinated *in vitro* on solid pollen germination medium for six hours and release of the sperm cells was achieved by induction of pollen tube burst through an osmotic shock (Figure 22). After release, the sperm cells were still located next to each other and appeared to be connected. 45 minutes after application of the GST-EC1.1 fusion protein an effect was not observed and the sperm cells were still located next to each other (Figure 22C, D). Similar results were obtained when liquid pollen germination medium was used instead of solid medium.

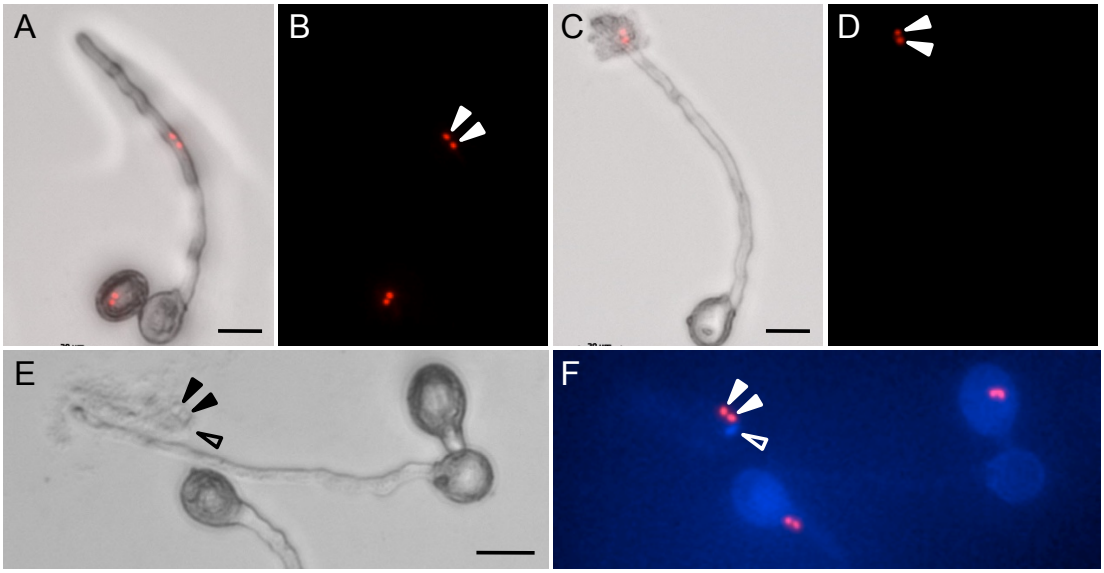

Figure 22: Effect of GST-EC1.1 on sperm cell pairs released from pollen tubes after osmotic shock. **A** *In vitro* germinated pollen of the sperm cell marker line, overlay of brightfield and mRFP1 fluorescence channel. Sperm cells are located within the growing pollen tube; mRFP1 fluorescence of sperm cell nuclei is shown in red. **B** Fluorescence channel of the same preparation. The sperm cell nuclei are shown in red (arrowheads). **C** Burst pollen tube after osmotic shock, 45 minutes after application of GST-EC1.1 protein. The sperm cells are released but are still located next to each other (overlay of brightfield and mRFP1 fluorescence channel). **D** Same sample as in C, sperm cell nuclei are shown in red (arrowheads), fluorescence channel only. **E** + **F** DAPI staining of burst pollen tubes. Sperm cells (closed arrowheads) are in close vicinity to the vegetative nucleus (open arrowhead). **E** Brightfield only. **F** Overlay of fluorescence channels for mRFP1 (red) and DAPI (blue) detection, respectively. Bars = 20 µm.

Since the sperm cells seemed to be tightly connected I asked whether the male germ unit (MGU) was still intact, i.e. the sperm cells were connected to the vegetative nucleus, mediating the adhesion of the two sperm cells to each other. *In vivo*, the MGU is likely to be dissolved upon pollen tube burst or during transport of the sperm cell to the site of fusion. In order evaluate whether the male germ unit might still be present, DAPI (4',6-diamidino-2-phenylindole) staining of DNA was performed to visualize the vegetative nucleus. Figure 22E and F show a ruptured pollen tube of the sperm cell marker line after DAPI staining. The vegetative nucleus is located in close vicinity to the two sperm cells. This indicates that the MGU might still be intact. Consequently, this bioassay likely does not reflect the *in vivo* situation and may thus not be suitable.

In summary, the expression and purification of EC1 turned out to be very challenging. Overexpression *in planta* did not work and it was not possible to purify EC1.1 and from *Pichia* supernatant. Most promising results were obtained with heterologous expression in *E. coli*. However, it remains questionable whether EC1.1 was correctly folded regarding disulfide bond formation, since the applied bioassay is probably not suitable and there was no other test to evaluate the biological functionality of the purified and refolded EC1 protein.

5.5 Post-translational regulation of EC1.1 stability

5.5.1 Proteasome inhibitor studies

As described in section 5.4.1 (page 54) plants expressing *EC1.1-eGFP* under control of the *CaMV35S* promoter were initially generated with the aim to purify the EC1.1-eGFP fusion protein. However, eGFP fluorescence could not be detected in any tissue, whereas the transcript of *EC1.1* was present abundantly (Figure 23A, inset). The absence of fluorescence could be explained by two simple scenarios: (i) the misexpressed protein is not translated at all, or (ii) it is degraded rapidly after translation, presumably via the ubiquitin-proteasome pathway. To test the latter hypothesis a proteasome inhibitor assay was established. Seedlings expressing $P_{CaMV35S}$*:EC1.1-eGFP* were grown on solid MS medium and after two weeks transferred to MS medium containing the proteasome inhibitor MG132. Seedlings were analyzed after 16 to 24 hours on plates. Microscopy analysis showed that only MG132 treated *EC1.1-eGFP* expressing roots showed eGFP fluorescence, mainly in the vasculature (Figure 23A). Protein extracts from these seedlings were made and analyzed by SDS-PAGE. The increased amount of fusion protein in *EC1.1-eGFP* expressing seedlings after MG132 treatment could also be confirmed by Western Blot analysis using a GFP antibody (Figure 23B, left side). Additionally, some degradation products were detectable in plants misexpressing the fusion protein under control of the *CaMV35S* promoter. In contrast, the control experiment with pistil extracts of plants expressing *EC1.1-eGFP* under control of the endogenous *EC1.1* promoter showed a single band of the size of the fusion protein without a prominent degradation product (Figure 23B, right side).

These data suggest that misexpressed *EC1.1-eGFP* is degraded rapidly via the ubiquitin-proteasome pathway. Endogenous EC1.1 localized in the egg cell did not seem to be affected by degradation and seems to be stabilized by a yet unknown mechanism (see section 5.5.3, page 70).

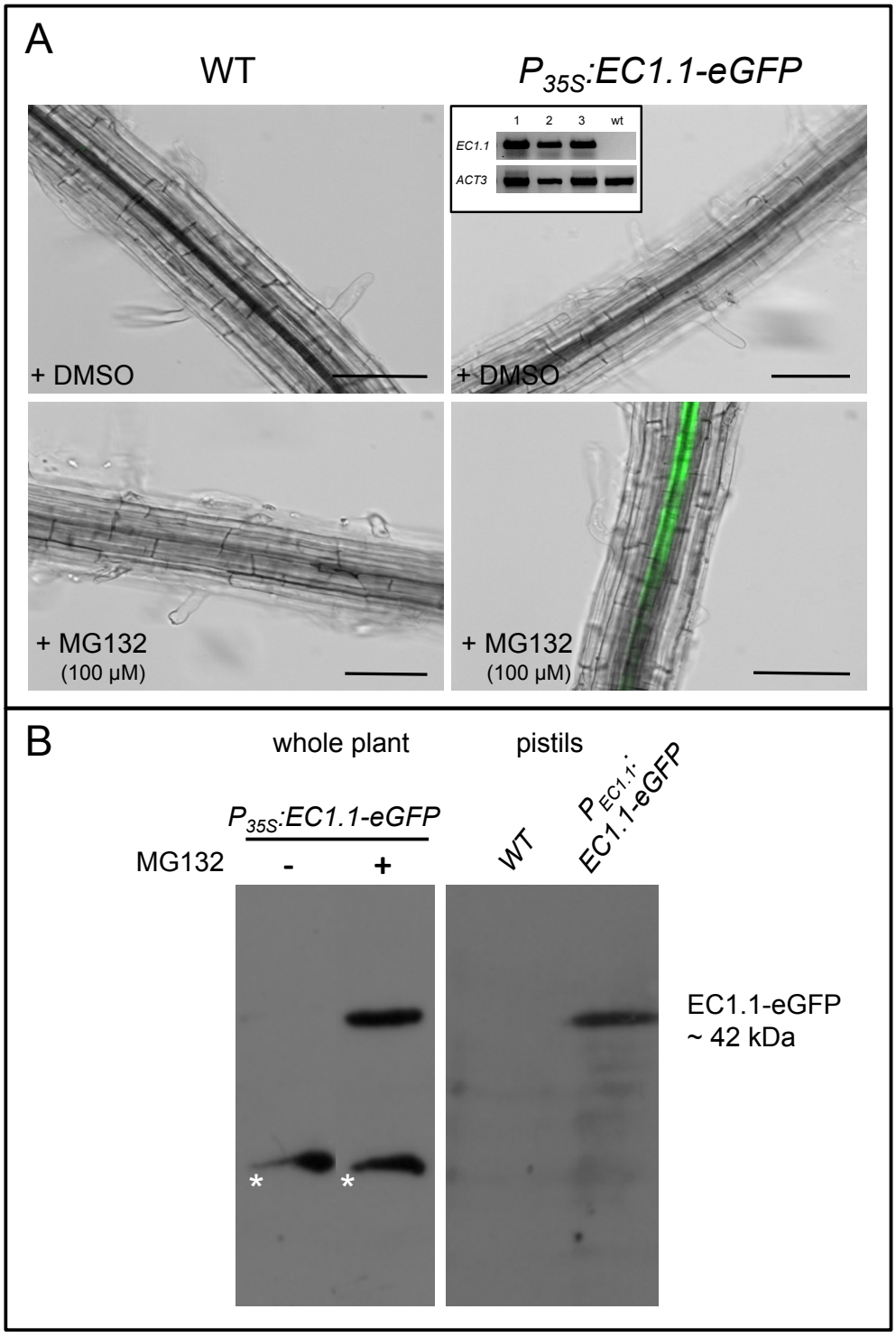

Figure 23: Misexpressed *EC1.1-eGFP* is degraded via the ubiquitin-proteasome pathway.
A Roots of wild type seedlings (left side) and seedlings expressing $P_{CaMV35S}$*:EC1.1-eGFP* (right side) 14 days after stratification. eGFP signals were investigated 24 h after transfer to solid MS medium including DMSO as a control (upper row) and on medium containing 100 µM MG132 (lower row). eGFP fluorescence is only detectable in roots expressing *EC1.1-eGFP* after MG132 treatment. Inset: RT-PCR of $P_{CaMV35S}$*:EC1.1-eGFP* and wild type seedling cDNA, *EC1.1* transcript is detectable in overexpressing lines but not in wild type seedlings. Bars = 50 µm. **B** Western Blots using a monoclonal anti-GFP antibody. Left side: whole plant protein extracts of P_{CaMV35}*:EC1.1-eGFP* plants. The fusion protein is only detectable after MG132 treatment. Degradation products are marked with asterisks. Right side: pistil protein extracts. Only the fusion protein is detectable in lines expressing *EC1.1-eGFP* under control of the endogenous promoter; 42 kDa represents the calculated molecular weight of the fusion proteins without the predicted leader peptide.

5.5.2 Identification of EC1.1 interacting proteins by yeast-two-hybrid approaches

As already mentioned above, the knockout of the sperm cell-specific *GCS1* gene causes a phenotype similar to *ec1*$^{+/-}$. GCS1 encodes for a protein with a predicted signal or leader peptide targeting it to the secretory pathway. Furthermore, it contains one large extracellular domain, a transmembrane domain and an intracellular histidine-rich C-terminal part (Figure 24A, B). Due to the observed phenotype GCS1 was tested as a putative interaction partner of EC1.1, which is secreted from the egg cell during fertilization. To analyze whether these two proteins interact, a direct yeast-two-hybrid test was performed. EC1.1 without the predicted signal peptide served as a bait and the N-terminal extracellular part of GCS1, which is sufficient for gamete fusion (Mori *et al.*, 2010), as a prey. However, the diploid yeast strain expressing *EC1.1* and *GCS1* did not grow on quadruple dropout medium selecting for interacting proteins indicating that the two proteins do not interact directly (Figure 24C).

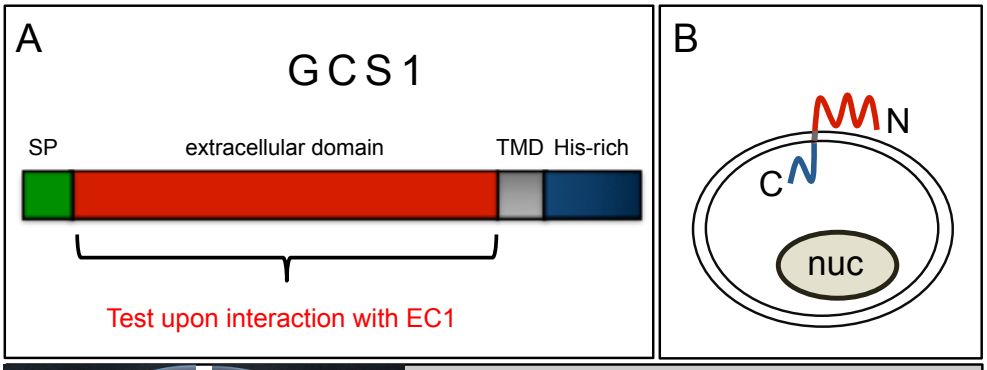

C

#	BD –vector (bait)	AD-vector (prey)
1/5	pGBKT7-53	pGADT7-T (positive ctrl)
2/6	empty	pGADT7-T (positive ctrl)
3/7	empty	GCS1 (extrac. domain)
4/8	EC1.1	GCS1 (extrac. domain)

Figure 24: GCS1-EC1.1 interaction analysis by mating based yeast-two-hybrid system.
A Schematic representation of the GCS1 protein domains. SP = signal peptide; TMD = transmembrane domain; His-rich = Histidine-rich domain. **B** Proposed topology of GCS1 in the sperm cell (according to Wong *et al.*, 2010); N- and C-termini are indicated; nuc = nucleus. **C** Growth of mated yeast strains on medium lacking leucine (L) and tryptophan (W) selecting for diploid clones and on medium lacking additionally adenine (A) and histidine (H) selecting for interacting proteins. The positive control is growing on medium selective for interaction of bait and prey (#5). Yeast expressing *GCS1* as a prey and *EC1.1* as a bait is not growing on –A/H/L/W medium (#8).

In addition to the direct yeast-two-hybrid interaction test with GCS1, cDNA libraries were screened with the aim to identify interaction partners of EC1.1. First, a cDNA library of mature ovules attached to the placenta was generated. After mating with the *EC1.1* bait strain 564 clones grew on quadruple dropout medium, but none of which activated the third reporter gene. This means that no interaction partners were identified in the ovule cDNA library. Since the phenotype of $ec1^{+/-}$ is related to the male gametes, a pollen tube cDNA library (generated by M. Gebert; Gebert, 2008) was screened. In total, 480 clones were identified that activated two reporter genes, 27 of which activated three reporter genes, i.e. diploid clones grew on quadruple dropout medium and additionally showed blue staining after an X-Gal assay (Table 6). After plasmid rescue and propagation in *E. coli*, isolated plasmids were subjected to a test digestion. Inserts of different sizes were sequenced and plasmids of interesting candidate clones were used for retransformation of yeast. The generated yeast strains were mated again with the strain expressing the *EC1.1* bait construct. Additionally, these strains were mated with a yeast strain transformed with the empty bait vector to evaluate auto-activation.

Table 6: Analysis of reporter-gene activating yeast-two-hybrid clones from a pollen tube cDNA library (Gebert, 2008) using EC1.1 without the predicted signal peptide as a bait. Clone number (#), staining intensity after X-Gal assay, success of transformation of *E. coli* with the rescued plasmid, sequence identity and length and verified interaction after retransformation and remating are indicated.

Clone #	X-Gal Assay; Staining intensity	Transformation of *E.coli*	Insert sequence, length of fragment	Interaction after retransformation /-mating
1	+	✓	At3g07820; putative polygalacturonase (PGA3); 206 bp	n.d.
2	+	✓	At3g07820; putative polygalacturonase (PGA3); 782 bp	-
3	+	✓	At3g07820; putative polygalacturonase (PGA3); 710 bp	n.d.
4	+	✓	n.d.	n.d.
5	++	✓	At3g29180, unknown protein, DUF1336; 261 bp	n.d.
6	++	✓	At3g29180, unknown protein, DUF1336; 261 bp	-
7	+	✓	At3g07820; putative polygalacturonase (PGA3); 1087 bp	n.d.
8	++	-	n.a.	n.a.
9	+	✓	n.d.	n.d.
10	+	✓	n.d.	n.d.
11	+	✓	At5g07410; pectinesterase family protein; 304 bp	n.d.

Clone #	X-Gal Assay; Staining intensity	Transformation of *E.coli*	Insert sequence, length of fragment	Interaction after retransformation /-mating
12	+	✓	At3g07820; putative polygalacturonase (PGA3); 599 bp	n.d.
13	+	✓	At3g07820; putative polygalacturonase (PGA3); 754 bp	n.d.
14	++	✓	At5g07410; pectinesterase family protein; 933 bp	n.d.
15	+	✓	n.d.	n.d.
16	++	✓	At1g13460; serine/threonine protein phosphatase 2A (PP2A) regulatory subunit B', putative; 320 bp	✓
17	+	✓	At3g28830; unknown protein, DUF1216; 252 bp	-
18	+	✓	At3g07820; putative polygalacturonase (PGA3); 578 bp	n.d.
19	+	✓	n.d.	n.d.
20	+	✓	At5g07410; pectinesterase family protein; 358 bp	n.d.
21	+	✓	At3g07820; putative polygalacturonase (PGA3); 617 bp	n.d.
22	++	✓	n.d.	n.d.
23	+	-	n.a.	n.a.
24	+	✓	At2g45800; putative LIM domain protein; 126 bp	-
25	+	✓	At5g24240; phosphatidylinositol 3- and 4-kinase family protein/ubiquitin family protein; 337 bp	✓
26	+	✓	At3g07820; putative polygalacturonase (PGA3); > 768 bp	n.d.
27	++	-	n.a.	n.a.

The clones encoding a putative polygalacturonase (At3g07820) and a pectin esterase family protein (At5g07410) were also identified in large numbers in another screening of this library but turned out to be false positives (Gebert, 2008) and were therefore not further analyzed here. For clones #16 and #25 the interaction could be verified, i.e. these clones showed activation of three reporter genes and did not reveal auto-activation (Figure 25A). These clones encoded a fragment of the regulatory subunit B'θ of the Phosphatase 2A (PP2A B'θ) and one of the ubiquitin-like domain kinase γ3 (UbDKγ3), respectively. *UbDKγ3* was formerly predicted to encode a type II phosphoinositide 4-kinase (PI4K) and was therefore also named as *AtPI4Kγ3*. However, it has been shown that UbDKγ4 – the most similar protein to UbDKγ3 – interacts with RPN10 and UFD1, which are both involved in the ubiquitin-proteasome pathway (Galvão *et al.*, 2008). It

was therefore suggested that UbDKγ4 functions in delivery of polyubiquitinated proteins to the proteasome. The EC1.1 interacting fragment of UbDKγ3 partly consists of the second UBL (ubiquitin-like) domain and a region between the UBL and the conserved PI3/4 kinase domain (Figure 25B). B'θ is a regulatory B' subunit of the Phosphatase 2A (PP2A). The fragment that was found to interact with EC1.1 consisted of 110 amino acids from residue 7 to 117 comprising a more variable part at the N-terminus and part of the conserved PP2A B domain (Figure 25C).

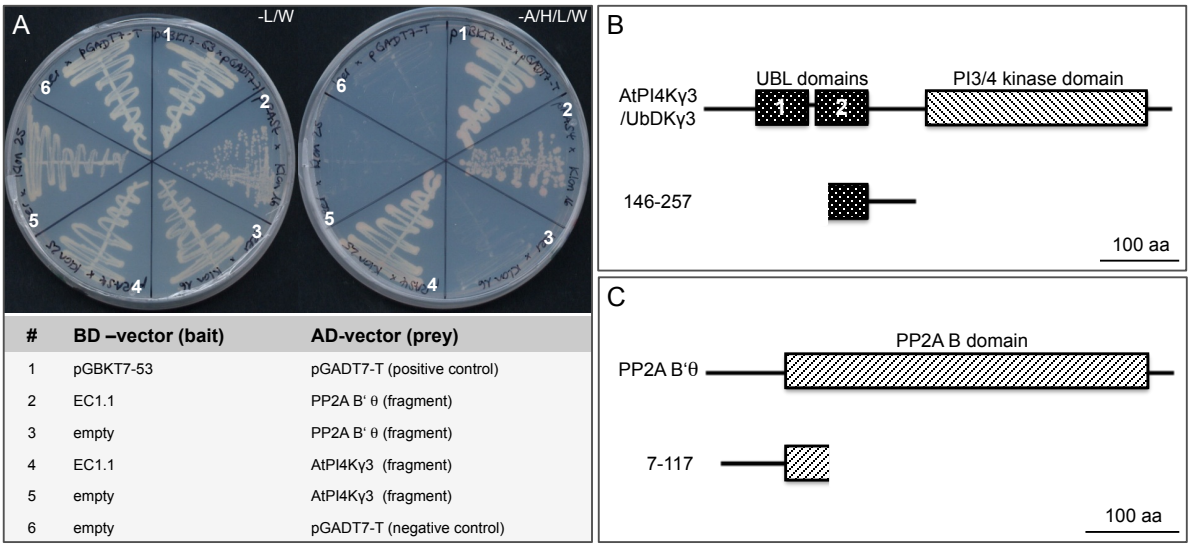

#	BD –vector (bait)	AD-vector (prey)
1	pGBKT7-53	pGADT7-T (positive control)
2	EC1.1	PP2A B' θ (fragment)
3	empty	PP2A B' θ (fragment)
4	EC1.1	AtPI4Kγ3 (fragment)
5	empty	AtPI4Kγ3 (fragment)
6	empty	pGADT7-T (negative control)

Figure 25: Identification of EC1.1 interaction partners by screening of a yeast-two-hybrid pollen tube cDNA library.
A Growth of mated yeast strains on medium lacking leucine (L) and tryptophan (W) selecting for diploid clones (left picture) and on medium lacking additionally adenine (A) and histidine (H) selecting for interacting proteins. Yeast strains expressing the *PP2A B'θ* fragment together with *EC1.1* (#2) but not without bait (#3) are able to grow on selective medium. Yeast strains expressing the *UbDKγ3* fragment are also able to grow on selection medium together with *EC1.1* (#4) but not without bait (#5). **B** + **C** Schematic representation of the identified EC1-interacting proteins. The full length protein (above) and the interacting protein fragment (below) are shown. **B** AtPI4Kγ3/UbDKγ3 contains two UBL domains and one kinase domain. **C** PP2A B'θ contains the PP2A B domain.

To verify the interaction of EC1.1 with PP2A B'θ and UbDKγ3, respectively, the full-length coding sequences of the two identified proteins were expressed in yeast as prey and mated with the *EC1.1* expressing bait strain. However, interaction with the full-length clones could not be confirmed (data not shown).

5.5.3 Stability of a phospho-mimicking variant of EC1.1 fused to eGFP

B' subunits of the PP2A determine substrate specificity and subcellular localization (Farkas *et al.*, 2007). According to *in silico* analysis (NetPhos 2.0) each of the *Arabidopsis* EC1 proteins exhibits numerous predicted phosphorylation sites, especially at serine residues at the C-terminal part of the protein behind the conserved cysteine-rich domain (Figure 26). These predictions together with the identified PP2A subunit in the yeast-two-hybrid screen suggest that phosphorylation of EC1.1 might occur and be possibly linked to the instability of the EC1.1 protein: phosphorylation might stabilize the protein and dephosphorylation of EC1.1 might mark it for degradation.

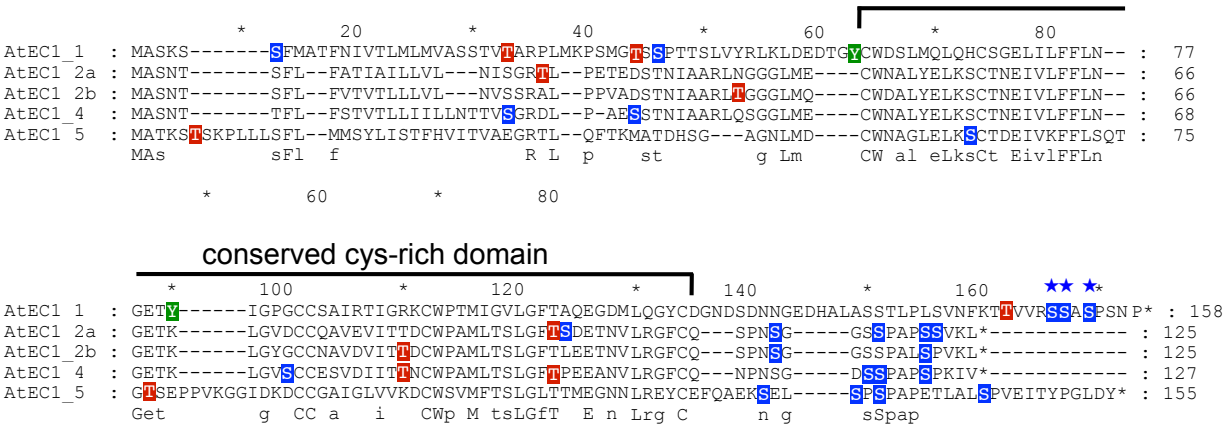

Figure 26: Alignment of *Arabidopsis* EC1 proteins showing predicted phosphorylation sites.
Full length AtEC1.1 to AtEC1.5 were aligned. Consensus sequence is shown below the alignment. Conserved cysteine-rich domain is indicated by the black line. The serine, threonine and tyrosine residues that are predicted to be phosphorylated (according to NetPhos 2.0) are highlighted in blue, red and green, respectively. Predicted phosphorylation sites of serine residues accumulate at the C-terminus of all proteins. Serine residues of EC1.1 that were exchanged against aspartate residues in the phospho-mimicking variant are indicated (blue stars).

To test this hypothesis, a phospho-mimicking construct was generated. The serine residues S151, S152 and S154 of EC1.1 (Figure 25, blue stars), which had – according to predictions – the highest probability to be phosphorylated, were exchanged against aspartate residues. This construct was used for transformation of agrobacteria and transiently expressed in *Nicotiana benthamiana* by leaf infiltration. Leaves infiltrated with the wild type form of EC1.1 fused to eGFP did almost not show fluorescence (Figure 27A, B), whereas eGFP fluorescence is clearly detectable in vesicle-like structures in leaves expressing the phospho-mimicking variant, (Figure 27C, D). This finding supported the hypothesis that the phosphorylated version of EC1.1 is more

stable and that the dephosphorylated form is marked for degradation. In contrast, fluorescence was not detected in stably transformed *Arabidopsis* expressing the phospho-mimicking variant of *EC1.1* fused to *eGFP* under control of the *CaMV35S* promoter indicating that there are additional mechanisms that regulate the stability of the EC1.1 protein (data not shown).

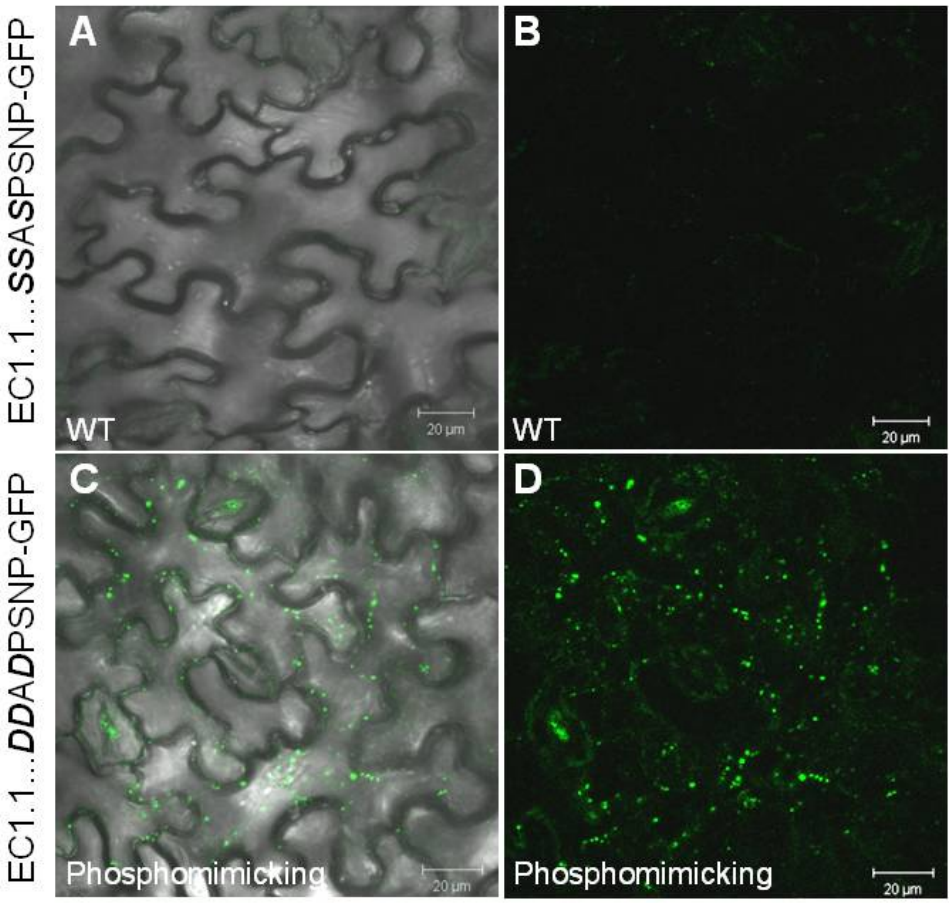

Figure 27: Fluorescence microscopy images of *N. benthamiana* leaf epidermal cells expressing the native *EC1.1-eGFP* or the phospho-mimicking variant of *EC1.1-eGFP*.
A + **B** Leaves expressing the wild type form of *EC1.1-eGFP*. eGFP fluorescence is not detectable. **C** + **D** Leaves expressing the phospho-mimicking form of *EC1.1* fused to *eGFP*; fluorescence is detectable and localizes to vesicle-like structures. **A** + **C** merge image of brightfield and fluorescence channel for eGFP. **B** + **D** Fluorescence channel for eGFP. Bars = 20 µm.

5.5.4 Misexpression of *PP2A B'θ* in synergid cells

According to publicly available array data, *PP2A B'θ* is ubiquitously expressed, but is absent in female gametophytic cells (Šoljić *et al*., unpublished). Due to this finding, it was proposed that the degradation of EC1.1, which is secreted by the egg cell during

fertilization, is initiated by dephosphorylation. PP2A B'θ would be delivered by the pollen tube to the female gametophyte where it is released into the degenerating synergid. After gamete fusion PP2A B'θ might dephosphorylate secreted EC1.1 and thereby trigger its inactivation and degradation. In order to support this model *PP2A B'θ* was misexpressed in the synergid cells using the strong synergid cell-specific promoter *DD31* (Steffen *et al*., 2007). For visualization, the *PP2A B'θ* was expressed as a translational fusion with e*GFP*. According to the hypothesis these plants should phenocopy *ec1*$^{+/-}$ plants because PP2A B'θ would then be present too early in the female gametophyte and EC1 would be degraded before it can induce sperm cell separation.

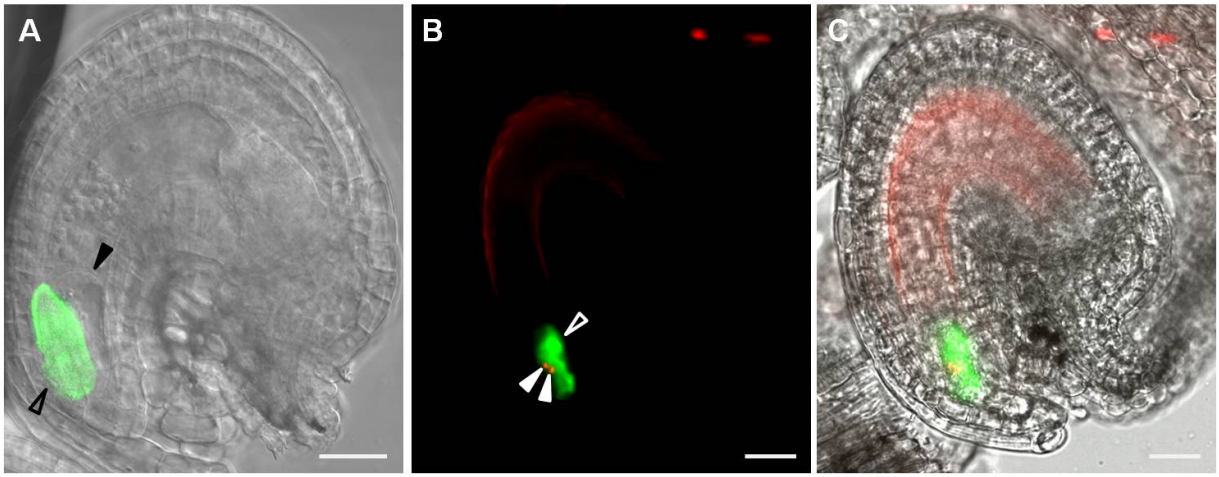

Figure 28: Misexpression of *PP2A B'θ-eGFP* in synergid cells.
A Confocal Laser Scanning Microscopy (CLSM) image of a flower stage 13 (Smyth *et al*., 1990) ovule expressing *PP2A B'θ-eGFP* in the cytoplasm of the synergid cell (open arrowhead); closed arrowhead points towards the egg cell. Overlay of DIC and eGFP channel. **B** + **C** Fluorescence Microscopy image of an ovule 12 hours after pollination of a P_{DD31}*:PP2A B'θ-eGFP* plant with *HTR10-mRFP1* pollen (Ingouff *et al*., 2007); eGFP fluorescence of *PP2A B'θ-eGFP* expressing synergid cells is shown in green (open arrowhead); mRFP1 fluorescence of sperm cell nuclei expressing *HTR10-mRFP1* is shown in red (closed arrowheads). Sperm cells do not separate and do not fuse with the female gametes. **B** Overlay of eGFP and mRFP1 fluorescence channels. **C** Overlay of brightfield, eGFP and mRFP1 fluorescence channels. Bars = 20 µm.

Figure 28A shows an ovule expressing P_{DD31}*:PP2A B'θ-eGFP* with strong eGFP fluorescence in the cytoplasm of the synergid cell. Plants expressing *PP2A B'θ* in the synergid cells were pollinated with the sperm cell marker line *HTR10-mRFP1*. Twelve hours after pollination a phenotype reminiscent of the *ec1*$^{+/-}$ phenotype was visible (Figure 28B, C). The pollen tube is normally attracted to the female gametophyte, pollen tube reception and discharge are also not affected, but the sperm cells are not separated and fusion of male and female gametes does not take place. Degenerated,

receptive synergid cells expressing *eGFP* were recognizable by their altered shape. Of all targeted ovules expressing *PP2A B'θ-eGFP* (n = 73) 70% showed non-fused sperm cells 14 to 17 hours after pollination.

The experiments described in this chapter show that additionally to its tight transcriptional regulation, EC1.1 is also strongly regulated at the post-translational level. A phospho-mimicking variant of EC1.1 fused to eGFP showed an increased stability, whereas misexpressed *EC1.1* was degraded quickly via the proteasome. Overexpression of the gene encoding the PP2A regulatory subunit B'θ interacting with EC1.1 in the synergid phenocopied the $ec1^{+/-}$ phenotype. Taken together, these data suggest that the regulatory subunit B'θ triggers dephosphorylation of EC1.1 and that this modification is a mark for degradation via the ubiquitin-proteasome pathway.

6 DISCUSSION

Double fertilization is the characteristic trait of angiosperms. During the double fertilization process, a lot of intercellular signaling events occur. The two male gametes are transported towards the female gametophyte by the pollen tube representing the male gametophyte. The pollen tube cell grows through the transmitting tract to the female gametophyte involving extensive cross-talk with the sporophytic tissue (Dresselhaus *et al.*, 2011). After arrival at the female gametophyte, the two immobile sperm cells are released from the pollen tube and are delivered to the female gametes, the egg cell and the central cell. In a coordinated manner one sperm cell fuses with the egg cell giving rise to the embryo and the second sperm cell fuses with the central cell giving rise to the nurturing endosperm. For the development of healthy and strong offspring, these mechanisms are based on cell-cell communication events between the male and female gametophytes as well as between the gametes and have to be tightly controlled to ensure successful fertilization and to inhibit polyspermy (reviewed by Dresselhaus, 2006; Higashiyama, 2010).

The egg cell-specific *EC1* gene family from *Arabidopsis* had been identified in a previous project. In the present work, the analysis of the physiological role of these small, cysteine-rich and secreted proteins during double fertilization in *Arabidopsis* was addressed in detail and events after fertilization including post-translational control and degradation of EC1 were analyzed.

6.1 EC1 proteins belong to the large class of 'ECA1 gametogenesis related family proteins' of cysteine-rich proteins

Silverstein *et al*. (2007) identified 825 cysteine-rich proteins in the *Arabidopsis* genome and clustered them into different classes according to their cysteine pattern and similarity. The proteins encoded by the *EC1* gene family are part of the class called 'ECA1 gametogenesis related family protein' comprising 118 members. This class is named after *ECA1* (*early culture abundant 1*), which was identified in a cDNA library of barley microspores and was shown to be strongly induced in early stages of microspore culture (Vrinten *et al.*, 1999). In BLAST searches, I identified the EC1

related- (ECR-) group comprising nine proteins with highest similarity to the EC1 proteins. The constructed phylogenetic tree of all proteins of the ECA1 gametogenesis class of *Arabidopsis* showed that the five EC1 family members clustered in an isolated clade. This was also true for the nine ECR proteins. At2g27315 (ECR1) of the ECR-group has been shown already to be synergid-specifically expressed (Punwani *et al.*, 2008). For At5g54062 (ECR6) and At5g52975/DD8 (ECR4) predominant expression in the synergid cell and weak expression in egg and central cell were observed (Jones-Rhoades *et al.*, 2007; Steffen *et al.*, 2007). Thus, the hypothesis arose that ECRs might be EC1 equivalents of the synergid cell. To date, there is no functional analysis available about ECR genes. Synergid cell-specific expression within the female gametophyte might point to a specific role in cell-cell communication during pollen tube guidance or reception. The cysteine-rich LURE proteins of the defensin-like class are secreted from the synergid cell in *Torenia fournieri* to attract pollen tubes towards the ovule (Okuda *et al.*, 2009). Moreover, Amien *et al*. (2010) recently showed that the defensin-like cysteine-rich ES4 protein (EMBRYO SAC 4) from maize is secreted from the synergid cells during fertilization and induces pollen tube burst via opening of the potassium channel KZM1. ECR proteins likely have different roles than these defensin-like proteins but might also be important during double fertilization.

Additionally, two putative central cell-specific groups among the defensin-like (DEFL) genes were identified in this thesis. Reverse transcriptase-PCR analyses showed that none of the tested genes is expressed in roots, leaves, stems or anthers. The absence of transcript in vegetative tissues tested so far makes these genes interesting candidates for detailed expression analysis and functional studies during the double fertilization process. Except for the fact that there are small cysteine-rich proteins among the prolamin superfamily of cereal seed storage proteins (Shewry and Halford, 2002), nothing is known about the function of central cell-specific cysteine-rich proteins. Especially the genes encoding the CCC proteins of the two identified putative central cell groups show a strong expression in siliques containing the embryo and the endosperm indicating a function after fertilization. Similarly, the paternally imprinted genes encoding cysteine-rich proteins of the MEG1 class are expressed in the endosperm and might play a role in nutrient trafficking to the developing seed (Gutierrez-Marcos *et al.*, 2004). Therefore, functional analysis of these genes might be very interesting and give new insights into the role of cysteine-rich proteins also after

fertilization such as endosperm development or communication of fertilization products with the surrounding maternal tissue (Marshall *et al.*, 2011).

6.2 EC1 homologs only occur in angiosperms

BLAST searches revealed that EC1 homologs were found exclusively in angiosperms. During the angiosperm characteristic trait of double fertilization, fusion of one sperm cell with the egg cell and of the second sperm with the central cells takes place in a highly coordinated manner. In gymnosperms such as white pine, which produces pollen with two sperm cells, the second sperm cell degenerates after fusion of the leading sperm with the egg cell (Bruns and Owens, 2000). Also in Ginkgo there is no classical double fertilization event. In ginkgo pollen two mobile sperm cells develop of which only one eventually fertilizes the egg cell (Nakao *et al.*, 2001). The phenotype of *ec1* knockout mutants, the non-separating and non-fusing sperm cells within the female gametophyte clearly involves double fertilization and thus underlines the importance of EC1 during the evolution of this angiosperm characteristic process.

The search for homologous proteins showed that *Arabidopsis thaliana* and *Arabidopsis lyrata* both contain an EC1.5 protein with a characteristic insertion within the conserved cysteine pattern. However, until now it is unclear whether this protein is functionally redundant to the other four proteins. The analysis of a quadruple mutant in *Arabidopsis thaliana* still remains standing to see if these plants also show the same phenotype like the knockdown of the entire gene family. On the other hand, *ec1.5* single knockout lines did not display a phenotype in terms of reduced seed set indicating that the protein is functionally redundant although experiments are still missing, which show that the protein is expressed and secreted during the double fertilization process.

6.3 *ec1*$^{+/-}$ mutants display a non-fusing sperm phenotype

The knockout of *EC1* genes lead to reduced seed set. More detailed analyses showed that earlier steps of the double fertilization process such as pollen tube growth, guidance and attraction to the female gametophyte were not affected in *ec1*$^{+/-}$ plants. Moreover, pollen tube reception, synergid degeneration and pollen tube burst occurred normally in these mutants. Only separation of the sperm cell pair did not take place and fusion of male and female gametes was impaired. In average, 45% of ovules of *ec1*$^{+/-}$ plants

showed non-fused sperm cells. The numbers of the different phenotypes varied between independent transgenic lines. This can be explained by an RNAi effect, i.e. differential transcriptional activities of the RNAi construct due to positional effects of the transgene. Moreover, the number of aborted seeds in *ec1*$^{+/-}$ siliques did not correlate with the frequency of ovules showing non-fused sperms. DIC microscopy analysis of siliques of selfed *ec1*$^{+/-}$ flowers showed that intermediate stages of female gametophytes with intact appearing cells occurred, which thus were probably still able to be fertilized. Post-transcriptional gene silencing of plant genes using RNAi constructs leads usually to a maximum of 90% gene silencing (Wesley *et al.*, 2001). Thus, in some of these ovules enough EC1 protein might accumulate over time, so that fertilization can take place and seeds will develop normally. In other ovules, fertilization might not happen due to an insufficient amount of EC1 protein. These seeds then would be aborted eventually.

Two other *Arabidopsis* mutants have been described that show a non-fusing sperm phenotype similar to *ec1*$^{+/-}$. Recently, Yu *et al.* (2010) showed that (i) the mitochondrial ankyrin repeat protein ANK6 is essential for gamete recognition. However, the phenotype of non-fusing sperm cells only occurred when an *ank6* sperm cell reaches an *ank6* female gametophyte. ANK6 interacts with SIG5 that functions as transcription initiation factor in mitochondria and chloroplasts. The authors propose that these two proteins together play a central role in gamete recognition by regulating mitochondrial gene expression. However, the mechanism of ANK6 activity is completely unclear. Due to the localization of the proteins, a direct interaction of ANK6 and EC1 is very unlikely. The loss of *GCS1/HAP2* (ii) also leads to non-fusing sperm cells within the *Arabidopsis* female gametophyte (Mori *et al.*, 2006; von Besser *et al.*, 2006). *GCS1/HAP2* is specifically expressed in sperm cells and encodes a protein anchored in the membrane where it presents its extracellular N-terminal domain (Mori *et al.*, 2010; Wong *et al.*, 2010). *EC1* is expressed in the egg cell and is secreted upon fertilization. Given these data about localization of the two proteins and their topology together with the similar loss-of-function phenotype, an interaction might be possible. Nevertheless, two facts indicate that GCS1/HAP2 and EC1 have different roles at different time points during gamete recognition and fusion: (i) In contrast to EC1, which only has homologs in angiosperms, GCS1/HAP2 homologous proteins have been identified also in green and red algae (*Chlamydomonas reinhardtii* and *Cyanidioschyzon merolae*), in slime molds (*Physarum polycephalum*) and parasites (*Plasmodium falciparum* and

Leishmania major) (Mori *et al.*, 2006). Liu *et al*. (2008) could show that *Chlamydomonas* and *Plasmodium berghei* each need one member of the conserved GCS1/HAP2 protein family and another species-specific protein for gamete fusion. The authors further showed that *Chlamydomonas* and *Plasmodium* GCS1/HAP2 functions in membrane merger downstream from gamete membrane attachment. Since GCS1/HAP2 is found in genomes of all major eukaryotic taxa, it was recently proposed that GCS1/HAP2 might represent an ancestral gamete fusogen (Wong and Johnson, 2010). Contrarily, EC1 is likely to be involved in a double fertilization-specific process upstream of gamete fusion. Moreover, (ii) pollen tube attraction of *ec1* and *gcs1* ovules differs. Multiple pollen tube attraction occurs only very rarely in wild type plants in order to avoid polyspermy (Shimizu and Okada, 2000). However, pollen tube entry alone seems not to the clue to prevent further pollen tube attraction. *sirene*/*feronia*, *abstinence by mutual consent* (*amc*) and *lorelei* mutants from *Arabidopsis* show pollen tube overgrowth within the female gametophyte but these ovules continue to attract further pollen tubes (Huck *et al.*, 2003; Rotman *et al.*, 2003; Escobar-Restrepo *et al.*, 2007; Boisson-Dernier *et al.*, 2008; Capron *et al.*, 2008). In *ec1*$^{+/-}$ plants multiple pollen tube attraction still occurred in at least 13% of all ovules indicating that the signal to stop pollen tube attraction occurs after gamete recognition. Interestingly, *gcs1* mutant ovules only rarely attract more than one pollen tube (Mori *et al.*, 2006) or not at all (von Besser *et al.*, 2006). The difference found here can probably be attributed to the two different alleles of *gcs1* and *hap2* that were analyzed. The clear difference regarding multiple pollen tube attraction in ovules of *ec1*$^{+/-}$ and *gcs1*$^{+/-}$ plants indicates that EC1 presumably acts upstream of GCS1/HAP2, i.e. the two proteins function at different levels during fertilization. Comparison of these data also suggests that the block of multiple pollen tube attraction can be narrowed down between the two mechanisms of gamete recognition or membrane adhesion and gamete fusion.

6.4 What is the mechanistic role of EC1?

Comparing pollination of *ec1*$^{+/-}$ plants with wild type pollen and with single sperm pollen of the *cdka;1*$^{+/-}$ mutant suggested that EC1 is rather needed for sperm cell separation than for sperm cell recognition or fusion. Recently, Aw *et al*. (2010) reported that the mRFP1 fluorescence intensity of the *HTR10-mRFP1* fusion in sperm-like cells of *cdka;1*$^{+/-}$ mutants varies and is in some cases lower than in wild type. Thus, it is

possible that some non-fused sperms were not detected within *ec1* female gametophytes due to a weak fluorescence signal, which might explain why a slightly higher number of fused sperm cells was observed than expected.

On their journey to the female gametophyte, the sperm cells are transported conjointly within the pollen tube. After the pollen tube has arrived at the receptive synergid, it ruptures, its content is released and the two sperm cells are delivered to the site of fusion in a sudden burst. Nevertheless, shortly after arrival they still appear to be attached to each other. Moreover, after induction of burst of *in vitro* grown pollen tubes, *Arabidopsis* sperm cells still seemed to be connected as well. Thus, for the fusion of one sperm cell with the egg cell and the other sperm cell with the central cell to take place, this robust connection probably has to be disintegrated. But what kind of connection holds the two sperm cells together? In maize, the two sperm cells do not seem to be as tightly associated. Analysis of an α-tubulin-YFP line showed that microtubule bundles form around the sperm cell nuclei and a microtubuli knot is visible at half distance between the two sperm cell nuclei (Kliwer and Dresselhaus, 2010). Moreover it was proposed that this cytoplasmic connection is rather labile and may disintegrate rapidly after delivery of the sperm cells to the egg apparatus.

Dumas *et al*. (1985) coined the term male germ unit (MGU) after studies in *Brassica.* The MGU comprises the vegetative cell linked to the two sperm cells. Ultrastructural analyses showed that in *Brassica oleracea*, the two sperm cells do not have cell walls but are held together in a common periplasm. However, in *Plumbago zeylanica* and *Nicotiana tabacum* the situation is different. Here it was shown that the two sperm cells are connected by a transverse cell wall and that a common periplasm binds the membranes of the sperm cells and of the vegetative cell thereby forming the MGU (Russell and Cass, 1981; Yu *et al.*, 1989). In most plants examined a MGU has been detected and in some it appears that a cytoplasmic projection of one sperm cell is connected to the vegetative nucleus. However, only little is known about the structure of this sperm cell cytoplasmic projection (McCue *et al.*, 2011).

Obviously, the detailed structure of the male germ unit differs among species. Unfortunately, there are no precise ultrastructural analyses for the *Arabidopsis* MGU. Instead, some genetic data are available. The progeny of an ethylmethane sulfonate (EMS) mutagenized population revealed two classes of mutants: *germ unit malformed* (*gum*) and *MGU displaced* (*mud*). In *gum1* mutants, the sperm cells are separated from the vegetative cell, which is located at the pollen wall. However, the two sperm cells are

not separated from each other. In wild type, the MGU is compact and located in the middle of the pollen grain, whereas in *mud1* mutants the whole MGU is displaced and shifted to the pollen wall. Both *mud* and *gum* mutants show a reduced male transmission (Lalanne and Twell, 2002). Interestingly, mutants were not described in which the connection of the two sperm cells to each other was disrupted.

Alternatively to a role directly in sperm cell separation, EC1 might function in membrane adhesion. The role of stigma/style cysteine-rich adhesion (SCA) proteins during pollination in lily has been described. The growth of the pollen tube through the style involves adhesion of the pollen tube wall to the extracellular matrix of the style. This adhesion is on the one hand mediated by basic, positively charged SCA molecules that are secreted from the pollen and epidermis cells of the transmitting tract (for review see Lord, 2000; Chae and Lord, 2011) and on the other hand by negatively charged pectin involved in forming an adhesive matrix between the pollen tube cell wall and the transmitting tract (Mollet *et al.*, 2000; Park *et al.*, 2000). A similar mechanism for adhesion of egg and sperm cell membranes would be conceivable. In *Plasmodium*, three cysteine-rich proteins have already been identified that are essential for the attachment of gametes. However, the molecular mechanism has not been clarified yet (van Dijk *et al.*, 2001; van Dijk *et al.*, 2010). Also in mammalians, cysteine-rich secretory proteins (CRISPs) have been identified that play a role in sperm-egg interaction (Da Ros *et al.*, 2007). CRISP1 is suggested to play a dual role during gamete interaction. First, it participates in the initial step of sperm cell binding to the *zona pellucida*. After the acrosome reaction and relocalization of CRISP1 to the site of fusion on the egg cell surface, it may mediate the fusion of the membranes of egg and sperm cell (Cohen *et al.*, 2008). It would be interesting to investigate whether there is a general mechanism involving cysteine-rich proteins in gamete attachment and/or recognition.

EC1 might also play a role in triggering sperm cells to acquire fusion competence. The PH-30 protein from pig sperm cells is essential for egg-sperm fusion and consists of two subunits that are both present as precursors in early developmental stages. The final processing of the two precursors, which is necessary for successful gamete fusion, is accomplished shortly before fertilization, i.e. the sperm cells acquire fusion competency (Blobel *et al.*, 1990). In a similar manner, EC1 might trigger events at the sperm cell to make them competent for membrane fusion. If this was the case, the tight post-translational regulation of EC1 in terms of rapid degradation would be reasonable to prevent some unfavorable membrane fusion events.

Another possibility could be that EC1 is a link between gamete recognition and the authorization for one sperm cell to fuse with the egg cell. If attachment of one sperm cell to the egg cell and separation from the second sperm cell occur more or less at the same time, EC1 might act as a checkpoint to ensure that there is only a single sperm that is going to fuse with the egg cell. This theory agrees with the result that single sperms are able to fuse with *ec1* but without obligatory direct involvement of EC1 in sperm cell separation.

6.5 *EC1* expression and protein purification is challenging

To study the mechanistic role of EC1 in more detail it was aimed to purify the protein and apply it in a bioassay. However, *EC1* expression and purification turned out to be very difficult. *In planta* systems were not suitable because of rapid degradation of misexpressed protein, which was indicated by the proteasome inhibitor assay. Although the phospho-mimicking form of EC1.1 fused to eGFP was more stable than the native variant it will probably not be useful for purification because the fluorescence was still much weaker compared to the positive control CAT6-eGFP or other fusion constructs. Moreover, in stably transformed *Arabidopsis* plants expressing the phospho-mimicking variant of *EC1.1* fused to *eGFP*, fluorescence could not be detected. This might indicate, that either reduced promoter activity prevents the accumulation of protein, or that additional mechanisms induce ubiquitination and thus mark the protein for degradation. The inhibition of EC1.1 protein accumulation indicates that the presence of this protein is harmful or even toxic to cells, perhaps due to its possible function in membrane adhesion. Misexpression of *Drosophila Reggie2/Flo1* requires the presence of the stabilizing protein Reggie1/Flo2 (Hoehne *et al.*, 2005). Similarly, misexpressed *EC1* might also need the co-expression of a (egg cell-) specific kinase mediating EC1 phosphorylation and stabilization.

The attempt to express *EC1.1* in *Pichia pastoris* also failed. Western Blot analyses showed that the induction of target protein expression was successful, but the signal on the Blot correlated to a molecular mass that was larger than expected. Additionally, the signal on the Western Blot did not appear as a clear band but was diffuse. The increased apparent molecular weight suggested some post-translational modification like glycosylation. However, only one Asn-X-Ser/Thr sequon for *N*-linked glycosylation was found in EC1.1. To clarify, whether EC1.1 is *N*-glycosylated in *P. pastoris* the

putative *N*-linked glycan could be cleaved off by performing an Endoglycosidase H digest. In yeast and fungi secreted proteins are substantially *O*-mannosylated (reviewed by Strahl-Bolsinger *et al*., 1999) and it has been also shown that *O*-mannosylation occurs on expressed proteins in *Pichia pastoris* (Duman *et al.*, 1998). To date, *O*-mannosylation has been found in fungi and in mammals, however homologs of the key enzymes that initiate *O*-mannosylation (protein *O*-mannoslytransferases, PMT) have not been found in *C. elegans* or in plants (reviewed by Lommel and Strahl, 2009). In *Pichia pastoris,* expressed *EC1.1* enters the secretory pathway. EC1.1 contains a large number of serine and threonine residues (22% of all amino acids are serine or threonine), which are the most commonly used hydroxy amino acids for *O*-linking of mannose. Thus, *Pichia pastoris* expressed *EC1.1* might be *O*-mannosylated, a post-translational modification that does not take place in plants, and which might be critical for the biological activity of EC1.1. Apart from this possible post-translational modification, EC1.1 could not be purified by Ni-NTA agarose affinity chromatography. The most prominent protein enriched after chromatography, which was visible on the Coomassie stained gel did not correlate in size with the specific signal obtained on the Western Blot. The enrichment of a 30 kDa non-target protein, presumably an endogenous secreted protein from *Pichia pastoris,* occurred also in other experiments during expression of a secreted cysteine-rich or another hydrophobic protein (I. Kliwer, personal communication).

TfCRP1 an *TFCRP3*, two genes encoding defensin-like LURE proteins from *Torenia fournieri* have been successfully expressed in *E. coli*, whereas *TfCRP2* could not be expressed (Okuda *et al.*, 2009). Although the cytoplasm of *E. coli* is too reducing to form disulfide bonds, it was tried to purify EC1 from *E. coli*. Expression of two constructs in several strains with different properties revealed various problems. In addition to the problem of disulfide bond formation and purification of N-terminally His-tagged protein, the major problem was insolubility of the target protein. Finally, the most promising results were obtained after expressing *EC1.2a* in the *T7* based LemoGami cells. Here, the problem of disulfide bond formation was solved due to the use of Origami cells that carry mutations in the genes encoding the thioredoxin reductase and the glutathione reductase. Moreover, the introduction of the pLEMO plasmid enables tunable expression and the target protein was partially soluble. However, the purification of EC1.2a by Ni-NTA agarose affinity chromatography did not work. On the other hand, the purification with a GSTrap column of refolded GST-

EC1.1 from Rosetta cells worked. Thus, the use of a vector with a GST-tag for *T7* based expression may represent the future solution for *EC1* expression and purification from *E. coli*.

6.6 EC1.1 interacts with a fragment of PP2A B'θ and UbDKγ3 in yeast

In a yeast-two-hybrid screen of a pollen tube cDNA library two putative interaction partners of EC1.1 were identified: the regulatory B'θ subunit of Phosphatase 2A and UbDKγ3, a protein with two ubiquitin-like domains. The interaction of the full length clones could not be verified in yeast. It has been observed before that full length proteins do not always interact in the yeast-two-hybrid system although fragments were found to interact and the interaction could be verified with other methods (Preuss *et al.*, 2006). Biochemical interaction of EC1 with PP2A B'θ and UbDKγ3 has not be shown so far, but at least for PP2A B'θ the experiments described in this thesis further support the hypothesis of interaction. The phospho-mimicking experiments suggest that phosphorylation plays a role in EC1.1 stability and misexpressed *PP2A B'θ* results in a phenotype similar to $ec1^{+/-}$ indicating genetic interaction.

PP2A B'θ is a regulatory subunit of serine/threonine phosphoprotein phosphatases (PPPs) that are found in all eukaryotes and which are grouped into different types. In general, all functional phosphatases consist of one catalytic subunit encoded by only few genes and one or more regulatory subunits, which mediate, for example, substrate specificity and subcellular localization. The regulatory subunits are usually encoded by several genes to ensure a large spectrum of specificity and diversity (reviewed by Virshup and Shenolikar, 2009). The *Arabidopsis* genome encodes for 5 ubiquitously expressed catalytical subunits of PP2A and for 21 regulatory subunits that are grouped into four major classes: A, B, B' and B'' (reviewed by Farkas *et al*., 2007). The gene encoding the B'θ subunit identified in the yeast-two-hybrid screen is ubiquitously expressed, according to publicly available expression data (Genevestigator and Arabidopsis eFP Browser), but not present in the cells of the female gametophyte (Šoljić *et al*., in preparation). This expression pattern suggests that B'θ might trigger dephosphorylation of misexpressed EC1.1 in any other tissue. In the endogenous situation, EC1.1 might be dephosphorylated to trigger its degradation after fertilization. According to our hypothesis, the pollen tube would not only deliver the sperm cells to

the female gametophyte but also the B'θ subunit to ensure that the first step of EC1.1 degradation after fertilization is accomplished in a controlled manner.

Matre *et al*. (2009) showed that the B'θ subunit of PP2A localizes to peroxisomes in transiently transformed tobacco and onion epidermal cells as well as in *Arabidopsis* cell suspension cultures. The authors could show that the C-terminal SSL peptide is necessary for localization to peroxisomes. Masking of the C-terminus by fusing a fluorophore resulted in an even distribution of fusion protein in the cytosol. This localization has not been verified yet for *Arabidopsis* pollen tubes and is currently investigated, but nevertheless complicates the model. After pollen tube arrival EC1 is secreted into the space that was occupied by the receptive synergid cell. If B'θ was still localized to peroxisomes the interaction of EC1 and B'θ is unlikely. However, it has been proposed that the molecular mechanisms during pollen tube guidance and burst are similar to defense mechanisms although the direct involvement of reactive oxygen species (ROS) in fertilization remains unclear (Dresselhaus and Márton, 2009). ROS act as signaling molecules and oxidative burst takes place during early events of plant-pathogen interactions and can induce hypersensitive cell death (reviewed by Nanda *et al*., 2010). Moreover, conserved molecular components for pollen tube reception and fungal invasion have been identified recently. *NORTIA* (*NRT*) encodes a Mildew resistance locus o (MLO) protein and is involved in pollen tube reception. In *nrt* female gametophytes, pollen tubes fail to arrest (Kessler *et al.*, 2010). Interestingly, a similar mutant phenotype has been described involving peroxisome function. When an *amc* pollen tube enters an *amc* female gametophyte, it fails to burst and to release its content. Instead *amc* pollen tubes continue to grow within the embryo sac. *AMC* encodes a peroxin and is involved in peroxisomal protein import (Boisson-Dernier *et al.*, 2008). If the synergid cell underwent cell death induced by an oxidative burst then presumably also the organelles of the pollen tube including the peroxisomes would disintegrate and thus enable the interaction of EC1.1 and PP2A B'θ. For the complete understanding of the interaction of EC1.1 and PP2A B'θ subcellular localization studies of both proteins and co-localization experiments have to be performed necessarily.

Additionally, a fragment of UbDKγ3 was found to interact with EC1.1 in the yeast-two-hybrid screen. Galvão *et al*. (2008) proposed that UbDKγ4 might assist in delivering polyubiquitinated proteins targeted for degradation. If UbDKγ3, the closest homolog to UbDKγ4, has a similar function, it could be assumed that polyubiquitinated EC1.1 is recognized and transported to the proteasome for degradation. Galvão *et al*.

(2008) could also show that UbDKγ4 interacts with RPN10 and UFD1, which are both known to bind forms of ubiquitin and which are involved in protein degradation via the ubiquitin proteasome pathway (reviewed by Elsasser and Finley, 2005). Moreover, RPN10 is directly associated to the 19S regulatory particle of the 26S proteasome. *Arabidopsis* plants that have a defect in *RPN10* accumulate ubiquitinated proteins (Smalle *et al.*, 2003). Although *rpn10* plants display a pleitropic phenotype like reduced growth and reduced fertility they might be a useful tool for overexpression of *EC1 in planta*.

Based on the available data, I established a model about EC1 function and its subsequent degradation (Figure 29): in the mature egg cell, EC1 is localized in vesicles (Figure 29A). The pollen tube carries the PP2A regulatory subunit B'θ as well as its main cargo, the two sperm cells. During fertilization, the pollen tube grows through the stigma and the transmitting tract, along the funiculus and finally enters the ovule at the micropylar opening (Figure 29B). Upon pollen tube arrival and/or synergid cell death, vesicles containing EC1 are secreted from the egg cell upon induced signaling (Figure 29B, C). After synergid degeneration the pollen tube ruptures and releases its content into the space of the degenerating, receptive synergid cell (Figure 29C). The sperm cells are rapidly transported to the site of gamete fusion through a yet unknown mechanism (Figure 29D). At this point we assume that EC1 acts on sperm cell separation and/or gamete recognition. Simultaneously, PP2A B'θ is also located at the site of gamete fusion and triggers EC1 degradation by dephosphorylation (Figure 29E, F). Finally, fusion of the two sperm cells with the central cell and the egg cell, respectively, is completed, and EC1 protein is degraded via the ubiquitin-proteasome pathway.

Legend for Figure 29: Model about EC1 function and degradation during double fertilization in *Arabidopsis*.
A Mature ovule: EC1 is localized in vesicles within the mature egg cell. **B** Pollen tube arrival: the receptive synergid cell degenerates; EC1 vesicles may localize polarly to the site of secretion. **C** Pollen tube reception, rupture and release of its content; EC1 is being secreted. **D** Sperm cells have been transported to the site of fusion between egg and central cell. EC1 functions in sperm cell separation and/or gamete recognition. PP2A B'θ is dispersed in the space of the degenerated synergid cell. **E** PP2A B'θ is also located at the site of fusion, EC1 degradation is initiated. **F** Fusion of gametes is completed, EC1 is completely degraded. Cell colors: yellow = synergid cell; blue = egg cell; dark green = central cell; red = antipodal cells in (A), sperm cells in (B)-(F); bright green dots = EC1; purple dots = PP2A B' θ; pollen tube is shown in light blue.

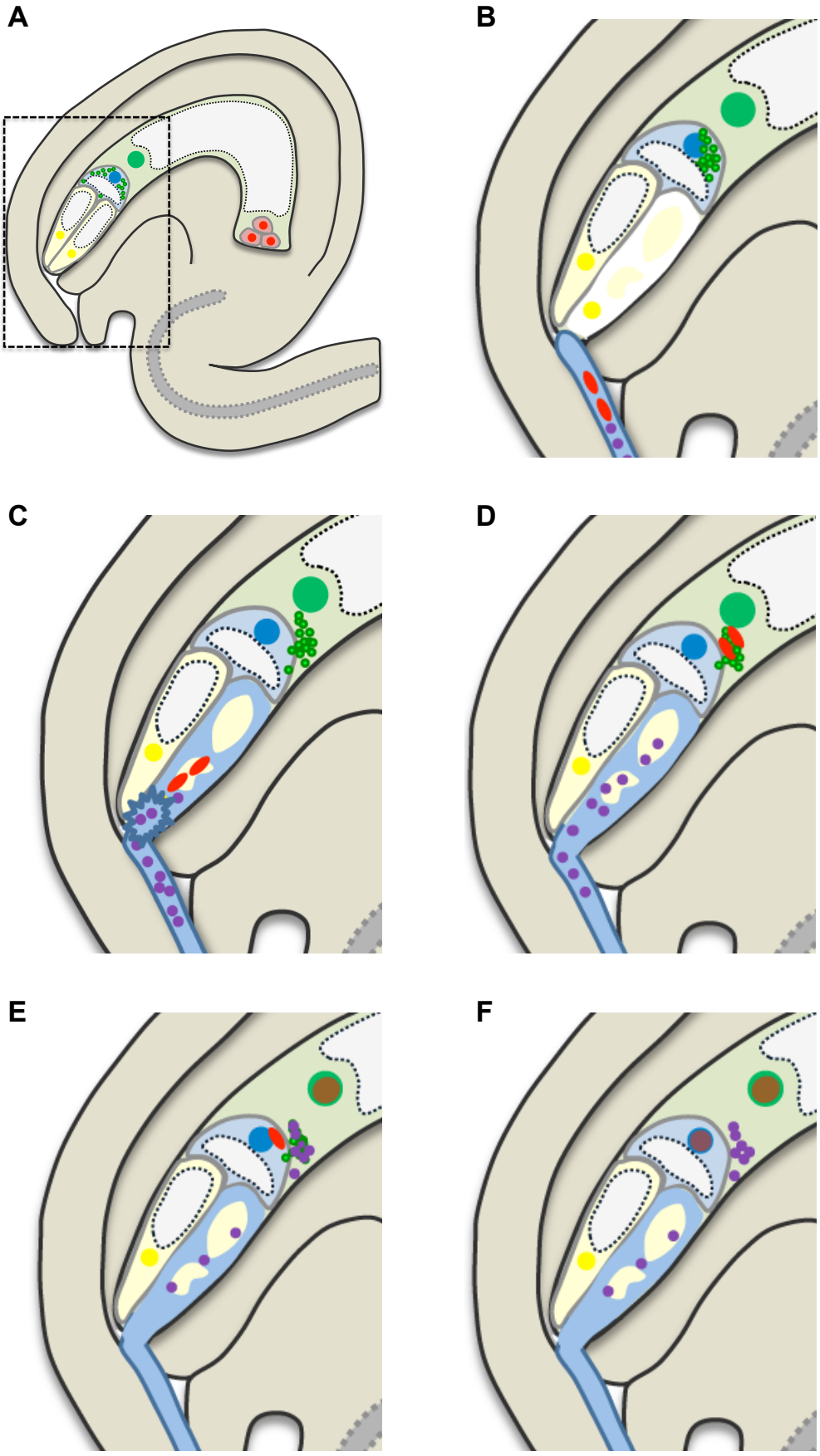

Figure 29: legend on previous page

6.7 A phospho-mimicking variant of EC1.1 shows increased stability

In order to study the role of phosphorylation for EC1.1 stability, an EC1.1 variant was generated, in which the three C-terminal serine residues that were predicted to have the highest probability to be phosphorylated were exchanged against aspartate residues. *N. benthamiana* leaf infiltration showed that this phospho-mimicking variant of EC1.1 fused to eGFP has an increased stability compared to the wild type form. This indicates that dephosphorylation of EC1.1 might trigger its degradation. However, it has not been analyzed, whether all three serines have to be phosphorylated for increased stability or if one or two serine phosphorylations are sufficient. To investigate this, single serine to aspartate exchanges or double exchanges in different combinations could be performed and analyzed for stability.

Nevertheless, one question remains open: how is the phosphorylated form stabilized and why is the non-phosphorylated form a better substrate for degradation? A look at the amino acid residues in the vicinity of the C-terminal serines shows that lysine residues appear in a distance of five to seven amino acids from these serine residues. It has been reported that phosphoserine-lysine saltbridges can stabilize the tertiary structure of proteins (Errington and Doig, 2005). Thus, on the one hand phosphorylated EC1.1 might be stabilized by electrostatic interaction of the positively charged lysine and the negatively charged phosphate group of phosphoserine and on the other hand the lysine residue might be masked for ubiquitination. To study this hypothesis it would be interesting to mutate these or maybe all lysine residues to amino acids such as histidine or arginine and analyze, for example, the stability of an EC1.1-eGFP fusion protein in the transient expression system in *N. benthamiana*.

6.8 EC1 degradation is initiated by dephosphorylation triggered by pollen tube delivered PP2A B'θ

Misexpression of the B'θ subunit of PP2A in the synergid cells could partially phenocopy the *ec1*$^{+/-}$ phenotype. Not all *PP2A B'θ-GFP* expressing ovules that were targeted and thus had a degenerated synergid cell showed non-fused sperms. This indicates the existence of a dosage effect: if there is enough EC1 that can act before the overexpressed *PP2A B'θ-GFP* can trigger its degradation by dephosphorylation, then gamete fusion will take place and fertilization will be successful. If, however,

PP2A B'θ-GFP is present abundantly and inhibits the function of EC1 by triggering its degradation, the phenotype similar to *ec1*$^{+/-}$ will occur. Taken together, the dosage of synergid cell-expressed *PP2A B'θ-GFP* will decide whether EC1 has enough time to induce the separation of the sperm cells (Figure 30). Moreover these data indicate that all EC1 proteins in *Arabidopsis* may be regulated by the same mechanism.

A tight regulation in terms of degradation of proteins involved in gamete fusion has also been observed in *Chlamydomonas*. The *plus* gamete specific FUS1 protein and the *minus* gamete specific GCS1 protein are degraded rapidly in the zygote. This degradation is triggered by gamete fusion and thus constitutes a membrane block of polygamy (Liu *et al.*, 2010). In addition to its egg cell-specific expression, EC1 seems also to be tightly regulated on the post-translational level. The rapid degradation of EC1 after gamete recognition and fusion and the fact that misexpressed EC1 is immediately degraded might indicate that EC1 acts in some fundamental cellular events that are commonly unwanted for all other cells comparable to GCS1 and FUS1 specific function in gamete membrane fusion. Since membrane fusion is rather unlikely, membrane adhesion or cell wall loosening might be possible mechanisms.

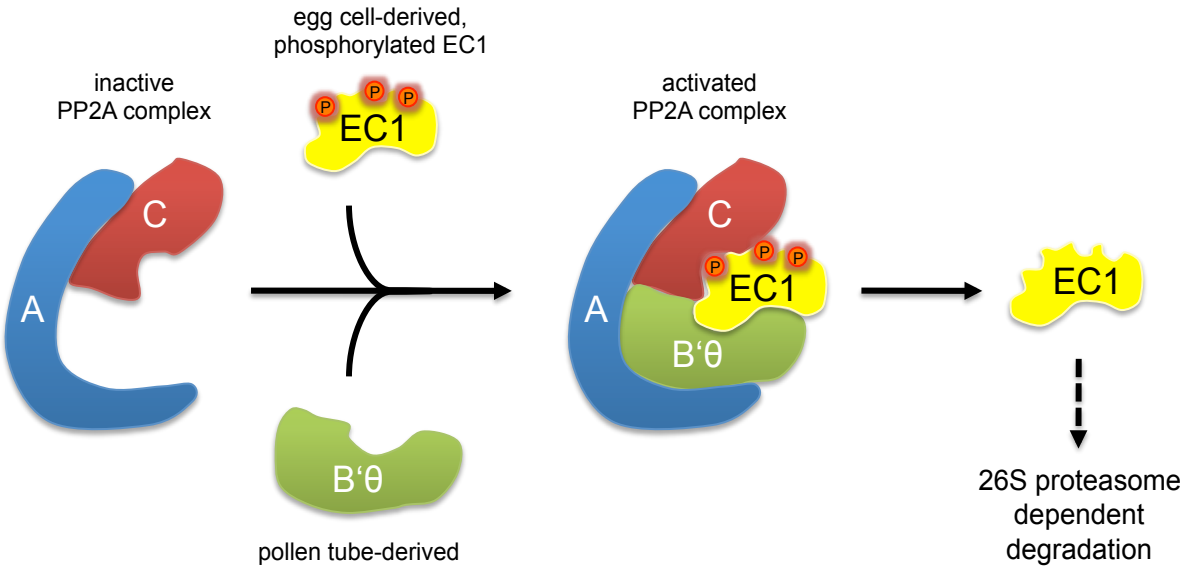

Figure 30: Model for EC1 dephosphorylation.
Inactive Phosphatase 2A (PP2A) consisting of catalytic subunit (C, red) and regulatory subunit A (blue). Activation of the complex upon binding of pollen tube derived B'θ regulatory subunit (green), which mediates substrate specificity for EC1 (yellow). Phosphorylated EC1 is secreted from the egg cell and becomes dephosphorylated by the activated PP2A complex. Dephosphorylated EC1 is destabilized and targeted for ubiquitin/proteasome dependent degradation. Adapted from Virshup and Shenolikar, 2009.

6.9 Outlook

In the future, the most interesting aspects regarding EC1 function are to find out how EC1 acts mechanistically during the process of membrane recognition or membrane attachment. Ultrastructural analyses of wild type and *ec1* female gametophytes will be indispensable. These analyses will be technically challenging though they may not only show at which point the defect caused by the loss of *EC1* occurs, but also give interesting insights into the *Arabidopsis* MGU organization during fertilization. Moreover, the identification of the sperm cell interaction partner is another important step towards the complete understanding of EC1 function. Since EC1 is a secreted protein and seems to act on the sperm cells, a receptor on the sperm cell surface might be expected. However, the exact function of EC1 has not been identified yet, which complicates the application of classical biochemical approaches like co-immunoprecipitation or pull-down assays. It is, for example, not clear whether EC1 acts during gamete adhesion or during separation of the sperm cells. In the first case, the membrane fraction would be the most interesting fraction of proteins for the search of an interaction partner, whereas in the latter case it would probably be important to have pairs of sperm cells with an intact connection. A more promising approach would be a mutant screen. *HTR10-mRFP1* expressing *Arabidopsis* lines could be mutagenized, e.g. chemically by ethylmethane sulfonate (EMS) and the progeny could then be screened for an $ec1^{+/-}$-like phenotype. The first trait for a candidate would be a reduced seed set. However, disruption of a housekeeping gene often leads to lethal defects in haploid gametophytes resulting in reduced seed. But since the screen for non-fusing sperm cells within the population of siliques with aborted seeds should be quite specific, I think that such a screen might be promising.

The generation of antibodies against EC1 might also be useful for e.g. whole mount protein localization in the female gametophyte. This method of protein immunolocalization has been described by Sauer *et al*. (2006) and has been already successfully applied for female gametophytes with different primary antibodies. With these antibodies the changing localization of the native protein during fertilization could be confirmed.

Another interesting aspect regarding EC1.1 post-translational modification and degradation would be to analyze which of the three serines residues are necessary for stabilization of the EC1.1 protein. Therefore, different combinations of serine-aspartate exchanges could be analyzed. Moreover, it needs to be shown, that the egg cell derived

EC1.1 protein is indeed phosphorylated. Due to the limited amount of protein it will be very difficult to show. However, it may be aimed to identify the EC1 kinase. Therefore, another yeast-two-hybrid screen with an egg cell library or a targeted approach with the most strongly expressed kinases in the egg cell could be performed. The identification of the ubiquitinated lysine residue(s) would also deepen the knowledge about the regulation of EC1.1 degradation. Similar to the analysis of serine phosphorylation, the lysine residues could be mutagenized and the protein could be analyzed for stability in the *N. benthamiana* system.

Furthermore, the interaction of PP2A B'θ and EC1.1 has to be confirmed using, for example, FRET analysis. In the future, plants expressing a fusion of *tagRFP-T* and *PP2A B'θ* under control of the endogenous *PP2A B'θ* promoter will be analyzed for subcellular localization. Moreover, these lines will be used for pollination of plants expressing *EC1.1-GFP* under control of the endogenous *EC1.1* promoter and localization of both fusion proteins will be observed within the gametophytes and simultaneously during fertilization. The phenotype of strongly misexpressed *PP2A B'θ* was already described in this thesis but data about a loss-of-function mutant remain still elusive. To investigate the *PP2A B'θ* knockout situation, an artificial microRNA (amiRNA) has already been generated that should target all genes encoding PP2A B' subunits, which are expressed in pollen and will be analyzed in the future.

7 BIBLIOGRAPHY

Amien, S., Kliwer, I., Márton, M.L., Debener, T., Geiger, D., Becker, D., and Dresselhaus, T. (2010). Defensin-like ZmES4 mediates pollen tube burst in maize via opening of the potassium channel KZM1. PLoS Biol **8,** e1000388.

Aw, S.J., Hamamura, Y., Chen, Z., Schnittger, A., and Berger, F. (2010). Sperm entry is sufficient to trigger division of the central cell but the paternal genome is required for endosperm development in *Arabidopsis*. Development **137,** 2683-2690.

Balandin, M., Royo, J., Gomez, E., Muniz, L.M., Molina, A., and Hueros, G. (2005). A protective role for the embryo surrounding region of the maize endosperm, as evidenced by the characterisation of *ZmESR-6*, a defensin gene specifically expressed in this region. Plant Mol Biol **58,** 269-282.

Blobel, C.P., Myles, D.G., Primakoff, P., and White, J.M. (1990). Proteolytic processing of a protein involved in sperm-egg fusion correlates with acquisition of fertilization competence. J Cell Biol **111,** 69-78.

Boisson-Dernier, A., Kessler, S.A., and Grossniklaus, U. (2011). The walls have ears: the role of plant CrRLK1Ls in sensing and transducing extracellular signals. J Exp Bot **62,** 1581-1591.

Boisson-Dernier, A., Frietsch, S., Kim, T.H., Dizon, M.B., and Schroeder, J.I. (2008). The peroxin loss-of-function mutation *abstinence by mutual consent* disrupts male-female gametophyte recognition. Curr Biol **18,** 63-68.

Boisson-Dernier, A., Roy, S., Kritsas, K., Grobei, M.A., Jaciubek, M., Schroeder, J.I., and Grossniklaus, U. (2009). Disruption of the pollen-expressed *FERONIA* homologs *ANXUR1* and *ANXUR2* triggers pollen tube discharge. Development **136,** 3279-3288.

Borg, M., and Twell, D. (2010). Life after meiosis: patterning the angiosperm male gametophyte. Biochem Soc T **38,** 577-582.

Borg, M., Brownfield, L., and Twell, D. (2009). Male gametophyte development: a molecular perspective. J Exp Bot **60,** 1465-1478.

Bradford, M.M. (1976). A rapid and sensitive method for the quantitation of microgram quantities of protein utilizing the principle of protein-dye binding. Anal Biochem **72,** 248-254.

Bruns, D., and Owens, J.N. (2000). Western white pine (*Pinus monticola* Dougl.) reproduction: II. Fertilisation and cytoplasmic inheritance. Sexual Plant Reproduction **13,** 75-84.

Capron, A., Gourgues, M., Neiva, L.S., Faure, J.E., Berger, F., Pagnussat, G., Krishnan, A., Alvarez-Mejia, C., Vielle-Calzada, J.P., Lee, Y.R., Liu, B., and Sundaresan, V. (2008). Maternal control of male-gamete delivery in *Arabidopsis* involves a putative GPI-anchored protein encoded by the *LORELEI* gene. Plant Cell **20,** 3038-3049.

Ceroni, A., Passerini, A., Vullo, A., and Frasconi, P. (2006). DISULFIND: a disulfide bonding state and cysteine connectivity prediction server. Nucleic Acids Res **34,** W177-181.

Chae, K., and Lord, E.M. (2011). Pollen tube growth and guidance: roles of small, secreted proteins. Ann Bot**,** doi: 10.1093/aob/mcr1015.

Cheung, A.Y., Wang, H., and Wu, H.M. (1995). A floral transmitting tissue-specific glycoprotein attracts pollen tubes and stimulates their growth. Cell **82,** 383-393.

Clough, S.J., and Bent, A.F. (1998). Floral dip: a simplified method for *Agrobacterium*-mediated transformation of *Arabidopsis thaliana*. Plant J **16,** 735-743.

Cohen, D.J., Busso, D., Da Ros, V., Ellerman, D.A., Maldera, J.A., Goldweic, N., and Cuasnicu, P.S. (2008). Participation of cysteine-rich secretory proteins (CRISP) in mammalian sperm-egg interaction. International Journal of Developmental Biology **52,** 737-742.

Da Ros, V., Busso, D., Cohen, D.J., Maldera, J., Goldweic, N., and Cuasnicu, P.S. (2007). Molecular mechanisms involved in gamete interaction: evidence for the participation of cysteine-rich secretory proteins (CRISP) in sperm-egg fusion. Soc Reprod Fertil Suppl **65,** 353-356.

Dickinson, H.G. (2000). Pollen stigma interactions: so near yet so far. Trends Genet **16,** 373-376.

Dresselhaus, T. (2006). Cell-cell communication during double fertilization. Curr Opin Plant Biol **9,** 41-47.

Dresselhaus, T., and Márton, M.L. (2009). Micropylar pollen tube guidance and burst: adapted from defense mechanisms? Curr Opin Plant Biol **12,** 773-780.

Dresselhaus, T., Lausser, A., and Márton, M.L. (2011). Using maize as a model to study pollen tube growth and guidance, cross-incompatibility and sperm delivery in grasses. Ann Bot**,** doi: 10.1093/aob/mcr1017.

Duman, J.G., Miele, R.G., Liang, H., Grella, D.K., Sim, K.L., Castellino, F.J., and Bretthauer, R.K. (1998). *O*-Mannosylation of *Pichia pastoris* cellular and recombinant proteins. Biotechnol Appl Biochem **28 (Pt 1),** 39-45.

Dumas, C., Knox, R.B., and Gaude, T. (1985). The spatial association of the sperm cells and vegetative nucleus in the pollen grain of *Brassica*. Protoplasma **124,** 168-174.

Elsasser, S., and Finley, D. (2005). Delivery of ubiquitinated substrates to protein-unfolding machines. Nat Cell Biol **7,** 742-749.

Errington, N., and Doig, A.J. (2005). A phosphoserine-lysine salt bridge within an alpha-helical peptide, the strongest alpha-helix side-chain interaction measured to date. Biochemistry **44,** 7553-7558.

Escobar-Restrepo, J.M., Huck, N., Kessler, S., Gagliardini, V., Gheyselinck, J., Yang, W.C., and Grossniklaus, U. (2007). The FERONIA receptor-like kinase mediates male-female interactions during pollen tube reception. Science **317,** 656-660.

Farkas, I., Dombradi, V., Miskei, M., Szabados, L., and Koncz, C. (2007). *Arabidopsis* PPP family of serine/threonine phosphatases. Trends Plant Sci **12,** 169-176.

Fobis-Loisy, I., Miege, C., and Gaude, T. (2004). Molecular evolution of the S locus controlling mating in the *Brassicaceae*. Plant Biology **6,** 109-118.

Foote, H.C., Ride, J.P., Franklin-Tong, V.E., Walker, E.A., Lawrence, M.J., and Franklin, F.C. (1994). Cloning and expression of a distinctive class of self-incompatibility (S) gene from *Papaver rhoeas* L. Proc Natl Acad Sci U S A **91,** 2265-2269.

Galvão, R.M., Kota, U., Soderblom, E.J., Goshe, M.B., and Boss, W.F. (2008). Characterization of a new family of protein kinases from *Arabidopsis* containing phosphoinositide 3/4-kinase and ubiquitin-like domains. Biochem J **409,** 117-127.

Gebert, M. (2008). The gametophyte specific ARM repeat protein AtARO1 is required for actin dynamics in *Arabidopsis* during pollen tube growth and double fertilization. In Cell Biology & Plant Biochemistry; PhD Thesis (Regensburg: University of Regensburg).

Gebert, M., Dresselhaus, T., and Sprunck, S. (2008). F-Actin organization and pollen tube tip growth in *Arabidopsis* are dependent on the gametophyte-specific Armadillo repeat protein ARO1. Plant Cell **20,** 2798-2814.

Gouy, M., Guindon, S., and Gascuel, O. (2010). SeaView version 4: a multiplatform graphical user interface for sequence alignment and phylogenetic tree building. Molecular Biology and Evolution **27,** 221-224.

Gutierrez-Marcos, J.F., Costa, L.M., Biderre-Petit, C., Khbaya, B., O'Sullivan, D.M., Wormald, M., Perez, P., and Dickinson, H.G. (2004). *maternally expressed gene1* is a novel maize endosperm transfer cell-specific gene with a maternal parent-of-origin pattern of expression. Plant Cell **16,** 1288-1301.

Hara, K., Kajita, R., Torii, K.U., Bergmann, D.C., and Kakimoto, T. (2007). The secretory peptide gene *EPF1* enforces the stomatal one-cell-spacing rule. Genes Dev **21,** 1720-1725.

Hara, K., Yokoo, T., Kajita, R., Onishi, T., Yahata, S., Peterson, K.M., Torii, K.U., and Kakimoto, T. (2009). Epidermal cell density is autoregulated via a secretory peptide, EPIDERMAL PATTERNING FACTOR 2 in *Arabidopsis* leaves. Plant Cell Physiol **50,** 1019-1031.

Harper, J.W., Adami, G.R., Wei, N., Keyomarsi, K., and Elledge, S.J. (1993). The p21 Cdk-interacting protein Cip1 is a potent inhibitor of G1 cyclin-dependent kinases. Cell **75,** 805-816.

Higashiyama, T. (2010). Peptide signaling in pollen-pistil interactions. Plant and Cell Physiology **51,** 177-189.

Higashiyama, T., Yabe, S., Sasaki, N., Nishimura, Y., Miyagishima, S., Kuroiwa, H., and Kuroiwa, T. (2001). Pollen tube attraction by the synergid cell. Science **293,** 1480-1483.

Hirai, M., Arai, M., Mori, T., Miyagishima, S.Y., Kawai, S., Kita, K., Kuroiwa, T., Terenius, O., and Matsuoka, H. (2008). Male fertility of malaria parasites is determined by GCS1, a plant-type reproduction factor. Curr Biol **18,** 607-613.

Hoehne, M., de Couet, H.G., Stuermer, C.A., and Fischbach, K.F. (2005). Loss- and gain-of-function analysis of the lipid raft proteins Reggie/Flotillin in *Drosophila*: they are posttranslationally regulated, and misexpression interferes with wing and eye development. Mol Cell Neurosci **30,** 326-338.

Hruz, T., Laule, O., Szabo, G., Wessendorp, F., Bleuler, S., Oertle, L., Widmayer, P., Gruissem, W., and Zimmermann, P. (2008). Genevestigator v3: a reference expression database for the meta-analysis of transcriptomes. Adv Bioinformatics **2008,** 420747.

Huang, B.Q., Fu, Y., Zee, S.Y., and Hepler, P.K. (1999). Three-dimensional organization and dynamic changes of the actin cytoskeleton in embryo sacs of *Zea mays* and *Torenia fournieri*. Protoplasma **209,** 105-119.

Huck, N., Moore, J.M., Federer, M., and Grossniklaus, U. (2003). The *Arabidopsis* mutant *feronia* disrupts the female gametophytic control of pollen tube reception. Development **130,** 2149-2159.

Ingouff, M., Hamamura, Y., Gourgues, M., Higashiyama, T., and Berger, F. (2007). Distinct dynamics of HISTONE3 variants between the two fertilization products in plants. Curr Biol **17,** 1032-1037.

Ingouff, M., Rademacher, S., Holec, S., Šoljić, L., Xin, N., Readshaw, A., Foo, S.H., Lahouze, B., Sprunck, S., and Berger, F. (2010). Zygotic resetting of the HISTONE 3 variant repertoire participates in epigenetic reprogramming in *Arabidopsis*. Curr Biol **20,** 2137-2143.

Iwakawa, H., Shinmyo, A., and Sekine, M. (2006). *Arabidopsis* CDKA;1, a cdc2 homologue, controls proliferation of generative cells in male gametogenesis. Plant J **45,** 819-831.

James, P., Halladay, J., and Craig, E.A. (1996). Genomic libraries and a host strain designed for highly efficient two-hybrid selection in yeast. Genetics **144,** 1425-1436.

Johnson, M.A., and Lord, E. (2006). Extracellular guidance cues and intracellular signaling pathways that direct pollen tube growth. Pollen Tube: Cellular and Molecular Perspective **3,** 223-242.

Jones-Rhoades, M.W., Borevitz, J.O., and Preuss, D. (2007). Genome-wide expression profiling of the *Arabidopsis* female gametophyte identifies families of small, secreted proteins. PLoS Genet **3,** 1848-1861.

Karimi, M., Depicker, A., and Hilson, P. (2007). Recombinational cloning with plant gateway vectors. Plant Physiol **145,** 1144-1154.

Kessler, S.A., Shimosato-Asano, H., Keinath, N.F., Wuest, S.E., Ingram, G., Panstruga, R., and Grossniklaus, U. (2010). Conserved molecular components for pollen tube reception and fungal invasion. Science **330,** 968-971.

Kim, S., Mollet, J.C., Dong, J., Zhang, K., Park, S.Y., and Lord, E.M. (2003). Chemocyanin, a small basic protein from the lily stigma, induces pollen tube chemotropism. Proc Natl Acad Sci U S A **100,** 16125-16130.

Kliwer, I., and Dresselhaus, T. (2010). Establishment of the male germline and sperm cell movement during pollen germination and tube growth in maize. Plant Signal Behav **5,** 885-889.

Koch, M.A., Haubold, B., and Mitchell-Olds, T. (2000). Comparative evolutionary analysis of chalcone synthase and alcohol dehydrogenase loci in *Arabidopsis*, *Arabis*, and related genera (*Brassicaceae*). Mol Biol Evol **17,** 1483-1498.

Lalanne, E., and Twell, D. (2002). Genetic control of male germ unit organization in *Arabidopsis*. Plant Physiol **129,** 865-875.

Li, H., Lin, Y., Heath, R.M., Zhu, M.X., and Yang, Z. (1999). Control of pollen tube tip growth by a Rop GTPase-dependent pathway that leads to tip-localized calcium influx. Plant Cell **11,** 1731-1742.

Liu, Y., Misamore, M.J., and Snell, W.J. (2010). Membrane fusion triggers rapid degradation of two gamete-specific, fusion-essential proteins in a membrane block to polygamy in *Chlamydomonas*. Development **137,** 1473-1481.

Liu, Y., Tewari, R., Ning, J., Blagborough, A.M., Garbom, S., Pei, J., Grishin, N.V., Steele, R.E., Sinden, R.E., Snell, W.J., and Billker, O. (2008). The conserved plant sterility gene *HAP2* functions after attachment of fusogenic membranes in *Chlamydomonas* and *Plasmodium* gametes. Genes Dev **22,** 1051-1068.

Lommel, M., and Strahl, S. (2009). Protein *O*-mannosylation: conserved from bacteria to humans. Glycobiology **19,** 816-828.

Lord, E. (2000). Adhesion and cell movement during pollination: cherchez la femme. Trends Plant Sci **5,** 368-373.

Lu, Y., Chanroj, S., Zulkifli, L., Johnson, M.A., Uozumi, N., Cheung, A., and Sze, H. (2011). Pollen tubes lacking a pair of K^+ transporters fail to target ovules in *Arabidopsis*. Plant Cell **23,** 81-93.

Macauley-Patrick, S., Fazenda, M.L., McNeil, B., and Harvey, L.M. (2005). Heterologous protein production using the *Pichia pastoris* expression system. Yeast **22,** 249-270.

Magnard, J.L., Le Deunff, E., Domenech, J., Rogowsky, P.M., Testillano, P.S., Rougier, M., Risueno, M.C., Vergne, P., and Dumas, C. (2000). Genes normally expressed in the endosperm are expressed at early stages of microspore embryogenesis in maize. Plant Mol Biol **44,** 559-574.

Maheshwari, P. (1950). An introduction to the embryology of angiosperms. (New York: McGraw-Hill).

Marshall, E., Costa, L.M., and Gutierrez-Marcos, J. (2011). Cysteine-Rich Peptides (CRPs) mediate diverse aspects of cell-cell communication in plant reproduction and development. J Exp Bot **62,** 1677-1686.

Márton, M.L., and Dresselhaus, T. (2010). Female gametophyte-controlled pollen tube guidance. Biochem Soc Trans **38,** 627-630.

Márton, M.L., Cordts, S., Broadhvest, J., and Dresselhaus, T. (2005). Micropylar pollen tube guidance by Egg Apparatus 1 of maize. Science **307,** 573-576.

Matre, P., Meyer, C., and Lillo, C. (2009). Diversity in subcellular targeting of the PP2A B'eta subfamily members. Planta **230,** 935-945.

McCue, A.D., Cresti, M., Feijo, J.A., and Slotkin, R.K. (2011). Cytoplasmic connection of sperm cells to the pollen vegetative cell nucleus: potential roles of the male germ unit revisited. J Exp Bot **62,** 1621-1631.

Mergaert, P., Nikovics, K., Kelemen, Z., Maunoury, N., Vaubert, D., Kondorosi, A., and Kondorosi, E. (2003). A novel family in *Medicago truncatula* consisting of more than 300 nodule-specific genes coding for small, secreted polypeptides with conserved cysteine motifs. Plant Physiol **132,** 161-173.

Miller, D.D., Scordilis, S.P., and Hepler, P.K. (1995). Identification and localization of three classes of myosins in pollen tubes of *Lilium longiflorum* and *Nicotiana alata*. J Cell Sci **108,** 2549-2563.

Miyazaki, S., Murata, T., Sakurai-Ozato, N., Kubo, M., Demura, T., Fukuda, H., and Hasebe, M. (2009). *ANXUR1* and *2*, sister genes to *FERONIA/SIRENE*, are male factors for coordinated fertilization. Curr Biol **19,** 1327-1331.

Mollet, J.C., Park, S.Y., Nothnagel, E.A., and Lord, E.M. (2000). A lily stylar pectin is necessary for pollen tube adhesion to an in vitro stylar matrix. Plant Cell **12,** 1737-1750.

Mori, T., Kuroiwa, H., Higashiyama, T., and Kuroiwa, T. (2006). GENERATIVE CELL SPECIFIC 1 is essential for angiosperm fertilization. Nat Cell Biol **8,** 64-71.

Mori, T., Hirai, M., Kuroiwa, T., and Miyagishima, S.Y. (2010). The functional domain of GCS1-based gamete fusion resides in the amino terminus in plant and parasite species. PLoS ONE **5,** e15957.

Muschietti, J., Dircks, L., Vancanneyt, G., and McCormick, S. (1994). LAT52 protein is essential for tomato pollen development: pollen expressing antisense *LAT52* RNA hydrates and germinates abnormally and cannot achieve fertilization. Plant J **6,** 321-338.

Nakao, Y., Kawase, K., Shiozaki, S., Ogata, T., and Horiuchi, S. (2001). The growth of pollen and female reproductive organs of ginkgo between pollination and fertilization. J Jpn Soc Hortic Sci **70,** 21-27.

Nanda, A.K., Andrio, E., Marino, D., Pauly, N., and Dunand, C. (2010). Reactive oxygen species during plant-microorganism early interactions. J Integr Plant Biol **52,** 195-204.

Nixon, B., Aitken, R.J., and McLaughlin, E.A. (2007). New insights into the molecular mechanisms of sperm-egg interaction. Cell Mol Life Sci **64,** 1805-1823.

Nowack, M.K., Grini, P.E., Jakoby, M.J., Lafos, M., Koncz, C., and Schnittger, A. (2006). A positive signal from the fertilization of the egg cell sets off endosperm proliferation in angiosperm embryogenesis. Nat Genet **38,** 63-67.

Okuda, S., Tsutsui, H., Shiina, K., Sprunck, S., Takeuchi, H., Yui, R., Kasahara, R.D., Hamamura, Y., Mizukami, A., Susaki, D., Kawano, N., Sakakibara, T., Namiki, S., Itoh, K., Otsuka, K., Matsuzaki, M., Nozaki, H., Kuroiwa, T., Nakano, A., Kanaoka, M.M., Dresselhaus, T., Sasaki, N., and Higashiyama, T. (2009). Defensin-like polypeptide LUREs are pollen tube attractants secreted from synergid cells. Nature **458,** 357-361.

Palanivelu, R., Brass, L., Edlund, A.F., and Preuss, D. (2003). Pollen tube growth and guidance is regulated by *POP2*, an *Arabidopsis* gene that controls GABA levels. Cell **114,** 47-59.

Park, S.Y., Jauh, G.Y., Mollet, J.C., Eckard, K.J., Nothnagel, E.A., Walling, L.L., and Lord, E.M. (2000). A lipid transfer-like protein is necessary for lily pollen tube adhesion to an in vitro stylar matrix. Plant Cell **12,** 151-164.

Pearce, G., Moura, D.S., Stratmann, J., and Ryan, C.A., Jr. (2001). RALF, a 5-kDa ubiquitous polypeptide in plants, arrests root growth and development. Proc Natl Acad Sci U S A **98,** 12843-12847.

Prado, A.M., Porterfield, D.M., and Feijo, J.A. (2004). Nitric oxide is involved in growth regulation and re-orientation of pollen tubes. Development **131,** 2707-2714.

Prado, A.M., Colaco, R., Moreno, N., Silva, A.C., and Feijo, J.A. (2008). Targeting of pollen tubes to ovules is dependent on nitric oxide (NO) signaling. Mol Plant **1,** 703-714.

Preuss, M.L., Schmitz, A.J., Thole, J.M., Bonner, H.K., Otegui, M.S., and Nielsen, E. (2006). A role for the RabA4b effector protein PI-4Kbeta1 in polarized expansion of root hair cells in *Arabidopsis thaliana*. J Cell Biol **172,** 991-998.

Primakoff, P., and Myles, D.G. (2007). Cell-cell membrane fusion during mammalian fertilization. FEBS Lett **581,** 2174-2180.

Punwani, J.A., Rabiger, D.S., Lloyd, A., and Drews, G.N. (2008). The MYB98 subcircuit of the synergid gene regulatory network includes genes directly and indirectly regulated by MYB98. Plant J **55,** 406-414.

Robzyk, K., and Kassir, Y. (1992). A simple and highly efficient procedure for rescuing autonomous plasmids from yeast. Nucleic Acids Res **20,** 3790.

Rotman, N., Rozier, F., Boavida, L., Dumas, C., Berger, F., and Faure, J.E. (2003). Female control of male gamete delivery during fertilization in *Arabidopsis thaliana*. Current Biology **13,** 432-436.

Rubinstein, E., Ziyyat, A., Wolf, J.P., Le Naour, F., and Boucheix, C. (2006). The molecular players of sperm-egg fusion in mammals. Semin Cell Dev Biol **17,** 254-263.

Russell, S.D. (1992). Double fertilization. International Review of Cytology - A Survey of Cell Biology **140,** 357-387.

Russell, S.D., and Cass, D.D. (1981). Ultrastructure of the sperms of *Plumbago zeylanica*. 1. Cytology and association with the vegetative nucleus. Protoplasma **107,** 85-107.

Sambrook, J., Fritsch, E.F., and Maniatis, T. (1989). Molecular cloning: a laboratory manual; Second edition vols. 1, 2 and 3. Cold Spring Harbor Laboratory Press: Cold Spring Harbor, New York, USA. .

Sandaklie-Nikolova, L., Palanivelu, R., King, E.J., Copenhaver, G.P., and Drews, G.N. (2007). Synergid cell death in *Arabidopsis* is triggered following direct interaction with the pollen tube. Plant Physiol **144,** 1753-1762.

Sauer, M., Paciorek, T., Benkova, E., and Friml, J. (2006). Immunocytochemical techniques for whole-mount *in situ* protein localization in plants. Nat Protoc **1,** 98-103.

Scheres, B., Van De Wiel, C., Zalensky, A., Horvath, B., Spaink, H., Van Eck, H., Zwartkruis, F., Wolters, A.M., Gloudemans, T., Van Kammen, A., and et al. (1990). The ENOD12 gene product is involved in the infection process during the pea-rhizobium interaction. Cell **60,** 281-294.

Schopfer, C.R., Nasrallah, M.E., and Nasrallah, J.B. (1999). The male determinant of self-incompatibility in *Brassica*. Science **286,** 1697-1700.

Serna, A., Maitz, M., O'Connell, T., Santandrea, G., Thevissen, K., Tienens, K., Hueros, G., Faleri, C., Cai, G., Lottspeich, F., and Thompson, R.D. (2001). Maize endosperm secretes a novel antifungal protein into adjacent maternal tissue. Plant J **25,** 687-698.

Shewry, P.R., and Halford, N.G. (2002). Cereal seed storage proteins: structures, properties and role in grain utilization. J Exp Bot **53,** 947-958.

Shimizu, K.K., and Okada, K. (2000). Attractive and repulsive interactions between female and male gametophytes in *Arabidopsis* pollen tube guidance. Development **127,** 4511-4518.

Shimizu, K.K., Ito, T., Ishiguro, S., and Okada, K. (2008). *MAA3* (*MAGATAMA3*) helicase gene is required for female gametophyte development and pollen tube guidance in *Arabidopsis thaliana*. Plant Cell Physiol **49,** 1478-1483.

Shpak, E.D., McAbee, J.M., Pillitteri, L.J., and Torii, K.U. (2005). Stomatal patterning and differentiation by synergistic interactions of receptor kinases. Science **309,** 290-293.

Silverstein, K.A., Moskal, W.A., Jr., Wu, H.C., Underwood, B.A., Graham, M.A., Town, C.D., and VandenBosch, K.A. (2007). Small cysteine-rich peptides resembling antimicrobial peptides have been under-predicted in plants. Plant J **51,** 262-280.

Smalle, J., Kurepa, J., Yang, P., Emborg, T.J., Babiychuk, E., Kushnir, S., and Vierstra, R.D. (2003). The pleiotropic role of the 26S proteasome subunit RPN10 in *Arabidopsis* growth and development supports a substrate-specific function in abscisic acid signaling. Plant Cell **15,** 965-980.

Smyth, D.R., Bowman, J.L., and Meyerowitz, E.M. (1990). Early flower development in *Arabidopsis*. Plant Cell **2,** 755-767.

Sprunck, S. (2010). Let's get physical: gamete interaction in flowering plants. Biochem Soc T **38,** 635-640.

Sprunck, S., and Gross-Hardt, R. (2011). Nuclear behavior, cell polarity, and cell specification in the female gametophyte. Sex Plant Reprod**,** doi: 10.1007/s00497-00011-00161-00494.

Sprunck, S., Baumann, U., Edwards, K., Langridge, P., and Dresselhaus, T. (2005). The transcript composition of egg cells changes significantly following fertilization in wheat (*Triticum aestivum* L.). Plant J **41,** 660-672.

Steffen, J.G., Kang, I.H., Macfarlane, J., and Drews, G.N. (2007). Identification of genes expressed in the *Arabidopsis* female gametophyte. Plant J **51,** 281-292.

Strahl-Bolsinger, S., Gentzsch, M., and Tanner, W. (1999). Protein *O*-mannosylation. Biochim Biophys Acta **1426,** 297-307.

Strasburger, E. (1879). Die Angiospermen und die Gymnospermen. (Jena, Germany: Fischer).

Sugano, S.S., Shimada, T., Imai, Y., Okawa, K., Tamai, A., Mori, M., and Hara-Nishimura, I. (2010). Stomagen positively regulates stomatal density in *Arabidopsis*. Nature **463,** 241-244.

Sundaresan, V., and Alandete-Saez, M. (2010). Pattern formation in miniature: the female gametophyte of flowering plants. Development **137,** 179-189.

Suzuki, G., Kai, N., Hirose, T., Fukui, K., Nishio, T., Takayama, S., Isogai, A., Watanabe, M., and Hinata, K. (1999). Genomic organization of the S locus: Identification and characterization of genes in SLG/SRK region of S(9) haplotype of *Brassica campestris* (syn. rapa). Genetics **153,** 391-400.

Tang, W., Kelley, D., Ezcurra, I., Cotter, R., and McCormick, S. (2004). LeSTIG1, an extracellular binding partner for the pollen receptor kinases LePRK1 and LePRK2, promotes pollen tube growth *in vitro*. Plant J **39,** 343-353.

Terras, F.R., Goderis, I.J., Van Leuven, F., Vanderleyden, J., Cammue, B.P., and Broekaert, W.F. (1992a). *In vitro* antifungal activity of a radish (*Raphanus sativus* L.) seed protein homologous to nonspecific lipid transfer proteins. Plant Physiol **100,** 1055-1058.

Terras, F.R., Schoofs, H.M., De Bolle, M.F., Van Leuven, F., Rees, S.B., Vanderleyden, J., Cammue, B.P., and Broekaert, W.F. (1992b). Analysis of two novel classes of plant antifungal proteins from radish (*Raphanus sativus* L.) seeds. J Biol Chem **267,** 15301-15309.

Tsukamoto, T., Qin, Y., Huang, Y., Dunatunga, D., and Palanivelu, R. (2010). A role for LORELEI, a putative glycosylphosphatidylinositol-anchored protein, in *Arabidopsis thaliana* double fertilization and early seed development. Plant J **62,** 571-588.

van Dijk, M.R., Janse, C.J., Thompson, J., Waters, A.P., Braks, J.A., Dodemont, H.J., Stunnenberg, H.G., van Gemert, G.J., Sauerwein, R.W., and Eling, W. (2001). A central role for P48/45 in malaria parasite male gamete fertility. Cell **104,** 153-164.

van Dijk, M.R., van Schaijk, B.C., Khan, S.M., van Dooren, M.W., Ramesar, J., Kaczanowski, S., van Gemert, G.J., Kroeze, H., Stunnenberg, H.G., Eling, W.M., Sauerwein, R.W., Waters, A.P., and Janse, C.J. (2010). Three members of the 6-cys protein family of *Plasmodium* play a role in gamete fertility. PLoS Pathog **6,** e1000853.

Van Went, J.L., and Willemse, M.T.M. (1984). Fertilization. (Berlin, West Germany; New York, N.Y., USA. Illus: Springer-Verlag).

Vielle-Calzada, J.P., Baskar, R., and Grossniklaus, U. (2000). Delayed activation of the paternal genome during seed development. Nature **404,** 91-94.

Virshup, D.M., and Shenolikar, S. (2009). From promiscuity to precision: protein phosphatases get a makeover. Mol Cell **33,** 537-545.

von Besser, K., Frank, A.C., Johnson, M.A., and Preuss, D. (2006). *Arabidopsis HAP2* (*GCS1*) is a sperm-specific gene required for pollen tube guidance and fertilization. Development **133,** 4761-4769.

Vrinten, P.L., Nakamura, T., and Kasha, K.J. (1999). Characterization of cDNAs expressed in the early stages of microspore embryogenesis in barley (*Hordeum vulgare*) L. Plant Mol Biol **41,** 455-463.

Wesley, S.V., Helliwell, C.A., Smith, N.A., Wang, M.B., Rouse, D.T., Liu, Q., Gooding, P.S., Singh, S.P., Abbott, D., Stoutjesdijk, P.A., Robinson, S.P., Gleave, A.P., Green, A.G., and Waterhouse, P.M. (2001). Construct design for efficient, effective and high-throughput gene silencing in plants. Plant J **27,** 581-590.

Wheeler, M.J., de Graaf, B.H., Hadjiosif, N., Perry, R.M., Poulter, N.S., Osman, K., Vatovec, S., Harper, A., Franklin, F.C., and Franklin-Tong, V.E. (2009). Identification of the pollen self-incompatibility determinant in *Papaver rhoeas*. Nature **459,** 992-995.

Willemse, M.T.M., and Van Went, J.L. (1984). The female gametophyte. (Berlin, West Germany; New York, N.Y., USA. Illus: Springer-Verlag).

Winter, D., Vinegar, B., Nahal, H., Ammar, R., Wilson, G.V., and Provart, N.J. (2007). An "Electronic Fluorescent Pictograph" browser for exploring and analyzing large-scale biological data sets. Plos One **2,** Article No.: e718.

Wong, J.L., and Johnson, M.A. (2010). Is HAP2-GCS1 an ancestral gamete fusogen? Trends Cell Biol **20,** 134-141.

Wong, J.L., Leydon, A.R., and Johnson, M.A. (2010). HAP2(GCS1)-dependent gamete fusion requires a positively charged carboxy-terminal domain. PLoS Genet **6,** e1000882.

Yang, H., Kaur, N., Kiriakopolos, S., and McCormick, S. (2006). EST generation and analyses towards identifying female gametophyte-specific genes in Zea mays L. Planta **224,** 1004-1014.

Yang, W.C., Shi, D.Q., and Chen, Y.H. (2010). Female gametophyte development in flowering plants. Annu Rev Plant Biol **61,** 89-108.

Yu, F., Shi, J., Zhou, J., Gu, J., Chen, Q., Li, J., Cheng, W., Mao, D., Tian, L., Buchanan, B.B., Li, L., Chen, L., Li, D., and Luan, S. (2010). ANK6, a mitochondrial ankyrin repeat protein, is required for male-female gamete recognition in *Arabidopsis thaliana*. Proc Natl Acad Sci U S A **107,** 22332-22337.

Yu, H.S., Hu, S.Y., and Zhu, C. (1989). Ultrastructure of sperm cells and the male germ unit in pollen tubes of *Nicotiana tabacum*. Protoplasma **152,** 29-36.

8 APPENDIX

8.1 Oligo nucleotides

8.1.1 Oligo nucleotides for expression analyses by RT-PCR

Table 7: Oligo nucleotides for expression analyses. Name of the amplified gene, AGI, primer name, oligo nucleotide sequence, annealing temperature and the resulting product size of genomic and cDNA are indicated.

					Product size	
Gene name	**AGI**	**Primer name**	**Sequence 5' – 3'**	**Annealing °C**	**gDNA**	**cDNA**
EC1.1	At1g76750	RT EC1.1 fw	ACAGTGACAGCTCGCCCTCTC	53	301	301
		RT EC1.1 rev	AGTCATTGCCATCACAGTAACCTT			
EC1.2a	At2g21740	qRT EC1.2a fw	ACAAAACAAAAACCCCAAAAAGAA	57	392	392
		qRT EC1.2a rev	GAAGGCGCCGGAGAAGAA			
EC1.2b	At2g21750	qRT EC1.2b fw	ACGCCGTTGATGTCATTACCACT	57	169	169
		qRT EC1.2b rev	ACGTCAGCGAGGAACATTTATCAA			
EC1.4	At4g39340	EC1.4 fw	CCAGCGGAGTCATCAACCAACATA	61	287	287
		EC1.4 rev	GGAGACGGAGCCGGAGAAGAGT			
EC1.5	At5g64720	EC1.5 fw	GCGCCGGAAACTTGATGGACT	57	277	277
		EC1.5 rev	GGCGCCGGTGAAGGAGATAAT			
ECR1	At2g27315	At2g27315 fw	TCCAACCAGGCTCACCCGTTG	64	136	136
		At2g27315 rev	AACGCCTTGCAACATGCGCC			
ECR2	At4g35165	At4g35165 fw	ATGAACAACCACCGCCCCGC	64	283	283
		At4g35165 rev	TCCCGCTTTCACTTTGAGGGAGA			
ECR3	At5g52965	At5g52965 fw	ACCACCAACGGTTCCAGGACTTCT	62	262	262
		At5g52965 rev	AGGGGAGTTGGGGACAATGCGA			
ECR4 / DD8	At5g52975	At5g52975 fw	AGCCGCATGTTGCAAGGCGT	64	116	116
		At5g52975 rev	TGGGGACAATACGAGCGCAGCTA			
ECR5	At5g53742	At5g53742 fw	TGGCGCACCAACACACACGAA	62	177	177
		At5g53742 rev	GCTGAAAACGCCTTGCAGCACA			
ECR6	At5g54062	At5g54062 fw	GCCCGGGCTAGCTCAACTCC	62	294	294
		At5g54062 rev	TGCGGTGTCTTGTGTGCTGGT			
LCR19	At4g30074	At4g30074 fw	GCCAGACACGGACCAGCGG	64	102	102
		At4g30074 rev	TTTGGGCTGCGGAGGCGATG			
LCR57	At5g42242	At5g42242 fw	TGCAAGGCCAAACACGGACCA	64	102	102
		At5g42242 rev	CGCACCGATGCACAGTTTGGC			
LCR58	At5g38317	At5g38317 fw	AGGCCAAACACGGGCCATCG	62	126	126
		At5g38317 rev	CAGTCCCACCGCTGCAAACG			
LCR59	At4g30070	At4g30070 fw	GCAAGGCCAAGCACGGACCA	62	138	138
		At4g30070 rev	TACCAGCCCCACCGTCGCAT			
LCR80 / DD22	At5g38330	At5g38330 fw	AGGCCAAACACGGGCCATCG	62	124	124

Gene name	AGI	Primer name	Sequence 5' – 3'	Annealing °C	Product size gDNA	Product size cDNA
		At5g38330 rev	TCACCGCAATTGCCAAGCCC			
CCC1	At1g24062	At1g24062 fw	GCGGCAACGCTTGTGATTCCA	62	143	143
		At1g24062 rev	GGGGGAAGATCATCAACCTCAGAAGG			
CCC2	At5g54220	At5g54220 fw	AGATGCGAGAACTGTGCCTCCG	62	129	129
		At5g54220 rev	ACCTCAGGAGGAGGATAAATGCAGC			
CCC3	At2g25305	At2g25305 fw	ACCTCCGACTTGTGGACCAGAT	62	110	110
		At2g25305 rev	GTCCTCGGAATAGAATGCAAACACCA			
CCC4	At5g54215	At5g54215 fw	GCCTCCCACTTGTGGACGAGAC	62	118	118
		At5g54215 rev	CGGAGGAAGTCCTTCGGATAGAATGC			
CCC5	At5g54225	At5g54225 fw	GCATCCGGGGAGGCTTCGAG	60	139	139
		At5g54225 rev	TGGAAGTAGGGGGAATTCCAAAACCA			
ACTIN3	At3g53750	AtACT3 fw	GATTTGGCATCACACTTTCTACAATG	60	740	657
		AtACT3 rev	GTTCCACCACTGAGCACAATG			
EUKARYOTIC TRANSL. INIT. FACTOR 4G	At3g60240	eIF4G fw	CGGCGATGTTCTTGGGAGTG	58	123	123
		eIF4G rev	CCGGTTAGGTGCATGAGGTTTG			

8.1.2 Oligo nucleotides for cloning

Table 8: Oligo nucleotides for cloning. Gene name and purpose of cloning, AGI, primer name and the oligo nucleotide sequence are indicated. Restriction endonuclease recognition sites are underlined and written in italic letters, start and stop codons are written in bold letters.

Gene name	AGI	Primer name	Sequence 5' - 3'
GCS1/HAP2 (Y2H)	At4g11720	GCS1c+73f EcoRI	GACACA*GAATTC*ATTCAGATTTTATCGAAATCA
		GCS1c+1650r EcoRI	GACACA*GAATTC*GAAGTCGAAGAAACTCGAGC
PP2A B'θ (Y2H)	At1g13460	PP2A B' theta SmaI +1f	GACACA*CCCGGG*T**ATG**TGGAAACAGATTCTGA
		PP2A B' theta XhoI +1479r	GACACA*CTCGAG***TTA**CAATGAACTCTTTTTTGCT
UbDK3γ (Y2H)	At5g24240	UbDk3gamma SmaI fw	GACACA*CCCGGG*T**ATG**TCAGTTGCTAGTGTAGC
		UbDK3gamma XhoI rev	GACACA*CTCGAG***TCA**GTTCCAAGCATACTGG
EC1.1 (phospho-mimicking)	At1g76750	P-mim EC1.1 fw	CACC**ATG**GCTTCCAAATCTAGTTTCATGGC
		AtEC1.1 3xSD	AGGGTTAGAAGGATCAGCATCATCTCTAAC
PP2A B'θ promoter (expression analysis/ subcellular localization)	At1g13460	PP2AB'tp fw SacI	GACACA*GAGCTC*TCCAATTCCAAGGAG
		PP2AB'tp rev kurz SpeI	GACACA*ACTAGT*AATTTTAATTGTTTTTTTATTCCCCTTTATT
		PP2AB'tp rev lang SpeI	GACACA*ACTAGT*GTATTAAACTCAGATTCTTCTTTG
PP2A B'θ (expression analysis/ subcellular localization)	At1g13460	PP2AB't cds fw PstI	TTA*CTGCAG*TC**ATG**TGGAAACAGATTCTGAGTAAG
		PP2AB't cds rev SmaI	ATAA*CCCGGG***TTA**CAATGAACTCTTTTGCTTTTGA
PP2A B'θ (mis-expression in synergid cells)	At1g13460	PP2A B'Θc+1f GW	CACC**ATG**TGGAAACAGATTCTGAGTAAGC
		PP2A B'Θ rev w/o stop	CAATGAACTCTTTTGCTTTTGATTACCAATTTC
DD31 promoter (misexpression in synergid cells)	At1g47470	DD31 prom fw (SacI)	AAGCTT*GAGCTC*GTTTATTTTTGTAACATTACT
		DD31 prom rev (SpeI)	TGATT*ACTAGT*TTTTTTATGGATGTAAGAATACTTTTAGTATTGA ATGTA
EC1.1-GFP (*A.th.* expr.)	At1g76750	AtEC1.1 SalI+1f	GACACA*GTCGAC***ATG**GCTTCCAAATCTAGTTTC
		GFP SalI rev	GACACA*GTCGAC***TCA**CTTGTAGAGTTCATCCAT
EC1.1 (*Pichia* expr.)	At1g76750	AtEC1.1 Pichia fw	CACA*GAATTC*GCCCTCTCATGAAACC
		AtEC1.1 Pichia rev	CTCT*TCTAGA*AACTTATCGTCATCGTCAGGGTTAGAAGGAGAA GCA

Gene name	AGI	Primer name	Sequence 5' - 3'
EC1.1 (*E.coli* expr.)	At1g76750	AtEC1.1+82f GW	CACCCGCCCTCTCATGAAACCATC
		AtEC1.1 rev GW	**TCA**AGGGTTAGAAGGAGAAGCAGAA
EC1.2a (E.coli expr.)	At2g21740	AtEC1.2a+67f GW	CACCAGAACTCTCCCGGAGACGG
		AtEC1.2a rev GW	**TCA**AAGTTTCACAGAGGAAGGCGC
amiRNA against	At1g13460	I miR-s B't	gaTTCTAGGATCCTCGGAGTCCAtctctcttttgtattcc
	At3g26020	II miR-a B't	gaTGGACTCCGAGGATCCTAGAAtcaaagagaatcaatga
	At3g54930	III miR*s B't	gaTGAACTCCGAGGAACCTAGATtcacaggtcgtgatatg
	At5g25510	IV miR*a B't	gaATCTAGGTTCCTCGGAGTTCAtctacatatatattcct
ami fw	Gateway® compatibility	HAU62	CACCAAACACACGCTCGGACGCATATTAC
ami rev		HAU63	CATGGCGATGCCTTAAATAAAGATAAACC

8.2 BLAST results

8.2.1 Plant GDB BLAST

Table 9: BLASTP results at plantgdb.org with AtEC1.1 as a query. The ID of the hit, BLAST score, E value and the term is indicated. The line before the third last row indicates the threshold that was used for EC1 homologs. * Annotation of nucleotide sequence is ambiguous and could therefore not be used for phylogeny construction

Query ID	#of hits	Hit (Subject) ID	BLAST Score	E value	Term
AtEC1.1	37	Q9SRD8_ARATH	328	1e-89	AtEC1.1
		D7KTW7_ARALY	277	2e-74	AlEC1.1
		B9SE79_RICCO	132	9e-31	RcEC1
		B9S177_RICCO	121	3e-27	RcEC2
		B9GGT7_POPTR	116	8e-26	PtEC1
		Q9SES8_HORVU	114	3e-25	HvECA1
		A5AIQ2_VITVI	113	7e-25	VvEC1*
		B9N9C7_POPTR	110	4e-24	
		A5AZZ7_VITVI	103	4e-22	VvEC2
		B9HN98_POPTR	103	6e-22	
		A2XFL4_ORYSI	103	7e-22	
		Q10MT0_ORYSJ	102	1e-21	OsEC1
		A2XFM3_ORYSI	102	1e-21	
		D7SWA7_VITVI	102	2e-21	
		B9NHC0_POPTR	100	3e-21	
		B4FS19_MAIZE	100	9e-21	ZmEC1
		Q53JF8_ORYSJ	99	1e-20	OsEC2
		A2ZBV3_ORYSI	99	1e-20	
		C5YSL3_SORBI	98	3e-20	SbEC1
		C5WNG6_SORBI	96	8e-20	SbEC2
		Q9T039_ARATH	96	1e-19	AtEC1.4
		A0MFC9_ARATH	96	1e-19	
		B9GGU6_POPTR	93	7e-19	PtEC2
		D7MGE0_ARALY	93	1e-18	AlEC1.4
		Q9SJ23_ARATH	92	1e-18	EC1.2b
		A0MEP0_ARATH	92	1e-18	
		D7LBY4_ARALY	92	2e-18	AlEC1.2b

Query ID	#of hits	Hit (Subject) ID	BLAST Score	E value	Term
		B9SVP8_RICCO	92	2e-18	RcEC3
		Q2QX72_ORYSJ	89	2e-17	OsEC3
		A2WMU5_ORYSI	89	2e-17	OsEC4
		B9SVP5_RICCO	86	1e-16	RcEC4
		Q9SJ24_ARATH	84	3e-16	AtEC1.2a
		A0MEN9_ARATH	84	4e-16	
		D7LBY3_ARALY	84	5e-16	AlEC1.2a
		D7MSJ0_ARALY	54	4e-07	AlEC1.5
		Q9FGG1_ARATH	54	8e-07	AtEC1.5
		B9T251_RICCO	51	4e-06	

8.2.2 *Brachypodium distachyon* BLAST

Table 10: BLASTP results at brachypodium.org with AtEC1.1 as a query. The ID of the hit, BLAST score, E value and term is indicated. Line after the third hit indicates the threshold for EC1 homology.

Query ID	Hit (Subject) ID	BLAST Score	E value	Term
AtEC1.1	Bradi1g65190.1	112	1e-25	BdEC1
	Bradi2g28070.1	105	2e-23	BdEC2
	Bradi4g24640.1	90	7e-19	BdEC3
	Bradi4g23900.1	62	1e-10	

8.2.3 *Medicago truncatula* BLAST

For the identification of EC1 orthologs in *Medicago truncatula*, BLAST version MT3.0 was used.

Table 11: BLASTP results at medicago.org with AtEC1.1 as a query. The ID of the hit, BLAST score, E value, position on BAC and the term is indicated. Threshold for EC1 homology after the second hit (indicated by thick line).

Query ID	Hit (Subject) ID	BLAST Score	E value	On BAC	Term
AtEC1.1	Medtr3g064370.1	115	6e-27	AC122170.28	MtEC1
	Medtr3g144340.1	98.2	2e-21	CU041253.11	MtEC2
	Medtr3g064340.1	67.8	2e-12	AC122170.28	

8.3 Prediction of disulfide bond formation in EC1.1

DISULFIND

Cysteines Disulfide Bonding State and Connectivity Predictor

>EC1.1

```
                                                                                +----------
                                                                       +--------|----------
                                                                       |        |
          .........10........20........30........40........50........60........70........
AA        MASKSSFMATFNIVTLMLMVASSTVTARPLMKPSMGTSSPTTSLVYRLKLDEDTGYCWDSLMQLQHCSGELILFFLNGE
DB_state                                                               1        1
DB_conf                                                                6        6

          -------+
          ------+|          +----------------------+
                ||          |                      |
          80........90........100.......110.......120.......130.......140.......150......
AA        TYIGPGCCSAIRTIGRKCWPTMIGVLGFTAQEGDMLQGYCDGNDSDNNGEDHALASSTLPLSVNFKTTVVRSSASPSNP
DB_state        11          1                      1
DB_conf         77          7                      7
```

Figure 31: Prediction of EC1 disulfide bond formation.
Disulfide bonds are predicted to form between the first and the third, the second and the fourth and the fifth and the sixth cysteine residue.

8.4 MS-Digest search and MALDI data

MS-Digest Search Results

[+] **Parameters**

Index Number: **1**
pI of Protein: **6.3**
Protein MW: **17283**
Amino Acid Composition: **A11 C6 D9 E5 F5 G16 H3 I5 K6 L16 M6 N6 P10 Q4 R7 S21 T14 V5 W2 Y5**

linker → EC1.1

```
1   MAGTSRSGAH RSLDPSTSLY KKAGSAAAPF TRPLMKPSMG TSSPTTSLVY RLKLDEDTGY CWDSLMQLQH CSGELILFFL
81  NGETYIGPGC CSAIRTIGRK CWPTMIGVLG FTAQEGDMLQ GYCDGNDSDN NGEDHALASS TLPLSVNFKT TVVRSSASPS
161 NP
```

Number	m/z (mi)	m/z (av)	Modifications	Start	End	Missed Cleavages	Sequence
1	622.2977	622.7251		1	6	0	(-)MAGTSR(S)
1	638.2926	638.7245	1Oxidation	1	6	0	(-)MAGTSR(S)
1	664.3083	664.7627	1Acetyl	1	6	0	(-)MAGTSR(S)
1	680.3032	680.7620	1Acetyl 1Oxidation	1	6	0	(-)MAGTSR(S)
1	746.3315	746.7561		155	162	0	(R)SSASPSNP(-)
1	999.5079	1000.0682	1Met-loss	1	11	1	(-)MAGTSRSGAHR(S)
1	1041.5184	1042.1057	1Met-loss+Acetyl	1	11	1	(-)MAGTSRSGAHR(S)
1	1110.5677	1111.2444		12	21	0	(R)SLDPSTSLYK(K)
1	1130.5483	1131.2660		1	11	1	(-)MAGTSRSGAHR(S)
1	1146.5433	1147.2654	1Oxidation	1	11	1	(-)MAGTSRSGAHR(S)
1	1172.5589	1173.3035	1Acetyl	1	11	1	(-)MAGTSRSGAHR(S)
1	1188.5538	1189.3029	1Acetyl 1Oxidation	1	11	1	(-)MAGTSRSGAHR(S)
1	1238.6627	1239.4196		12	22	1	(R)SLDPSTSLYKK(A)
1	1302.6648	1303.4231		150	162	1	(K)TTVVRSSASPSNP(-)
1	1618.8184	1619.7853		7	21	1	(R)SGAHRSLDPSTSLYK(K)
1	2982.5176	2984.4880		23	51	0	(K)AGSAAAPFTRPLMKPSMGTSSPTTSLVYR(L)
1	2998.5125	3000.4874	1Oxidation	23	51	0	(K)AGSAAAPFTRPLMKPSMGTSSPTTSLVYR(L)
1	3014.5074	3016.4868	2Oxidation	23	51	0	(K)AGSAAAPFTRPLMKPSMGTSSPTTSLVYR(L)
1	3110.6125	3112.6632		22	51	1	(K)KAGSAAAPFTRPLMKPSMGTSSPTTSLVYR(L)
1	3126.6075	3128.6626	1Oxidation	22	51	1	(K)KAGSAAAPFTRPLMKPSMGTSSPTTSLVYR(L)
1	3142.6024	3144.6619	2Oxidation	22	51	1	(K)KAGSAAAPFTRPLMKPSMGTSSPTTSLVYR(L)
1	3223.6966	3225.8237		23	53	1	(K)AGSAAAPFTRPLMKPSMGTSSPTTSLVYRLK(L)
1	3239.6915	3241.8230	1Oxidation	23	53	1	(K)AGSAAAPFTRPLMKPSMGTSSPTTSLVYRLK(L)
1	3255.6864	3257.8224	2Oxidation	23	53	1	(K)AGSAAAPFTRPLMKPSMGTSSPTTSLVYRLK(L)

Figure 32: Results of the MS digest research.
Amino acid sequence comprises the linker between the N-terminal GST and EC1 the identified fragments are highlighted in red. Table below lists the expected fragments after trypsin digest and their respective masses. Identified fragments (see MALDI data) are marked in red.

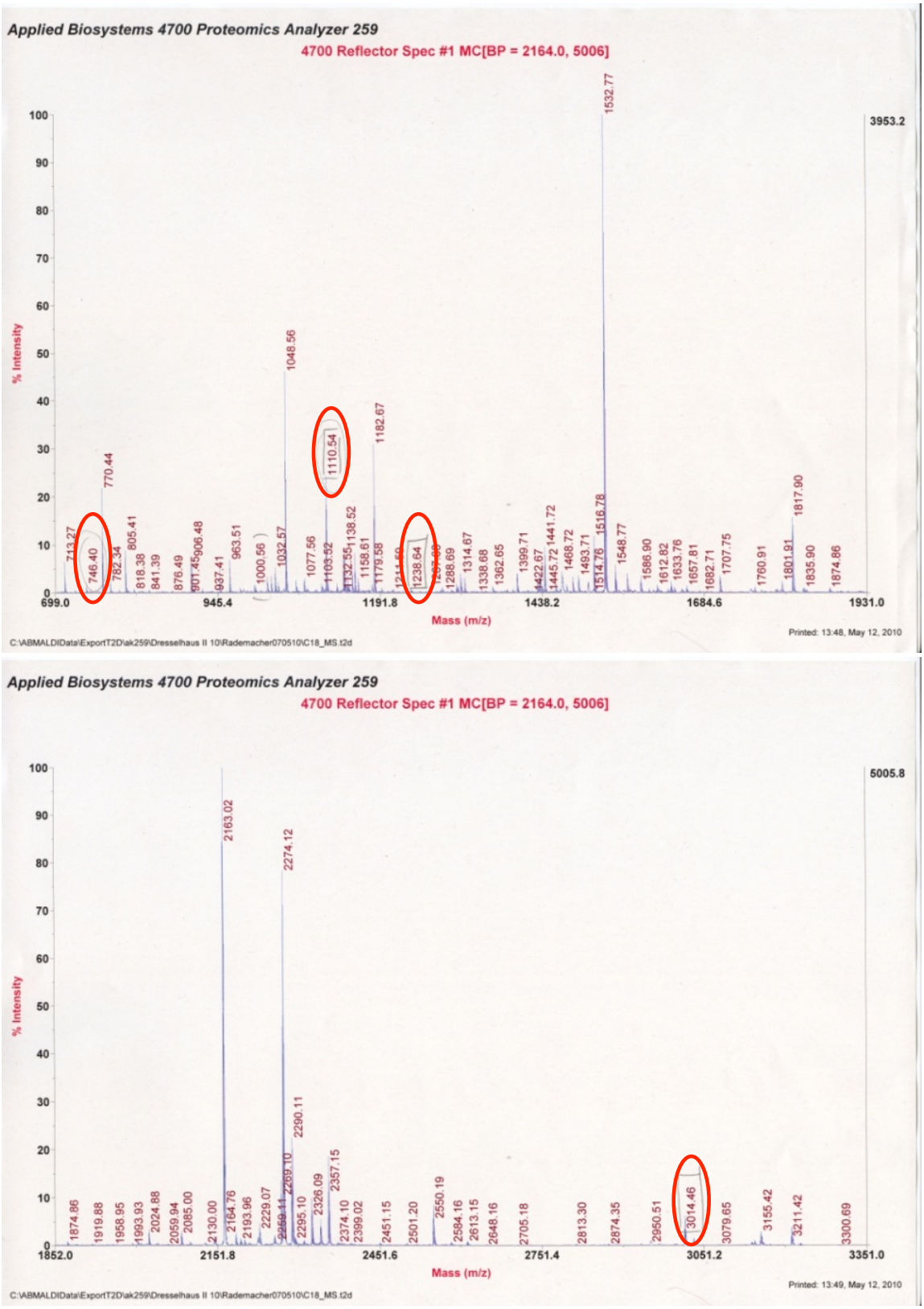

Figure 33: Reflector Spectrum of MALDI analysis.
Predicted masses of fragments after GST-EC1 trypsin digest identified in the spectrum are marked in red.

8.5 Vector maps

Yeast-two-hybrid vectors

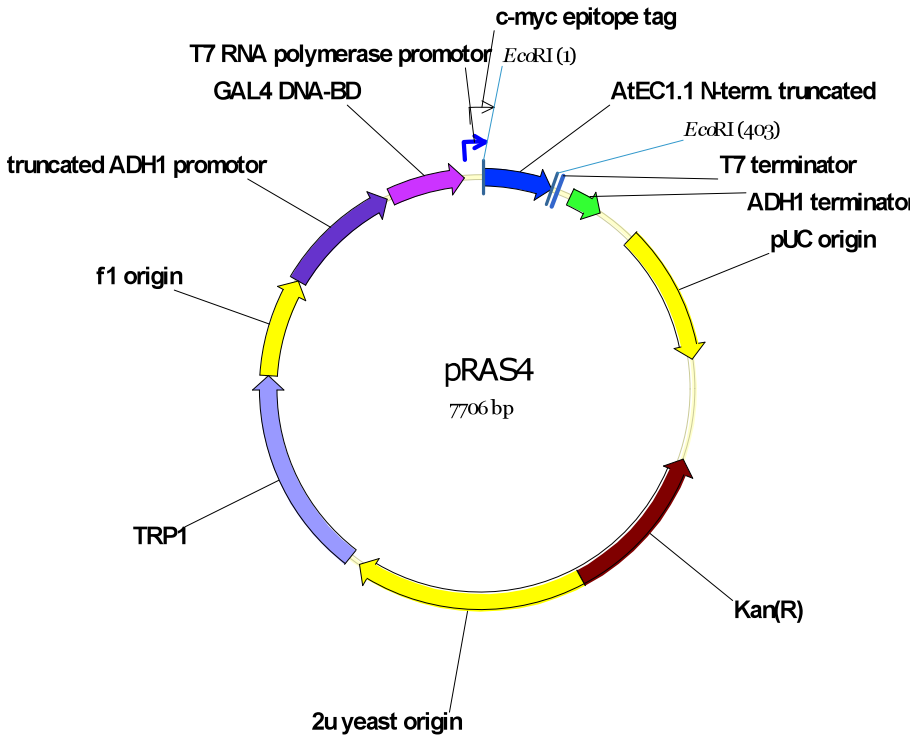

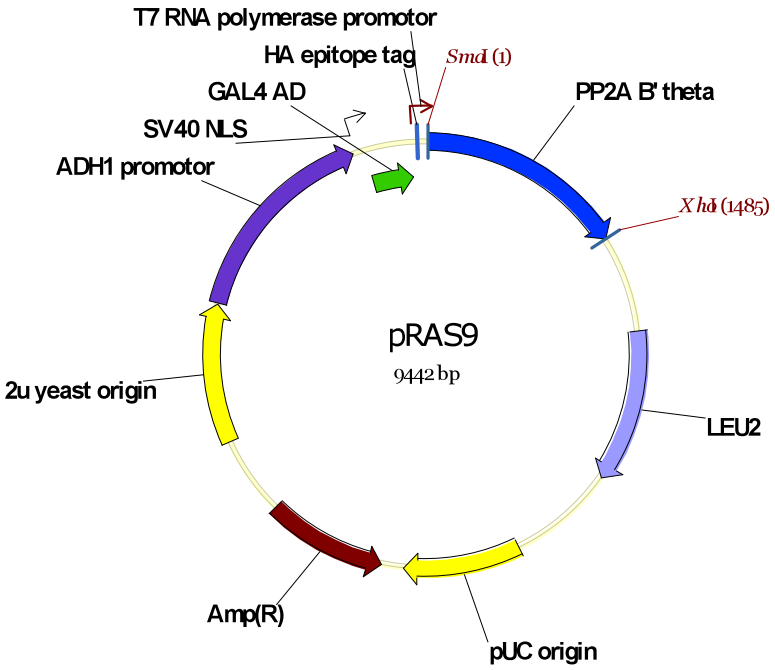

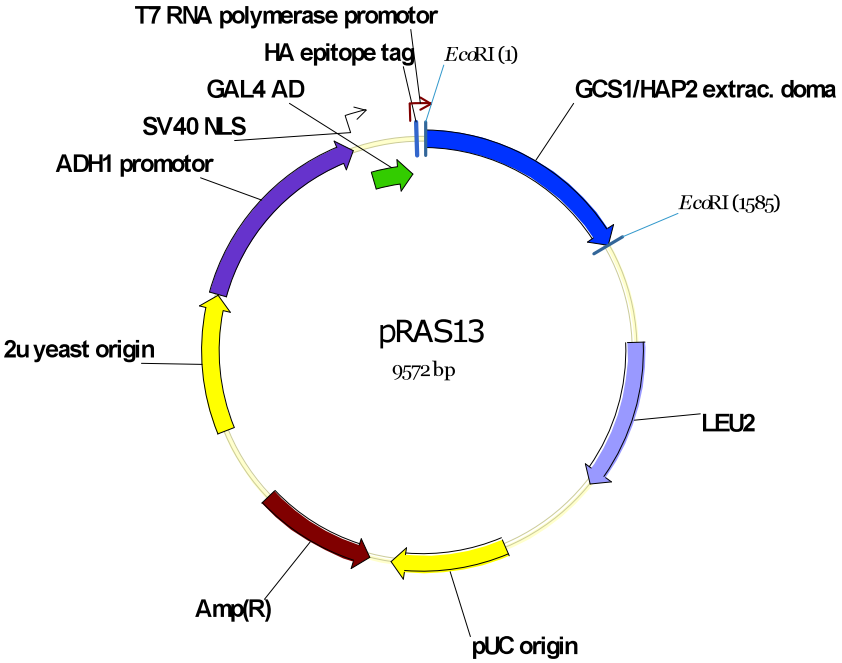
T7 RNA polymerase promotor
HA epitope tag
EcoRI (1)
GAL4 AD
GCS1/HAP2 extrac. doma
SV40 NLS
ADH1 promotor
EcoRI (1585)
pRAS13
9572 bp
2u yeast origin
LEU2
Amp(R)
pUC origin

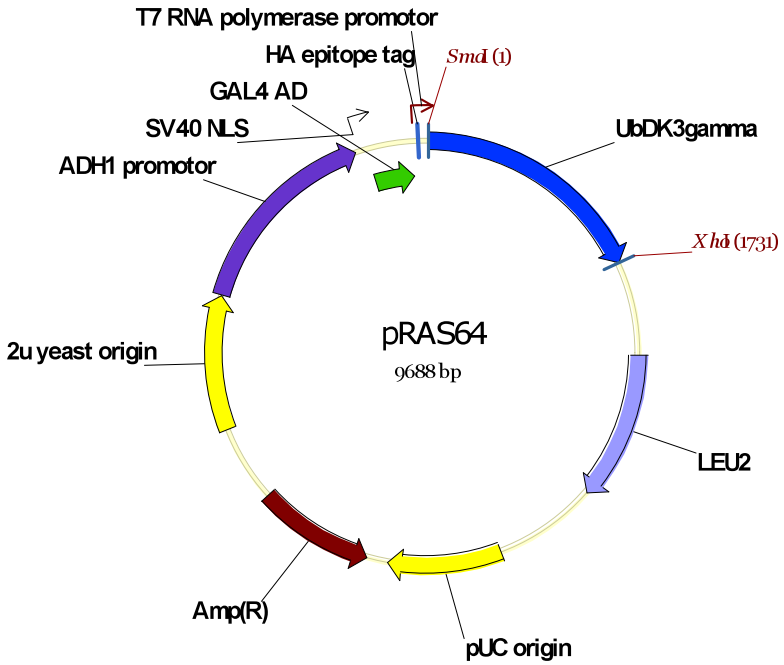
T7 RNA polymerase promotor
HA epitope tag
SmaI (1)
GAL4 AD
SV40 NLS
UbDK3gamma
ADH1 promotor
XhoI (1731)
pRAS64
9688 bp
2u yeast origin
LEU2
Amp(R)
pUC origin

Binary vectors for expression in plants

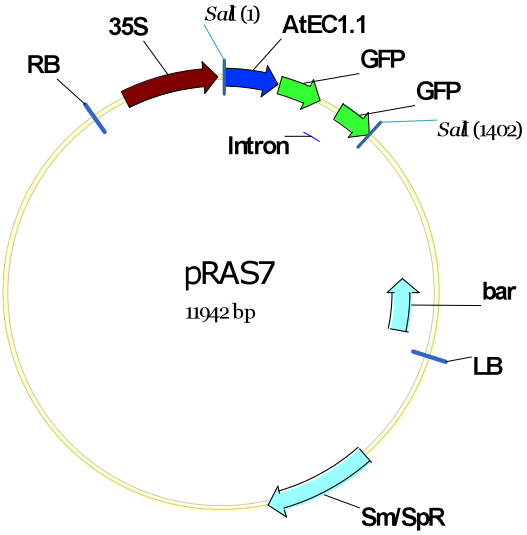

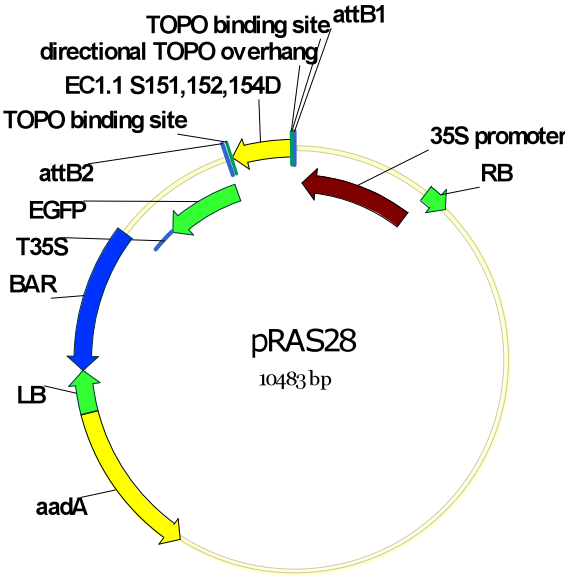

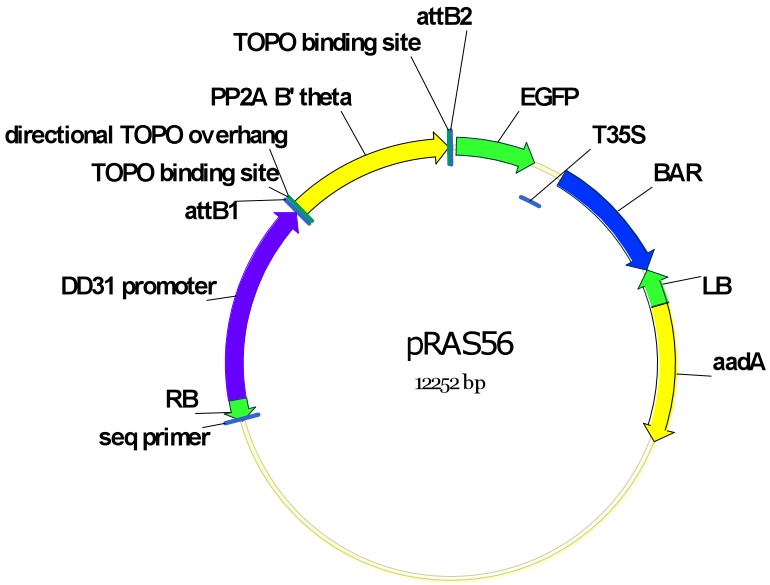

Pichia pastoris expression vector

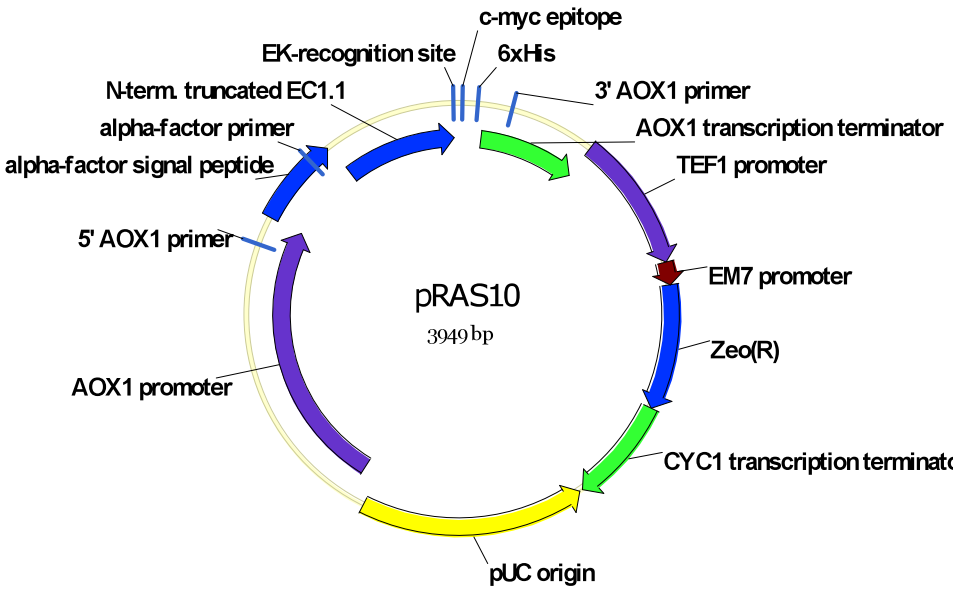

E.coli expression vectors

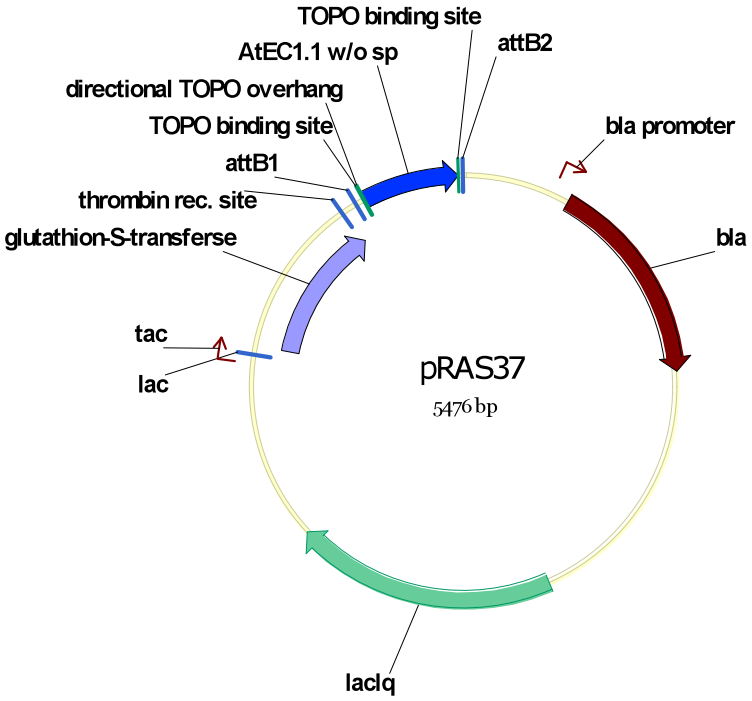

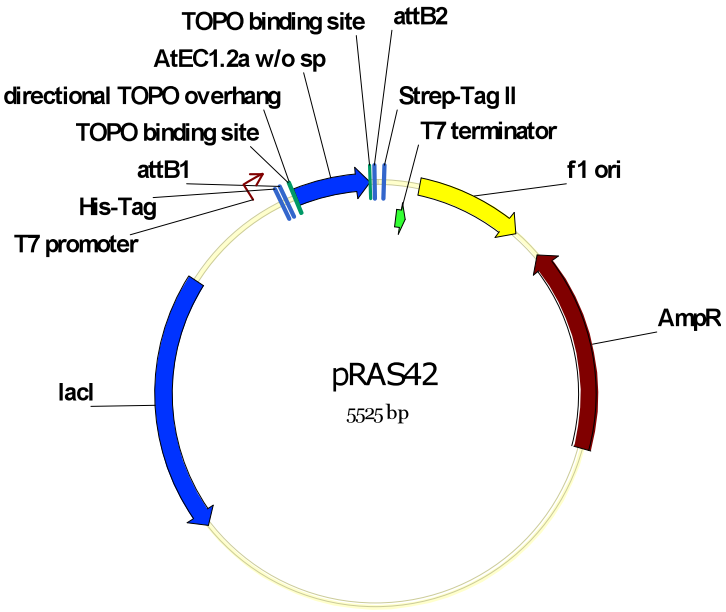

Parts of this work are reported in:

Ingouff, M., **Rademacher, S.**, Holec, S., Šoljić, L., Xin, N., Readshaw, A., Foo, S.H., Lahouze, B., Sprunck, S., and Berger, F. (2010). Zygotic resetting of the HISTONE 3 variant repertoire participates in epigenetic reprogramming in *Arabidopsis*. Curr Biol 20, 2137-2143.

Sprunck, S., **Rademacher, S.**, Grossniklaus, U., Dresselhaus, T. Egg-sperm crosstalk by EC1 mediates double fertilization in *Arabidopsis thaliana* (manuscript in preparation).

Rademacher, S., Dresselhaus, T., Sprunck, S. Rapid turnover of egg cell-specific EC1 is triggered by a pollen tube-derived regulatory subunit of PP2A (manuscript in preparation).

Šoljić, L., **Rademacher, S.**, Becker, J., Dresselhaus, T., Sprunck, S. The transcriptome of *Arabidopsis* female gametophyte cells (manuscript in preparation).

Acknowledgements

I am very grateful to Prof. Dr. Thomas Dresselhaus for giving me the chance to do my PhD in Regensburg. I would like to thank him for writing the proposal for the ‚Bayerische Eliteförderung' at the beginning of my PhD and for his continuous support in financial issues and last but not least, for scientific discussions, advice and the correction of my thesis.

I am very thankful to my supervisor Dr. Stefanie Sprunck for handing over this interesting project to me, for her support and for her scientific advice. Moreover, I thank her for giving me the opportunity to work independently and for the correction of my thesis.

I thank Prof. Dr. Herbert Tschochner for being an expert of my thesis.

I am very obliged to my friend and ex-roommate Dr. Ulrich Hammes. Again, like already during my diploma thesis in Erlangen he was of great help and support. I thank you not only for scientific discussions and advice and proofreading of my thesis but also for your friendship.

I would like to thank my friend Dr. Nádia Krohn, also known as just ‚Krohn'. I miss you! Thanks for reading my thesis and giving helpful comments for improvement.

I am indebted to Dr. Mariana Mondragon. She introduced me to bioinformatics and the construction of phylogenetic trees. Thank you also for correcting the worst mistakes I made!

Of course I would like to thank all my colleagues of the department of Cell Biology and Plant Biochemistry. Special thanks to my colleagues of the Arabidopsis lab: Lucija, Marc and Monika. Klemens and Uli: Thanks for the time we had together in our lab, I had a lot of fun, I guess so did you! ☺

Moreover I thank my Badminton and Squash partners Andi, Birgit, Frank, Julius „JD", Joe, Jürgen, Klemens, Martin, Martina and Philipp for athletic balance during my PhD!

Special thanks to Vroni for the administration of bureaucratic issues and of course to Günther for sowing, picking and taking care of hundreds or maybe thousands of *Arabidopsis* plants.

Regarding technical issues I would like to thank Eduard Hochmuth for conducting the MALDI analysis and Dr. Susanne Dietrich for help with the Äkta system.

I am deeply thankful to Philipp Alter. Thank you for supporting me, building me up and believing in me!

Last but not least, I would like to thank my parents Elke and Karl-Heinz. I am very grateful for your continuous support and your love, without you this would not have been possible!

Eidesstattliche Erklärung

Ich erkläre hiermit an Eides statt, dass ich die vorliegende Arbeit ohne unzulässige Hilfe Dritter und ohne Benutzung anderer als der angegebenen Hilfsmittel angefertigt habe; die aus anderen Quellen direkt oder indirekt übernommenen Daten und Konzepte sind unter Angabe des Literaturzitats gekennzeichnet.

Svenja Rademacher

Regensburg, den 08. März 2011